UNIVERSITY OF OKLAHOMA

GRADUATE COLLEGE

ENCAPSULATED THROMBOLYTIC MICROSPHERES TO PREVENT

REOCCLUSION AFTER THROMBOLYSIS AND TRIGGERED RELEASE

MICROSPHERES TO DELIVER THERAPEUTIC DRUGS

A DISSERTATION

SUBMITTED TO THE GRADUATE FACULTY

in partial fulfillment of the requirements for the

Degree of

DOCTOR OF PHILOSOPHY

By

HOAI XUAN NGUYEN
Norman, Oklahoma
2015

ENCAPSULATED THROMBOLYTIC MICROSPHERES TO PREVENT
REOCCLUSION AFTER THROMBOLYSIS AND TRIGGERED RELEASE
MICROSPHERES TO DELIVER THERAPEUTIC DRUGS

A DISSERTATION APPROVED FOR THE
DEPARTMENT OF BIOMEDICAL ENGINEERING

BY

_____
Dr. Edgar A. O'Rear III, Chair

_____
Dr. Matthias U. Nollert

_____
Dr. Roger G. Harrison

_____
Dr. Rong Z. Gan

_____
Dr. David A. Sabatini

I dedicate this dissertation to my wife, Duong Le, and my daughter, Annie Nguyen, for their company and support during my PhD study at the University of Oklahoma.

Acknowledgements

I would like to express my deepest gratitude to my advisor Dr. Edgar O'Rear for his guidance, encouragement, motivation, and support throughout my PhD study. I appreciate his time and efforts spending to help me improve my personal skills and build my career. Without his guidance and support, this project would not have been completed.

I also would like to thank Dr. Matthias Nollert, Dr. Roger Harrison, Dr. Rong Gan, and Dr. David Sabatini for serving in my committee. I appreciate their comments and advice in improving my dissertation.

Special thanks go to Dr. Preston Larson and Greg Strout from the Samuel Roberts Noble Electron Microscopy Laboratory of OU for technical assistance with the SEM and TEM experiments. I am also grateful to Evonic Röhm for supplying Eudragit polymer for this study.

I would like to acknowledge our staff Terri Colliver, Vernita Farrow, Donna King, Wanda Gress, and PJ Roberts Meek for their kindness and very professional assistance.

Finally, I appreciate the unconditional support from my family. I would like to thank my parents, Quy Nguyen and Tam Vo, my brothers, Ha Nguyen and Hieu Nguyen, my father and mother-in-law, Chuong Le and Loan Le, my wife, Duong Le, and my daughter, Annie Nguyen, for their endless love, support and patience.

Table of Contents

List of Tables

List of Figures

List of Abbreviations

Abbreviation	Definition
AA	Acetic anhydride
AGU	Anhydroglucose unit
ATTEMPTS	Antibody targeted, triggered, electrically modified prodrug strategy
BSA	Bovine serum albumin
CS	Chitosan
CV	Crystal violet
DA	Dextran acetate
DAC	Acetalated dextran
DEXAM	Dextran-amine conjugates
DMF	Dimethyl formamide
DMSO	Dimethyl sulfoxide
DO	Oxidized dextran
EDC	1-ethyl-3-(3-dimethylaminopropyl)-carbodiimide
EE	Encapsulation efficiency
Eud	Eudragit
FT-IR	Fourier transform infrared
HP	Heparin
IU	International unit

LESK	Liposome-encapsulated streptokinase
MES	2-(N-morpholino)ethanesulfonic acid
MESK	PEG-encapsulated streptokinase microspheres
MWCO	Molecular weight cut-off
NHS	N-hydroxysuccinimide
NMR	Nuclear magnetic resonance
PA	Plasminogen activator
PAI	Plasminogen activator inhibitor
PBS	Phosphate-buffered saline
PEG	Polyethylene glycol
Pg	Plasminogen
PLGA	Poly(D,L-lactic-*co*-glycolic acid)
Pm	Plasmin
PPP	Platelet-poor plasma
PRP	Platelet-rich plasma
PVA	Poly(vinyl alcohol)
RGD	Arg-Gly-Asp peptides
SEM	Scanning electron microscope
SK	Streptokinase
TEM	Transmission electron microscope
TNBS	2,4,6-trinitrobenzenesulfonic acid
tPA	Tissue-type plasminogen activator
W/O/W	Water-in-oil-in water double emulsion

Abstract

Cardiovascular diseases, including acute myocardial infarction, stroke, peripheral arterial diseases, and pulmonary embolism, are the most common and growing cause of morbidity and mortality in the United States. Early reperfusion of occluded blood vessels can be achieved by using thrombolytic therapy. However, thrombolysis is associated with its side effects, including bleeding complications and reocclusion. The hours after treatment for myocardial infarction represent a critical period when the patient is subject to reocclusion and a second coronary event. While rapid release on the order of minutes is desirable initially, an extended half-life of a thrombolytic agent functions better to address reocclusion.

The overall goal of this research was the design, synthesis, characterization and testing of microspheres which *i*) are suitable for extension the half-life of a thrombolytic agent for prevention of reocclusion *in vitro*, and *ii*) provide a general controlled release by triggered release mechanism for cardiovascular delivery of therapeutic drugs.

The first project of this thesis is to synthesize dextran acetate (DA) with various degrees of substitutions (DA1<DA2<DA3) and prepare, characterize polyethylene glycol (PEG)/DA microspheres which were combined with PEG microspheres to provide short and intermediate term release. Bovine serum albumin (BSA) was used as a model protein. PEG/DA3 microspheres exhibited the release of BSA on the scale of hours (180 min), more slowly than that of PEG microspheres. The percentage of BSA released from PEG and PEG/DA3 microspheres with time (min) was modeled mathematically [$Y_{PEG} = 100(1 - e^{-0.12t})$; $Y_{PEG/DA3} = 100(1 - e^{-0.024t})$] in order to predict

cumulative delivery from mixtures *in vitro* over a period of hours when constrained to a target level at 30 min. The system is examined for potential application in thrombolytic therapy.

The second project is to develop and characterize eudragit (Eud) microspheres which were coated with chitosan (CS) by the covalent bonding in order to meet short and longer term needs. The extension of thrombolytic activity of these microspheres in *in vitro* experiments was also examined. CS-Eud/SK microspheres had a lower encapsulation efficiency of streptokinase (SK), reduced activity of SK, and a much slower release of SK when compared with those of Eud/SK microspheres. Release of SK from Eud/SK microspheres obeyed first-order kinetics model [$Y_{Eud/SK} = 100(1 - e^{-0.6t})$] while release of SK from CS-Eud/SK microspheres obeyed the Hixson-Crowell model [$Y_{CS-Eud/SK} = 100(1 - (1 - 0.1t)^3)$]. Counter-intuitively, slower release leads to faster thrombolysis as a result of greater penetration of agent into the thrombus and the mechanism of distributed intraclot thrombolysis. In the *in vitro* lysis experiment, the presence of CS coating on the surface of Eud/SK microspheres induced a much slower release of SK up to 8 h which would seem to provide clot-lytic efficacy in prevention of second blockage up to 4 h. This study has demonstrated that longer release times leading to extended half-life in plasma can be expected to offer prevention of reocclusion.

The third project is to synthesize and characterize a novel amine-modified acetalated dextran polymer which is combined with heparin to develop triggered release microspheres for the delivery of therapeutic agents. In this study, we extend the underlying concept of Yang's ATTEMPTS (antibody targeted, [protamine] triggered,

electrically modified prodrug-type strategy) system to enable controlled release from microspheres. By encapsulating a drug in a cationic dextran-heparin microsphere, we broaden the protamine initiated release mechanism so that delivery can be generalized to a greater range of agents. In particular, a drug need not be electrically modified with this approach.

Chapter 1 - Introduction

In the United States, cardiovascular diseases are estimated to account for greater than 32% of all deaths annually, in which myocardial infarction and ischemic stroke are considered the most severe cases of thrombosis (1). The formation of an occlusive thrombus in an artery has been identified as a leading cause of common cardiovascular diseases. To decrease the incidence of morbidity and increase patient survival, early detection and using thrombolytic therapy are necessary. Thrombolytic therapy with the administration of a plasminogen activator (PA) or a so-called "clot-busting" drug breaks up the clot and restores flow with proven efficacy in saving lives and reducing morbidity (2). Multiple PAs [tissue-type plasminogen activator (tPA), streptokinase (SK), urokinase] are available and being used in clinical practice. PAs activate the proenzyme plasminogen to plasmin, which can lyse a solid fibrin clot, resulting in clearing the occluded blood vessel and allowing the blood flow to be re-established (3, 4).

Despite the benefit of fibrinolysis achieved with PAs, thrombolytic therapy has some limitations, including high risk of bleeding complications and reocclusion (5). Intracerebral hemorrhages occur in approximately 1% of patients treated for acute myocardial infarction (6) and in 7% of those treated for stroke by thrombolysis agents (5). Reocclusion of coronary arteries after reperfusion occurs in 7-32% of patients (7)

and associates with the increase the level of infarct and mortality (8). The mechanism of reocclusion is not well understood, but it may be induced by several factors including thrombi traveling downstream, the release of various chemicals that cause restenosis due to spasm of the blood vessel or the exposure of active surface that initiates platelet response (9). Reocclusion after thrombolysis associates with the residual thrombus because the surface of the residual thrombus is highly thrombogenic (10, 11). Moreover, it has been noticed that reocclusion occurs inversely to the plasma half-life of the thrombolytic agent used (12). Therefore, maintenance infusion of PAs after thrombolysis for prolonging the half-life of PAs was used to prevent coronary artery reocclusion (13, 14). However, due to high risk of bleeding (15), this method has not gained wide acceptance. It is therefore reasonable to infuse of PAs in delivery vehicles that protect them from enzymes and antibodies in the circulatory system in order to prolong drug retention for prevention of reocclusion.

Encapsulation PAs in liposomes, microspheres, and nanospheres shows great promise in improving the performance of PAs by accelerating thrombolysis and reducing bleeding complications (9, 16, 17). The greater advantages of encapsulation have been achieved when drug vehicles have been targeted to thrombi by attaching ligands, e.g. RGD (Arg-Gly-Asp) peptides, to their surfaces (18, 19) or by using magnetic devices (20, 21). Encapsulation also extents the half-life of PAs and maintain the drug activity for long-term effects (19, 22). Therefore, encapsulation shows some promise in addressing reocclusion but few studies have been conducted using encapsulated PA for reducing the rate of reocclusion. For these reasons, this study has

focused towards the development of formulations of encapsulated PA that provide benefit in prevention of reocclusion.

The purpose of this research is to develop formulations that would not only restore blood flow rapidly, but also would act to prevent formation of secondary thrombus. Our group has shown that polyethylene glycol (PEG) microspheres provide the release of the encapsulated SK on the scale of minutes, which dissolves blood clots more quickly by enabling the penetration of SK into the interior of the clot with faster digestion (9, 23). We aim to prepare microspheres which exhibit the release of active agent on the scale of hours. These microspheres can be used with PEG microspheres to provide complementary action with delayed release to prevent a putative second thrombus. To reach this stage, we first need to synthesize the polymer that facilitates the release of thrombolytic agent within hours in order to address reocclusion. Then, we characterize the ability of the polymer and microspheres for that purpose.

In another approach for producing the effective thrombolysis and reducing bleeding complication, Yang et al. have pioneered the ATTEMPTS (antibody targeted, triggered, electrically modified prodrug strategy) concept for targeted and triggered delivery of thrombolytics (24-26). In this approach, cation-modified tPA was attached to a heparin-antifibrin complex via ionic attraction. Protamine, a competitive heparin inhibitor, was used as a triggering agent to release the active tPA from the prodrug for clot dissolution. In this study, we extend the underlying concept of Yang's ATTEMPTS system to enable an on-demand controlled release from microspheres that might enhance therapeutic efficacy and reduce systemic side effects of thrombolysis.

In the light of the above-mentioned aspects, the objectives of our research project were threefold:

1) To synthesize and characterize dextran acetate (DA), prepare and characterize PEG/DA microspheres which were combined with PEG microspheres to provide short and intermediate term release.

2) To develop and characterize the covalent linking of chitosan to eudragit/SK microspheres to meet short and longer term needs. The extension of thrombolytic activity of these microspheres in *in vitro* experiments was also examined.

3) To synthesize and characterize a novel amine-modified acetalated dextran polymer which are combined with heparin to develop triggered release microspheres for cardiovascular delivery of therapeutic agents.

Chapter 2 gives a detailed background and the biological processes related to thrombosis, thrombolysis and reocclusion, and the development of encapsulation of PAs in order to better understand the pathogenesis and prevention of reocclusion. Chapter 3 describes the synthesis of DA and the characterization of DA/PEG microspheres. Chapter 4 presents the development of delayed release chitosan-eudragit/SK microspheres and describes *in vitro* thrombolytic experiment for prevention of a putative second thrombus. Chapter 5 describes the synthesis of a novel amine-modified acetalated dextran polymer for the preparation of triggered release microspheres. Finally, Chapter 6 includes an overall summary and suggests important areas of further research based on the findings of the current study.

Chapter 2 - Background

2.1. Thrombosis

Vascular thrombosis is a major event in the pathogenesis of ischemic conditions including myocardial infarction, stroke, venous thromboembolism (deep vein thrombosis), pulmonary embolism , and other vascular obstructions (27). Thrombosis is the most common and growing cause of morbidity and mortality in the United States. Most cases of myocardial infarction and of about 80% of strokes are caused by acute arterial thrombosis (28) which lead to the death rates of myocardial infarction and stroke between 10-20%, and 20-50%, respectively (1) Deep vein thrombosis and pulmonary embolism are the third leading cause of cardiovascular-associated death, after myocardial infarction and stroke (28).

Thrombosis is the pathological presence of a thrombus in the circulation. When an injury occurs at a blood vessel, platelets and fibrin form an immediate thrombus to prevent bleeding (29). Although this process is a protective response to cardiovascular injury to halt bleeding, the unnecessary changes that occur in the blood vessel wall and in the blood itself result in thrombosis: alteration in vessel wall, alteration in blood flow, and alteration in blood constituents (30). These three categories of thrombosis are known as Virchow's triad (31). However, clot formation is thus a more complex

interplay between the three criteria of Virchow's triad rather than a simple occurrence of one condition.

Under normal condition, intact vascular endothelium acts as a barrier for limiting the access and permeability of procoagulant proteins to the procoagulant surfaces that lie beneath it, thus helping to maintain patency of blood vessels. Moreover, the endothelial cells provide antithrombotic substances which defend against thrombus formation, including nitric oxide (NO) that regulate vasodilation and antiplatelet activities (32), endothelin-1 (ET-1) that is a potent vasoconstrictor (33), and a prostaglandin (PGI2) with the most potent endogenous inhibitor of platelet aggregation (34). Vascular endothelium injury can occur as a result of multiple factors such as smoking, hypertension, hypercholesterolemia, and hyperlipidemia (30). Damaged endothelium exposes the underlying collagen and tissue factor to flowing blood. Exposed collagen triggers the accumulation and activation of platelets, whereas exposed tissue factor initiates the generation of thrombin, which not only converts fibrinogen to fibrin but also activates platelets, initiating formation of a thrombus (29).

The second portion of Virchow's triad is abnormal forms of blood flow which include turbulence and stasis (31). Turbulence can arise from specific regions such as vessel branches, bifurcation and curvatures or from pathological atherosclerotic plaques and blood hyperviscosity. When blood flow moves from laminar flow to turbulent flow, countercurrents and local pockets of stasis can occur. Stasis is a major factor in the development of thrombi and can arise from several sources. For example, irregular contraction due to atrial fibrillation or a faulty valve can reduce the cardiac ejection fraction, causing the blood that is not ejected to pool, creating a thrombogenic

environment. In addition, a non-contractile myocardium following infarction can lead to formation of a mural thrombus. Blood can also become trapped in an aneurysm or remain stagnant downstream of an occluded vessel. When blood is no longer in circulation and becomes static, thrombi are prone to form.

The last portion of Virchow's triad, abnormal blood constituents, refers to abnormalities in platelets, as well as coagulation and fibrinolytic pathways. Cardiovascular risk factors, including smoking, hypertension and diabetes mellitus cause chronic endothelial cell injury, resulting in increased platelet adhesion to the endothelium (30). Acute endothelial injury or rupture of a complicated plaque leads to exposure of the sub-endothelium and binding of platelets via sub-endothelial bound von Willebrand factor (vWF) thus potentiating thrombosis. Altered shear stress states also induce platelet activation, aggregation and microparticle formation, further potentiating thrombogenesis (35).

Thrombosis may cause vascular blockage, leading to a lack of blood or oxygen supply to the organs in the body. Depending on the site of thrombus and the extent of its growth to occupy the cross-section of a blood vessel, thrombotic events can cause tissue death, dysfunction of the organs and possible death. A number of cardiovascular diseases are the direct results of vascular thrombosis: myocardial infarction, stroke, deep vein thrombosis, pulmonary embolism. However, the pathophysiology of arterial thrombosis differs from that of venous thrombosis (28).

Arterial thrombosis is typically associated with atherosclerotic plaque rupture (36, 37). This pathogenic process results in exposure or release of subendothelial cells and procoagulant material such as tissue factor, collagen from within the plaque and

activation and aggregation of platelets (Figure 2.1). The growing thrombus increases the degree of stenosis which can result in extremely high shear rates (up to 70,000 s^{-1}) within the stenotic region (38). In some cases, depending on stenosis geometry and location in the blood vessel, turbulent flow may develop downstream of the stenosis. Ultimately, platelet accumulation and fibrin deposition produces an occlusive platelet-rich intravascular thrombus (28, 31)
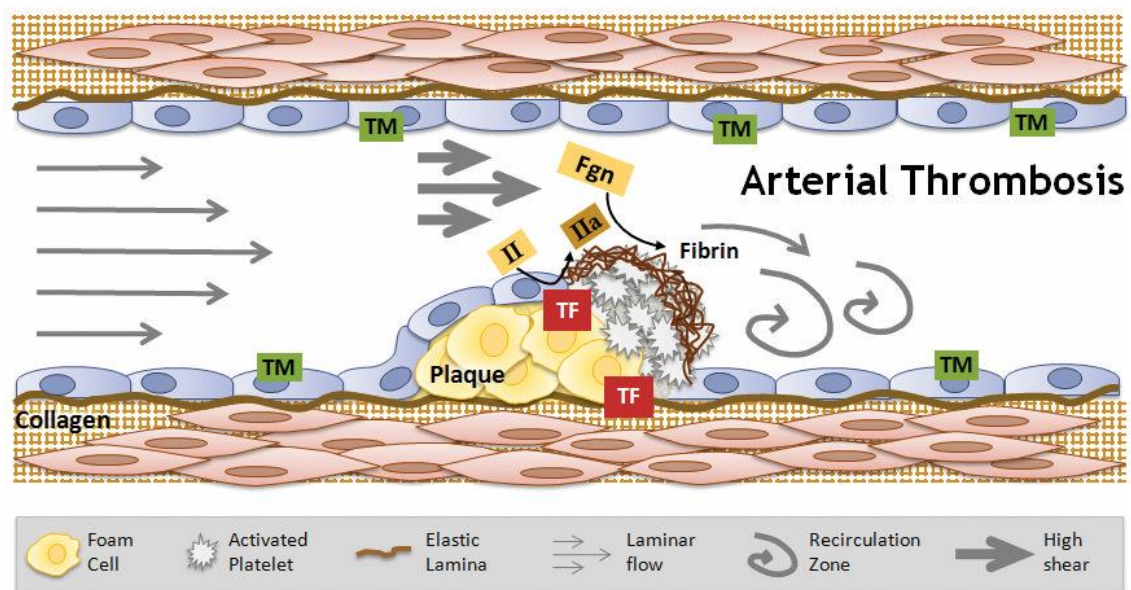
Figure 2.1. The Development of Arterial Thrombosis (31).

In contrast, venous thrombosis is typically associated with plasma hypercoagulability and thought to be triggered by expression of procoagulant activity on intact endothelium from inflammation and/or low blood flow and shear stress resulting from prolonged immobility (Figure 2.2). Venous clots have regions or layers showing substantial erythrocyte incorporation or "red thrombi" (28, 31, 39).

8
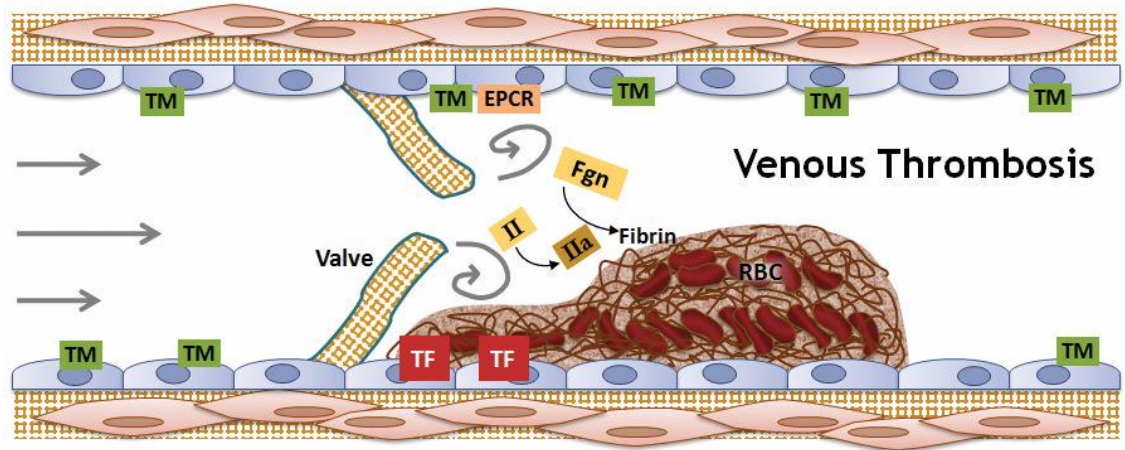
Figure 2.2. The Development of Venous Thrombosis (31).

Understanding the interplay between the components of Virchow's triad and its associated disorders will allow us to design more effective and safe therapeutics to treat thrombotic events.

2.2. Thrombosis treatment

The general methods of treatment for cardiovascular thrombosis involve administering anticoagulant drugs or thrombolytic agents, percutaneous transluminal coronary angioplasty, and bypass graft surgery depending on the location and size of thrombus, time of occlusion. Many of these factors must be weighed before determining the use of thrombolytic agents or surgical interventions.

Anticoagulants such as heparin and coumarin derivatives are mainstays in prevention and treatment of arterial or venous thrombosis where rapid clot dissolution is not necessary, including prevention of venous thromboembolism and long-term prevention of ischemic stroke in patients with atrial fibrillation (28, 40). However, these

9

drugs have the problem of increasing the risk of bleeding during their administration (41).

Both invasive techniques such as angioplasty and bypass graft surgery require personnel with expertise, equipment and might not be life-saving, where time is an important factor, as most of the deaths due to thrombosis occur within the first 6 hours of attack.

Thrombolytic therapy use activators of the fibrinolytic system, namely 'clot busters", to degrade fibrin, which stabilizes the structure of a thrombus (3). The success of thrombolysis depends crucially on the timing of intervention, with earlier intervention generally having a better outcome. For example, fibrinolytic therapy seems to be beneficial for at least 12 hours after the onset of symptoms of acute myocardial infarction and proven beneficial only when used within 3 hours for stroke. Therefore, thrombolytic therapy has the advantage that they are quicker, inexpensive method and can reach a large population.

2.2.1. Thrombolysis

Thrombolytic therapy uses plasminogen activators (PAs) such as tissue type plasminogen activator (tPA), streptokinase (SK), staphylokinase, urokinase and their derivatives to degrade the fibrin network that provides the structure of the thrombus and dissolve the clot (2, 3). PAs initiate a cascade of events that result in the dissolution of the blood clot and the recanalization of the blood vessel. PAs converse inactive blood plasminogen to its active form of plasmin, upon which plasmin degrades fibrin network into soluble fibrin degradation (Figure 2.3). The systemic plasmin is rapidly inactivated by α_2-antiplasmin, but, by contrast, the plasmin generated at the fibrin surface is

protected from neutralization of α_2-antiplasmin and thus localizes the action of fibrinolysis only on the fibrin clot. The free activators in the plasma are regulated by plasminogen activator inhibitor (PAI-1) (3, 4). The available thrombolytic agents are presented in Table 2.1 (42).
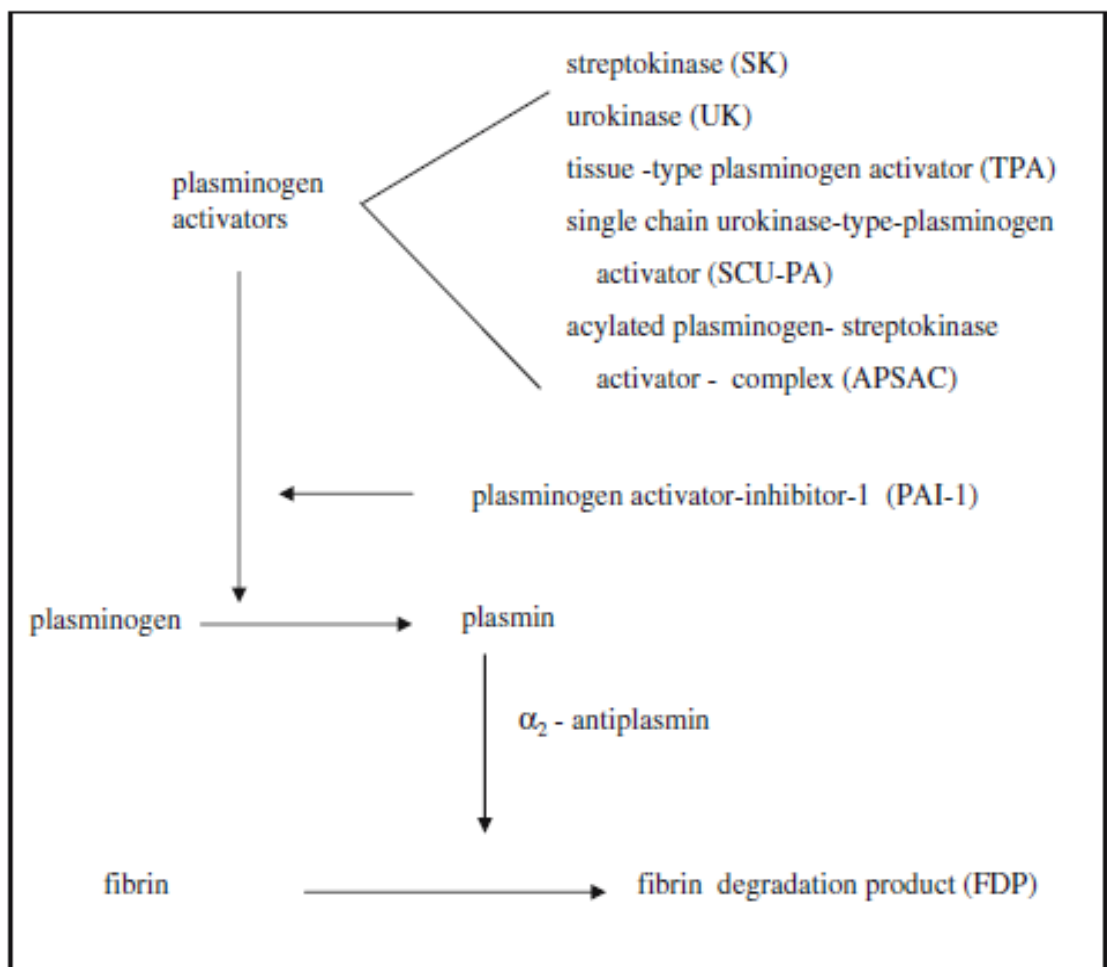
Figure 2.3. Mechanism of Fibrin Degradation with PAs (4).

The activation mechanism and the affinity of thrombolytic agents towards plasminogen in the presence or absence of fibrin are different. Based on the activation mechanism, PAs are classified into the direct and indirect activators. tPA and its variants, urokinase are direct activators which convert plasminogen to plasmin directly. By contrast, SK and staphylokinase are indirect activators. They must first combine with plasminogen to form a 1:1 molar ratio activator-plasminogen complex, which then becomes the activators.

In term of their affinity to fibrin, the activators are divided into two groups (37): fibrin-specific plasminogen activators, including tPA, recombinant single chain urokinase, and staphylokinase; and nonfibrin-specific activators which comprise two chain urokinase, SK, and acylated plasminogen streptokinase activator complex (APSAC).

Despite of its achievements, thrombolytic therapy has several limitations. Thrombolytic drugs are rapidly inactivated by PAI-1 and antibodies in the circulation. Plasmin produced in the circulating system is rapidly neutralized by α_2-antiplasmin. In addition, thrombolytic agents have very short half-lives (Table 2.1) (42) which are the consequences of the fast renal clearance due to their hydrophilic properties and small size or the enzymatic degradation in blood, liver and kidney (27). Therefore, in order to be effective in clinic treatment, the infused dosage of thrombolytic agents must be sufficiently high enough over the period of time (e.g., I.V. infusion of SK for 12-72 h) to overcome their short half-lives (43). This leads to increase the side effects such as uncontrolled bleeding as well as the cost of treatment. During thrombolysis, depletion of circulating plasminogen and plasma fibrinogen has been reported as a cause of

potential bleeding complications. The limited fibrin specificity and the nonspecific uptake of a large fraction of the administered drug dosage result in activation of circulating plasminogen to form plasmin, which, in turn, degrades plasma fibrinogen, leading to systemic hemorrhaging. There arises a need to use of advanced drug delivery systems to circumvent these problems and optimize efficacy and safety of thrombolytic drugs, especially in patients at high risk of thrombosis and bleeding.

Table 2.1. Available Thrombolytic Agents (42)

Name	Mechanism of Action	Half-life
tPA	Fibrin-selective. Binds and activates fibrin by cleavage of an arginine-isoleucine bond after which it activates plasminogen by cleaving Arg_{560}-Val_{561}	2-6 min
Streptokinase (SK)	Irreversible binding and activation of SK to plasminogen. Indirect activation. Vaguely fibrin-specific	12-18 min
Urokinase	Cleavage of the Arg_{560}-Val_{561} bond in plasminogen leading in active plasmin	7-20 min
Anisteplase	Similar to SK	70-120 min
Alteplase	Tissue plasminogen activator produced by recombinant DNA technology. Fibrin-enhanced conversion of plasminogen to plasmin. It produces limited conversion of plasminogen in the absence of fibrin	3-6 min
Reteplase	Similar to Alteplase. Lower fibrin binding and superior penetration ability	14-18 min
Tenecteplase	Similar to Alteplase. Greater binding affinity for fibrin	20-24 min

2.2.2. Streptokinase (SK)

SK was first discovered by Tillet and Garner in 1933 (44). It is a 414-residue protein secreted by hemolytic strains of Streptococci with the molecular weight of 47 kDa. The isoelectric pH for SK is 4.7 and it has a maximum activity at a pH of approximately 7.5. It consists of multiple structural domains (α-, β- and γ-domains) with different associated functional properties. The residues 1–59 of the α-domain play a key role in plasminogen activation (45). The C-terminal is involved in substrate recognition and activation. The Asp_{41}-His_{48} region is an important region of SK for its binding to plasminogen. The β- and the γ-domain are involved in SK-plasminogen complex formation and the plasminogen activation process (3, 4).

Unlike tPA and urokinase, SK possesses no enzymatic activity of its own and thus activates plasminogen (Pg) to produce plasmin (Pm) indirectly by forming a stoichiometric complex with either plasminogen or plasmin (2, 46). SK binds specifically to Pg and Pm, converting both the zymogen and proteinase into Pg activators. Binding of SK to Pg results in the conformational expression of an active catalytic site on the zymogen that cleaves specifically the Arg_{561}-Val_{562} activation bond in the catalytic domain of Pg to form Pm (47, 48). SK also binds to Pm, transforming the substrate specificity of the proteinase from one which is incapable of Pg activation into a specific activator, and protects Pm from inactivation of α_2-antiplasmin (47, 49).

The mechanism of coupling between conformational activation and Pm formation by SK was investigated in kinetic studies (Figure 2.4) (50). The first step of the trigger catalytic cycle is rapid binding of SK to the catalytic domain of Pg and conformationally induced activation of Pg in the SK·Pg* catalytic complex. SK·Pg*

binds a second Pg molecule in the substrate mode and proteolytically activates it to Pm. Free Pm and free Pg compete for SK in the catalytic mode, where the formation of SK·Pm is highly preferred over SK·Pg* because of its 500–900-fold higher affinity. This results in transition of the catalytic complexes from SK·Pg* to SK·Pm as the sole catalyst, terminating the trigger cycle and initiating the bullet cycle. The SK·Pm catalytic complex binds free Pg as the substrate and proteolytically converts the remaining free Pg to Pm (49).
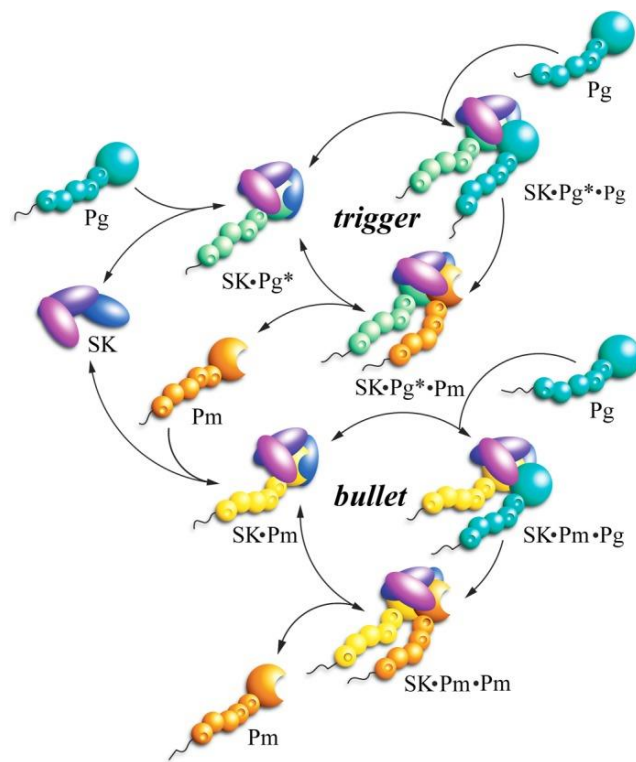
Figure 2.4. Mechanism of Plasminogen Activation by SK (50).

The advantages of SK over other PAs include high catalytic efficiency in the reaction of plasminogen activation, low price, and extensive experience of clinical applications. Its disadvantages comprise low stability, immunogenicity, and rapid elimination from circulation (51). For improvement, efforts have focused primarily on structural modification of streptokinase in order to prolong its half-life, reduce or eliminate its immunogenicity, and enhance its resistance to the proteolytic action of plasmin (4).

2.3. Development of drug carriers for prolonging the half-life of thrombolytic agents

Drug delivery systems have the potential to help overcome the limitation and thereby broaden the therapeutic window of thrombolytic therapy through two keys: *i)* prolonging the circulation time and minimizing the side effects and *ii)* spatiotemporally localizing drug action (52). This dissertation focuses on the strategies to extend the half-life of PAs.

To increase the half-life and activity of PAs in the circulation, multiple approaches have been developed, including chemical modification (53, 54) and the use of drug carriers (5). PEGylation, the covalent attachment of polyethylene glycol (PEG) to proteins, has proven to enhance the therapeutic potentials of many proteins. PEG chains form a hydrated shell that masks the protein's surface and increases the molecular size of the polypeptide, thus reducing its renal ultrafiltration, preventing the approach of antibodies or antigen processing cells and reducing the degradation by proteolytic enzymes (55). PEGylation of tPA (53), SK (51, 56, 57), urokinase (58), and staphylokinase (59) has been prepared. The results showed that PEGylation has

significantly increased circulating time and stability in plasma, and reduced loss of activity and immunogenicity of the PAs.

Another approach for prolonging the half-life of PAs is using properly designed drug carriers without chemical modification of these agents. Drug carriers can shield PAs for transport throughout the vasculature from premature inactivation, systemic removal or degradation by antibodies or enzymes.

Liposomes, spherical vesicles with diameters from 100 to 250 nm, composed of a phospholipid bilayer surrounding an aqueous core, are widely investigated as drug carrier for thrombolytic agents *in vitro* and *in vivo*. They can entrap hydrophilic or hydrophobic drugs into their internal water compartment or into the membrane, making them to be isolated from the inactivating effect of external conditions and at the same time not causing any undesirable side effects (27, 60). By encapsulation in liposomes, the systemic delivery of PAs has been extended.

As an approach to prolong the half-life of PAs, liposomes composed of distearoylphosphatidyl ethanolamine-N-poly(ethylene glycol) (DSPE-PEG$_{2000}$) increased the half-life and improved the area under curve (AUC$_\infty$) of the SK by 16.3- and 6.1-fold, respectively, as compared to free SK (43). PEGylated liposomes composed of egg phosphatidylcholine, cholesterol and cholesterol-3-sulfate and DSPE-PEG$_{2000}$ prolong the half-life of tPA by 21-fold, compared to tPA alone (61).

By encapsulation in large liposomes, Nguyen et al. showed that the fibrinolytic potential of SK was preserved because the liposomes limited its exposure to plasma components (16). Encapsulation of tPA, SK, urokinase in liposomes has demonstrated enhanced thrombolysis in *vivo* by reducing the time required to obtain reperfusion (16)

and increasing the percentage of the digested clot (62, 63) as compared with free PAs. In a jugular vein model in rabbit, liposomal tPA displayed a significantly better thrombolysis efficiency than equimolar doses of free tPA, in which a dose of about 0.24 mg/kg of liposomal tPA was nearly as effective as 1.0 mg/kg free tPA (62). In a rabbit thrombosis model, SK-entrapped liposomes improved the thrombolysis by increasing a 30% clot lysis as compared with free SK (63).

The mechanism of acceleration of thrombolysis by encapsulated liposomes is not completely understood. The studies of Heeremans et al. and Perkin et al. in animal models demonstrated that increased thrombolytic effects of liposomes encapsulated PAs were not due to pressure at the leading edge of the thrombus created by blocking of the channels inside the thrombus (62, 63). Nguyen et al. suggested that the liposomes were ruptured due to the shear stress on the vesicles when they arrive at and begin to pass the clot. Then, the liposomes then release their payload and lysis begins (16). Other studies have shown that plasminogen binds to the surface of the liposome and acts as a homing device for the blood clot. Then, the plasminogen would reduce the free circulation of the liposomes and attract the encapsulated thrombolytic agent to the blood clot (9, 64).

Although some benefits have been achieved from encapsulating PAs in liposomes, such delivery system suffers a limited stability. In order to develop encapsulated thrombolytic carriers with improved stability, polymeric carriers have been widely investigated to protect PAs from inactivation in the circulatory system and lengthen their short half-life (27).

Leach et al. developed two types of drug carriers: liposome-encapsulated SK (LESK), and PEG-encapsulated SK microspheres (MESK). The *in vivo* results showed

that both the formulations improved thrombolysis for multiple end points when compared to free SK but MESK demonstrated comparatively better results. In a rabbit model of carotid artery thrombosis, MESK achieved accelerated thrombolysis with reduced residual clot mass and greater return of arterial blood flow when compared to both free SK and LESK (9). In a canine model of coronary artery thrombosis, MESK significantly reduced the time to achieve sustained reperfusion of the occluded artery, infarct size, residual clot mass, bleeding complication and reocclusion episodes (23). The mechanism for increased thrombolysis by MESK was also explored: PEG polymer provides the resistance to adsorption and blocks the binding of SK to the leading edge of the thrombus, and enables the microspheres to penetrate into the interior of the clot with the help of permeation pressure (65). This leading to the higher thrombolytic effects of MESK.

In the absence of hydrodynamic pressure, the surface of the microparticles was modified to promote the interaction of the microparticles with the components of the clot in order to attract more particles into the interior of the clot. Following this trend, Chung et al. developed tPA loaded PLGA nanoparticles coated with chitosan (CS) and CS-GRGD (Gly-Arg-Gly-Asp peptides) to promote the electrostatic interactions between positive charge of CS and negative charge of fibrin as well as the ligand-receptor interactions between GRGD and GP IIb/IIIa receptors expressed on the activated platelets. The results showed that PLGA/CS-GRGD nanoparticles achieved a nearly 40% shorter clot lysis time and more effective thrombolytic potential due to they were adhered more to the clot front and aggregated in the interior of the clot, compared to PLGA/CS and PLGA nanoparticles (17, 18).

With the development of nanotechnology in drug delivery, nanoparticles have been applied in thrombolytic therapy for effective delivery of thrombolytic agents to the site of thrombus and subsequently to the interior of the clot (37). Taking advantage of their small size, nanoparticles can avoid the resistance of the pores of fibrin clots to the penetration and permeation of drug carriers with size of 1 μm of larger (27). Piras et al. developed nanoparticles with an average diameter of 125–130 nm for targeting delivery as well as long circulation time (66). Nanoparticles was prepared as based on polymer which was synthesized by covalently binding of PEG moieties and monoclonal antibody anti-fibrin Fab fragment to the synthetic bioerodible copolymer chain, poly[(maleic anhydride)-alt-(butylvinyl ether)] (67). The results gave evidence that the release of enzyme from nanoparticles is time controlled and that nanoparticles have a preserving effect on urokinase activity in solution (66).

Similarly, Tang et al. developed a tPA/gold nanoparticle (t-PA/AuNP) conjugate via bio-affinity ligation. The surfaces of gold nanoparticles were modified with 3-lysine-terminated polyvinyl pyrrolidone, serving as a spacer. tPA was immobilized to the surface of gold nanoparticles under physiological conditions through affinity interactions between the specific domain in tPA and 3-lysine exposed on the nanoparticle surface. The results showed that the conjugate can not only retain almost full enzymatic activity and clot dissolving efficiency, but also protect tPA from inhibition by PAI-1 to some extent as compared with free tPA *in vitro*. Moreover, the conjugate showed prolonged circulation time *in vivo* (68).

But concerns have been raised regarding the mechanisms of nanoparticles to concentrate locally at the thrombus site, and then, modulate the drug release nearby,

21

which restricted their use to treat acute events like acute myocardial infarction when immediate drug action is required (19). Recently, some approaches have used the targeting moieties such as anti-fibrin or anti-platelet antibodies for the delivery of nanocarriers to the thrombus site (37). Yurko et al. designed a prototype nanodevice capable of binding to fibrin clots and initiating their dissolution. The devices consist of tPA and anti-fibrin antibody covalently attached to a 40 nm polystyrene-latex nanoparticles. These nanoscale devices can directly deliver tPA to the clot site through fibrin-specific antibody. The results showed that *in vitro* fibrinolytic activity of these nanodevices was comparable to that of free tPA (69).

Most recently, Korin et al described an alternative biomimetic approach based on high shear stress caused by vascular narrowing to trigger deliver of tPA rather than relying on molecular targeting or ultrasound (70). Shear-activated nanotherapeutics was prepared as aggregates of multiple smaller nanoparticles by spray-drying technique and was similar in size to nature platelets (1 to 5 μm in diameter). The nanoparticles were fabricated of PLGA and were further coated with tPA by means of biotin-streptavidin chemistry. Shear stress between 10 and 1000 dynes/cm^2 caused aggregates of nanoparticles coated with tPA to burst apart, which then breaks down the clots. The results showed that when administered intravenously in mice, shear-activated nanotherapeutics clear rapidly clots induced by ferric chloride in mouse arteries, restore the normal flow, and increase survival in other fatal mouse pulmonary embolism model. This approach provides new potential treatment for vascular occluded diseases.

2.4. Development of Antibody Targeted Triggered Electrically Modified Prodrug Strategy (ATTEMPS)

Despite the liposomes, microspheres and nanoparticles of PAs have been developed for extension of the half-life of PAs, the release of PAs from these formulations tends to be rather slow considering that a quick onset of action is required for treating acute thrombotic conditions. Therefore, a targeted prodrug approach where drug release can be triggered locally is necessary for treating thrombotic events. Yang and coworkers have pioneered the ATTEMPS (antibody targeted, triggered, electrically modified prodrug strategy) concept for targeted and triggered delivery of thrombolytics (24-26, 71). This system is composed of two components: *i*) a targeting component consists of an anionic heparin molecule (Hep) conjugated to an anti-fibrin antibody (Ab) (termed Hep–Ab) and *ii*) a drug component consists of a cation-modified t-PA drug (termed CM-tPA) (Figure 2.5). These two components are linked via a tight yet reversible electrostatic interaction between the anionic heparin on the antibody and the cationic species on tPA. Once bound, the modified tPA is deprived of its enzymatic activity, due to blocking of the active site by the appended Hep–Ab conjugates. Thus, tPA will be inactive during administration. Once in circulation, the antibody component can direct the complex to reach the appropriate target site (fibrin clot), localizing and accumulating a high concentration of the inactivated CM-tPA at the thrombus. The active tPA can be subsequently released by the addition of protamine, a competitive heparin inhibitor, yielding dissolution of the clot. The results showed that both *in vitro* characterization and *in vivo* studies using a rat thrombosis model clearly demonstrated that Heb–Ab conjugate induced inhibition of CM-tPA could be effectively reversed

upon addition of protamine. Therefore, this delivery system would allow tPA to react

only with plasminogen at the clot site, reducing bleeding complications associated with

non-specific tPA action. Besides thrombolytics, this concept is also applicable to other

macromolecular anticancer drug delivery offering a solution to overcoming dose-

limiting side effects (72).
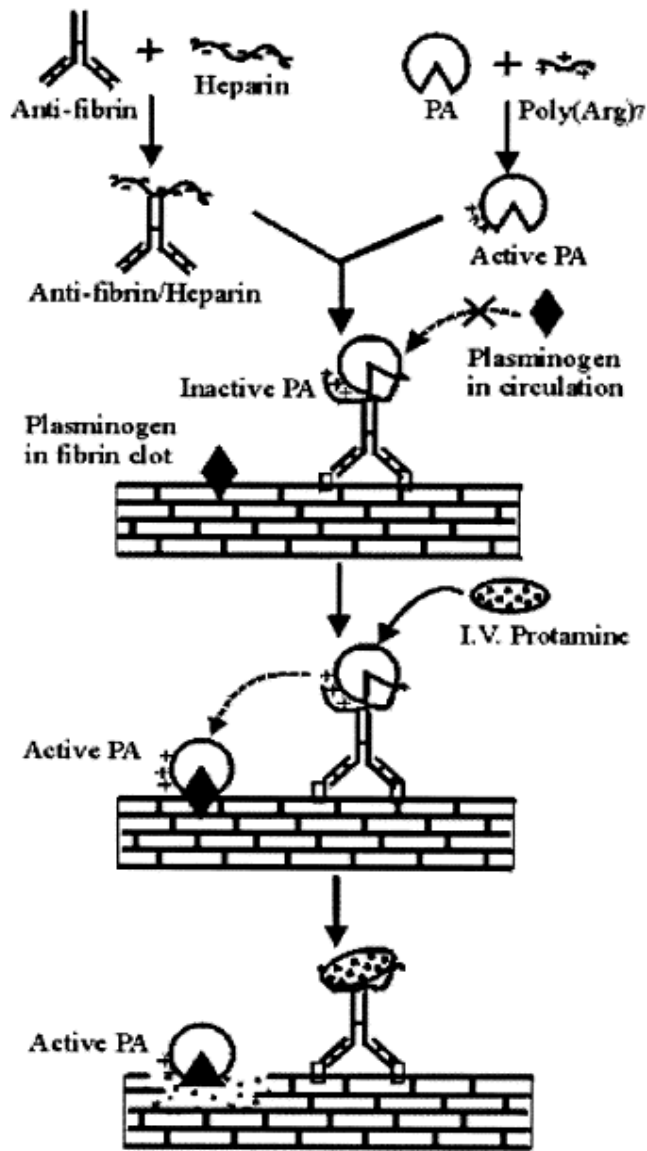
Figure 2.5. Schematic Design of the ATTEMPTS Approach (26).

2.5. Reocclusion

Thrombolytic therapy aims to restore the blood flow by dissolving or removing thrombotic material at the site of coronary lesion. However, the initially successful dissolution of the thrombus is complicated by reocclusion after thrombolysis. Reocclusion is a major drawback of thrombolytic therapy besides bleeding complications and resistance to thrombolysis. Reocclusion of coronary arteries after reperfusion occurs in 7-32% of patients (7). It has been associated with a 2- to 3-fold increased risk of mortality (8) and complications of left ventricular dysfunction, including heart failure and dysrhythmias (73).

The mechanism of reocclusion is not well understood but it may be induced by plasmin-mediated activation of the coagulation system, procoagulant activity of the residual thrombus, presence of high shear forces that promote platelet deposition, and attenuation of physiologic fibrinolytic activity after thrombolysis (11). Early after reperfusion, the stimulus for reocclusion is strongest because of the re-exposure of the cracked plaque, the hypercoagulability and activation of platelets induced by thrombolytic therapy, and the presence of locally vasoactive substances released by activated platelets (74). The activation of platelets after thrombolysis and the released thrombin from the site of vascular injury due to the thrombus dissolution are mainly responsible for the pathogenesis of reocclusion. The residual thrombus may protrude into the lumen, leading to a small residual diameter and increasing local shear rate that promote platelet activation and deposition at the lesion are. Moreover, the surface of residual thrombus is highly thrombogenic (10). Thrombin is bound to fibrin and remains active on the surface of the residual thrombus, where it may activate factors V

and VIII, promote fibrin formation and platelet activation. Thrombin activates platelets with subsequent elaboration of serotonin and thromboxane A_2, which are not only vasoconstrictors but also strongly supports platelet aggregation which can contribute to early reocclusion (74, 75). Moreover, the residual fibrin-bound thrombin stimulates the formation of prothrombinase which, in turn, converts prothrombin to thrombin at a rate approximately 5 orders of magnitude greater than would normally occur in its absence (76).

Multiple strategies have been applied to reduce the incidence of reocclusion after thrombolysis. Some strategies focus on inhibition of the platelet activation using antiplatelet agents (77, 78) or platelet glycoprotein IIb/IIIa inhibitors (79, 80). Another strategy is using anticoagulant agents as an adjunct to thrombolytic therapy in the treatment of patients with myocardial infarction (40). These studies have shown some benefits in preventing reocclusion. However, early reocclusion still occurs despite the use of such agents indicates the necessity for more potent interventions.

In an attempt to prevent reocclusion, the structure of thrombolytic agents has been modified to have three parts: one part for activation of the fibrinolysis, another part to inhibit the aggregation of platelets and a third part to inhibit thrombin. Recently, a multifunctional recombinant staphylokinase linked with RGD (Arg-Gly-Asp) and Hirulog peptides was constructed in which RGD acts as an antiplatelet agent and Hirulog acts as an antithrombin agent (81). The results showed that the multifunctional staphylokinase retained the fibrinolytic activity and effectively inhibited the thrombin activity and platelet aggregation. The multifunctional staphylokinase can be an efficient candidate for reduction of reocclusion after thrombolysis

Alternative approach in prevention of reocclusion is to lyse the residual thrombus because of its procoagulant activity resulting in increased probability of reocclusion (11). Therefore, further lysis is required to reduce the rate of reocclusion following recanalization. Reocclusion after reperfusion has been noticed that it occurs in inverse proportion to the plasma half-life of the thrombolytic agent used (12). Accordingly, prolong the half-life of PAs by maintaining infusion of PAs after thrombolytic therapy was used to dissolve the residual thrombus for prevention of coronary artery reocclusion (13, 14). However, this approach suffered from the high risk of bleeding (15). It is therefore reasonable to assume that the infusion of PAs in a delivery vehicle would result in improved lysis by overcoming some their limitations, including short plasma half-life, rapid inactivation and clearance by PAI-1, circulating antibodies, and α2-antiplasmin. The new vehicle can be designed to maintain drug concentrations and prolong drug retention in the circulatory system in order to further lyse the residual thrombus.

Recently, tPA-loaded liposomes have been developed and their surfaces have been decorated with a homing peptide that can guide the vehicle to accumulate on the thrombus and produce localized action (19). The liposomes demonstrated an affinity to bind with activated platelets and exhibited an initial burst release (40-50% in 30 min) followed by a continuous release of tPA (80-90% in 24 h) *in vitro*. The authors assume that 40-50% of tPA released during the burst phase would dissolve the existing clot, whereas continuous release thereafter would help prevent reocclusion. The results suggested that both reperfusion and prevention of reocclusion could be achieved by a single bolus dose with minimal systemic bleeding incidence.

In this study, we have developed formulations that would not only restore blood flow rapidly but would also act to prevent formation of another occlusion. We combine PEG microspheres which provide the release of the encapsulated SK on the scale of minutes for the clot digestion, with delayed release microspheres designed to prevent a putative second thrombus. The development of encapsulated thrombolytic formulations has been investigated and is described in the forthcoming chapters.

Chapter 3 - Biphasic Release of Protein from Polyethylene Glycol (PEG) and PEG/Modified Dextran Microspheres[1]

3.1. Introduction

Ischemia caused by the presence of an occlusive thrombus in a coronary or cerebral artery leads to the immediate result of a heart attack or stroke, possibly causing death. Administration of a "clot-busting" drug or plasminogen activator (PA) can break up the clot and restore flow with proven efficacy in saving lives and reducing morbidity if applied in a timely manner (82, 83). However, reocclusion of coronary arteries after thrombolytic therapy occurs in 7-32% of patients (7) and increases the level of mortality (8). As mentioned in Chapter 2, the mechanism of reocclusion is obscure but it may be due to multiple factors including thrombi traveling downstream, the release of various chemicals that cause restenosis due to spasm of the blood vessel or the exposure of active surface that initiates platelet response (9). In clinical practice, reocclusion is addressed by administration of antithrombotic treatment following thrombolysis (78, 84). But early reocclusion still occurs despite the use of such agents leading to the necessity for more potent and specific pharmaceutical procedures.

---

[1] This chapter has been published previously in *Journal of Biomedical Materials Research Part A* 2013, 101A: 2699-2705. This current version has been reformatted for this dissertation.

Encapsulation of antithrombotic agents in liposomes (85) and microcapsules has been used widely to modify their performance. Wang et al. (17) and Vaidya et al. (86) targeted nanoparticles and liposomes, respectively, with RGD (Arg-Gly-Asp) peptides on the surface of the delivery vehicles while others have investigated magnetic carriers to localize thrombolysis (87, 88). Similarly, ultrasound has been employed in combination with encapsulation with the objective of facilitating release at a specific site (89-91). Even in the absence of a targeting mechanism, significant acceleration of thrombolysis for faster reperfusion has been shown with encapsulation of streptokinase (SK) in polyethylene glycol (PEG) microspheres. PEG microspheres provide the release of the encapsulated PA on the scale of minutes, which dissolves blood clots more quickly by enabling PA administered intravenously to be delivered more effectively (9). While slow flow of free SK through a fresh thrombus coupled with the high surface area of fibrin strands results in thrombolysis only at the leading edge, encapsulation blocks the binding and enables penetration into the interior of the clot with faster digestion (65). Using an animal model of myocardial infarction, Leach also reported a reduction in reocclusion episodes with SK in rapid release microcapsules (23). Coupling the extended circulatory lifetimes of tPA in PEGylated liposomes (61) with the fact that reocclusion varies inversely with plasma half-life (12) provides further indication of the potential of encapsulation to address a second occlusive event. Therefore, a time release frame of minutes is necessary to address an acute thrombotic crisis, while the release of a PA over several hours is desirable to address reocclusion.

Polymers that have been widely used for controlled release of proteins and drugs over a period of days and months such as poly(D,L-lactic-*co*-glycolic acid) (PLGA)

(92) and poly(ε-caprolactone) (93) are not well-suited for addressing a secondary thrombus if one should form. Instead, a polymer that allows the release of active agent within hours is required. Dextran is a polysaccharide consisting mainly of linear 1,6-glucosidic linkage with some degree of branching via 1,3-glucosidic linkage (94). It has great promise for drug delivery and has been used clinically as a plasma volume expander, peripheral flow promoter, and antithrombotic agent (95). Due to a large number of hydroxyl groups, derivatives of the compound have been investigated as potential macromolecular carriers for the delivery of drugs and proteins (94-96) while a recent review highlights the potential of degradable dextran micro- and nano-particles for gene delivery (97). Dextran, however, cannot be used directly for drug delivery itself due to its solubility in water. Therefore, mostly hydrophobically modified forms have been employed with solubility properties orthogonal to those of dextran (98-101). But depending on the extent of degree of substitution, i.e. the number of substituted groups in an anhydroglucose unit (AGU) (102), either water-soluble or water-insoluble dextran derivatives can be synthesized (99, 100). With the degree of substitution higher than 1.75, dextran acetate (DA) is soluble in organic solvents and insoluble in distilled water (103). Water-insoluble DA is not suitable for delivery of PA because its degradation is on the scale of days (104). As such, we have fabricated formulations that combine moderately water-soluble DA with PEG to create extended release microspheres by a modified double emulsion method.

In this study, DAs were synthesized by the reaction of dextran with acetic anhydride, and then utilized to prepare PEG/DA microspheres by a modified double emulsion method. Bovine serum albumin (BSA) functioned as a model protein in order

31

to determine whether or not PEG/DA microspheres of various compositions were effective in providing release over a period of hours. Microsphere characteristics such as particle size, morphology, encapsulation efficiency, and time dependent *in vitro* drug release were investigated, and the release profile of PEG/DA microspheres compared with that of PEG microspheres. Lastly, as an illustration, we have predicted the mass of encapsulated BSA delivered at 3 hours for various mixtures of PEG and PEG/DA microspheres constrained to provide sufficient release at 30 minutes as would be needed for rapid perfusion.

3.2. Materials and Methods

3.2.1. Materials

Dextran from *Leuconostoc spp.* (average molecular weight: 70 kDa), acetic anhydride, poly(vinyl alcohol) (PVA, 87-90% hydrolyzed, average molecular weight: 30-70 kDa), BSA, chloroform (HPLC grade), lithium chloride, dimethyl formamide (DMF, anhydrous 98%), triethylamine, and methylene chloride were purchased from Sigma-Aldrich (St. Louis, MO). PEG (molecular weight: 20 kDa) was obtained from Polysciences (Warrington, PA) and hexane (HPLC grade) from Fisher Scientific (Denver, CO).

3.2.2. Synthesis of DA

DA was synthesized by the reaction of dextran with acetic anhydride in a lithium chloride (LiCl/DMF 2% (w/v)) aprotic solvent system (105). 1 g dextran (hydroxyl group 0.0185 mol) was dissolved in 20 mL of LiCl/DMF at 90°C under nitrogen gas. After complete dissolution, the mixture was cooled down to 60°C and

triethylamine (20 mol% to acetic anhydride) was added to the reaction vessel. The solution was stirred for 15 min at 60°C, and then acetic anhydride was introduced at a very slow rate. In separate runs, the amount of acetic anhydride was 0.75, 1.0, and 1.5 times the molarity of the hydroxyl group in the AGU of dextran and designated as DA1, DA2, and DA3, respectively. The reaction continued at 60°C for 10 h under nitrogen gas. Product isolation followed from precipitation in cold isopropyl alcohol, filtration and washing several times with isopropyl alcohol, before drying in a vacuum oven at room temperature.

The degree of substitution was determined by a titration method (103, 106): 100 mg of DA was dissolved in 10 mL of distilled water, and 20 mL of sodium hydroxide 0.1N added. Phenolphthalein served as indicator. Excess base was titrated with hydrochloric acid 0.1N until a color change from pink to colorless occurred. A blank test was also carried out with dextran using the same procedure.

The weight percent of the acetate group (A%) in the product and the degree of substitution were calculated using equations (1) and (2), respectively:

$$A\,(\%) = \frac{(V_1 - V_2) \times N_{HCl} \times MW_A \times 100}{m} \tag{1}$$

$$DS = \frac{MW_{AGU} \times A}{MW_A \times 100 - \Delta AGU \times A} \tag{2}$$

Equation (2) was derived from equation (3):

$$A\,(\%) = \frac{MW_A \times DS \times 100}{MW_{AGU} + \Delta AGU \times DS} \tag{3}$$

where

V_1, V_2: the volumes (mL) of HCl 0.1N used in titration for the blank and sample, respectively

DS: degree of substitution

N_{HCl}: normality of hydrochloric acid

MW_A: molecular weight of the acetate group (43 g/mol)

m: mass of DA (g)

MW_{AGU}: molecular weight of the AGU (162 g/mol)

ΔAGU: net increment in the AGU for every substituted acetate group (42 g/mol)

3.2.3. Fourier Transform Infrared (FT-IR) Spectroscopy

Infrared spectra were obtained by Nicolet 6700 FT-IR Spectrometer. Dried samples were ground with KBr powder, and pressed into pellets for FT-IR examination.

3.2.4. Preparation of PEG/DAs Microspheres

PEG/DAs microspheres were prepared by a modified double emulsion method (9). BSA (50 mg) and DA (0.3 g) were dissolved in 0.5 mL distilled water at room temperature. PEG (1 g) was dissolved separately in 1.5 mL chloroform. The two solutions were mixed and sonicated at 45 W for 1 min with a Sonic Dismembrator 60 (Fisher Scientific). The protein/polymer mixture was mixed with 4 mL of PVA 2% (w/v). The mixture was vortexed for 40 s and frozen at -80°C for 1 h, and then lyophilized for 15 h. The lyophilized product was washed with hexane three times by centrifugation at 1000 × g for 5 min each at 4°C, and then was filtered under vacuum through 0.45 μm pore size membranes to remove any externally bound protein. Then, the washed particles were resuspended in hexane and were filtered under vacuum through 10 μm pore size membranes to remove the large particles. The particles were

isolated by centrifugation several times and finally dried in a fume hood for 1 h. Blank microspheres lacking entrapped BSA were prepared by replacing the BSA solution with an identical volume of distilled water.

Plain PEG microspheres were prepared by a modified double emulsion method without DA in inner water phase (65).

3.2.5. Particle Size

Particle diameter was determined using a laser diffraction particle size analyzer (Beckman Coulter LS230). The LS series uses light with a wavelength of 750 nm to measure sizes of particles ranging from 0.4 to 2000 μm. Microspheres (300 mg) were suspended in 3 mL of methylene chloride. Then, the microsphere suspension was loaded in the sample well, which had 700 mL of methylene chloride circulating throughout the system. Particle size measurements are based on diffraction patterns formed by the scattering of light by microparticles. Particle sizes were obtained and analyzed using the accompanying software (107).

3.2.6. Morphology of the Microspheres

The surface morphology of the microspheres was examined using a scanning electron microscope (SEM) (Jeol JSM-880). A small amount of freeze-dried microspheres was loaded on an aluminum stub with double-sided adhesive tape. Samples were sputter coated with gold and examined by SEM at 15 kV.

To assess the mechanism of protein release from microspheres, the morphological change of PEG/DA3 microspheres in phosphate-buffered saline (PBS) pH 7.4 was monitored via SEM. Microspheres (100 mg) were dispersed in 10 mL PBS

pH 7.4 at 37°C. After 30 min, samples were collected by centrifuge at $1000 \times g$ for 5 min, and then lyophilized for 15-20 h.

3.2.7. Drug Encapsulation Efficiency

100 mg microspheres were allowed to dissolve completely in 10 mL distilled water for approximately 5 h. Protein concentration was determined by the bicinchoninic acid protein assay (Pierce Chemical, Rockford, IL).

Encapsulation efficiency, EE (%), was calculated using the following equation:

$$EE\ (\%) = \frac{\text{Actual BSA loading} \times 100}{\text{Total BSA}} \tag{4}$$

3.2.8. In Vitro Release Study

Microspheres (150 mg) were dispersed in 10 mL PBS pH 7.4 in test tubes. The test tubes were placed in an orbital shaker at 37°C and agitated at 80 rpm. At specified time points, a small volume of solution (300 µL) was drawn for testing. Samples were collected using filters of 0.2 µm pore sizes and 25 mm diameter over 360 min. PBS solution (300 µL) was replenished to maintain a constant sink volume. The bicinchoninic acid method yielded the amount of the released protein. Similar tests were performed to analyze the dissolution of blank microspheres, and the corresponding absorbance of each blank sample as a function of time was subtracted from the absorbance of each sample. Samples were analyzed with Shimadzu UV-2450 spectrophotometer at a wavelength of 562 nm (107).

3.2.9. Statistical Analysis

Unless otherwise stated, all data are presented as mean ± standard error of the mean. The Student's t-test was used to determine significance between two groups. P-values less than 0.05 were considered significant.

3.3. Results and Discussion

3.3.1. Synthesis and Characterization of DA

In the present study, dextran was modified by acetylating a fraction of the hydroxyl groups of dextran to produce a hydrophobically modified dextran, DA (Figure 3.1). Esterification of hydroxyl groups in dextran proceeded by reaction with varying amounts of acetic anhydride. The degree of substitution of DA in different preparations appears in Table 3.1. The weight percent of the acetyl group (A%) and the degree of substitution increased with increasing molar ratio of acetic anhydride to hydroxyl groups of dextran. Dextran is (1 → 6) linked α-D-glucopyranosyl residues and carries three hydroxyl groups per AGU (105). As shown in Table 3.1, the degrees of substitution of DAs were 0.60 − 0.96, indicating that only 0.60 − 0.96 of available hydroxyl groups of AGU were modified. Increasing degree of substitution of DA means increasing the introduction of acetyl groups into the backbone of dextran, resulting in increasing the hydrophobicity of dextran. Because of low degree of substitution, DA1, DA2 and DA3 were soluble in distilled water and insoluble in organic solvents such as chloroform and methylene chloride. The solubility of DAs in water is DA1>DA2>DA3. DAs with higher degree of substitution, which also were prepared, exhibited orthogonal properties, insoluble in water, and not suited for encapsulation in this study.

Table 3.1. Results of Acetylation of Dextran with Acetic Anhydride (AA) ($n = 5$)

Sample	Molar Ratio[a]	Yield (%)	Acetyl Group (A%)	Degree of Substitution
DA1	1:0.75	82	13.8	0.60
DA2	1:1	80	17.2	0.78
DA3	1:1.5	83	20.4	0.96

[a] AGU: AA
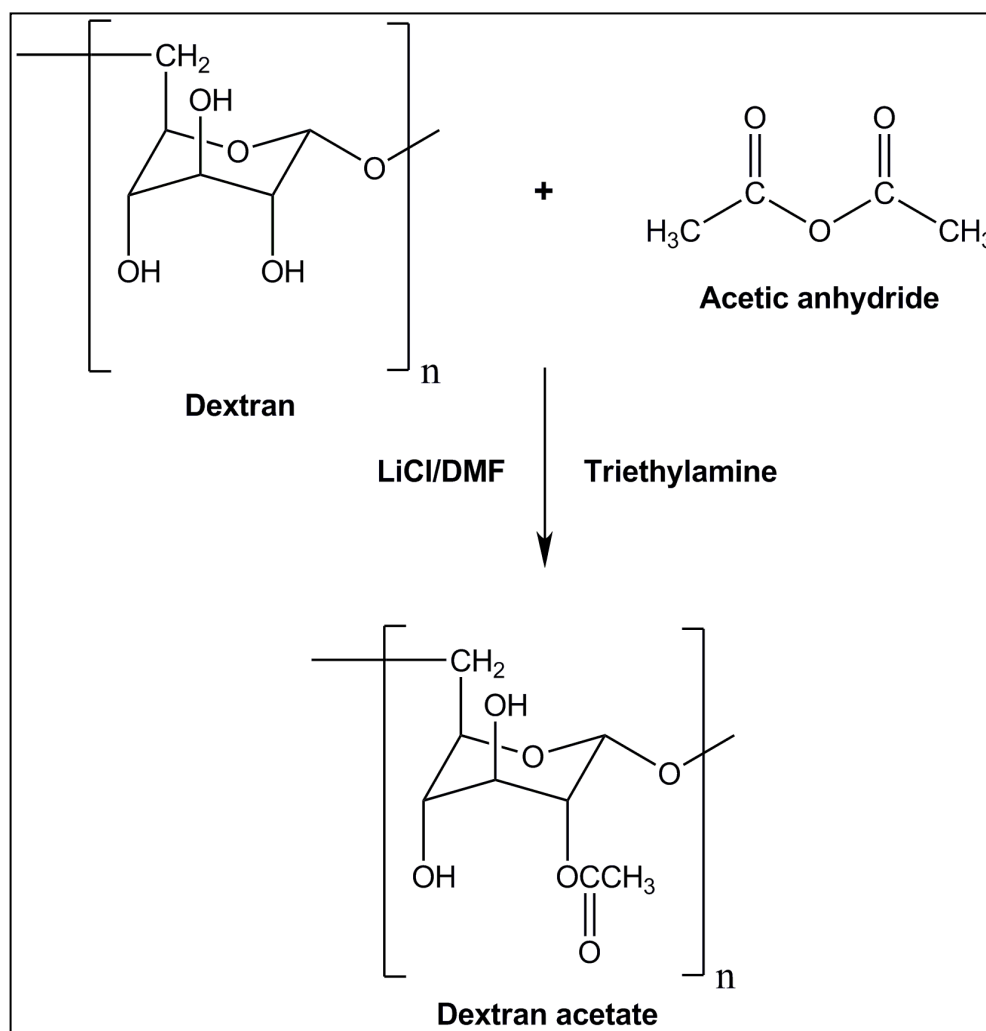
Figure 3.1. Synthesis of DA.

The FT-IR spectra of DA (Figure 3.2) confirmed introduction of the acetyl group, as indicated by C=O stretching of ester at 1735 cm^{-1}, and the C-O-C stretching of esters at 1250 cm^{-1}. The original dextran did not show such a carbonyl peak. A broad peak about 3500 cm^{-1} was related to the OH absorption of the unreacted hydroxyl groups of dextran, which is indicative of incomplete modification of the hydroxyl group.
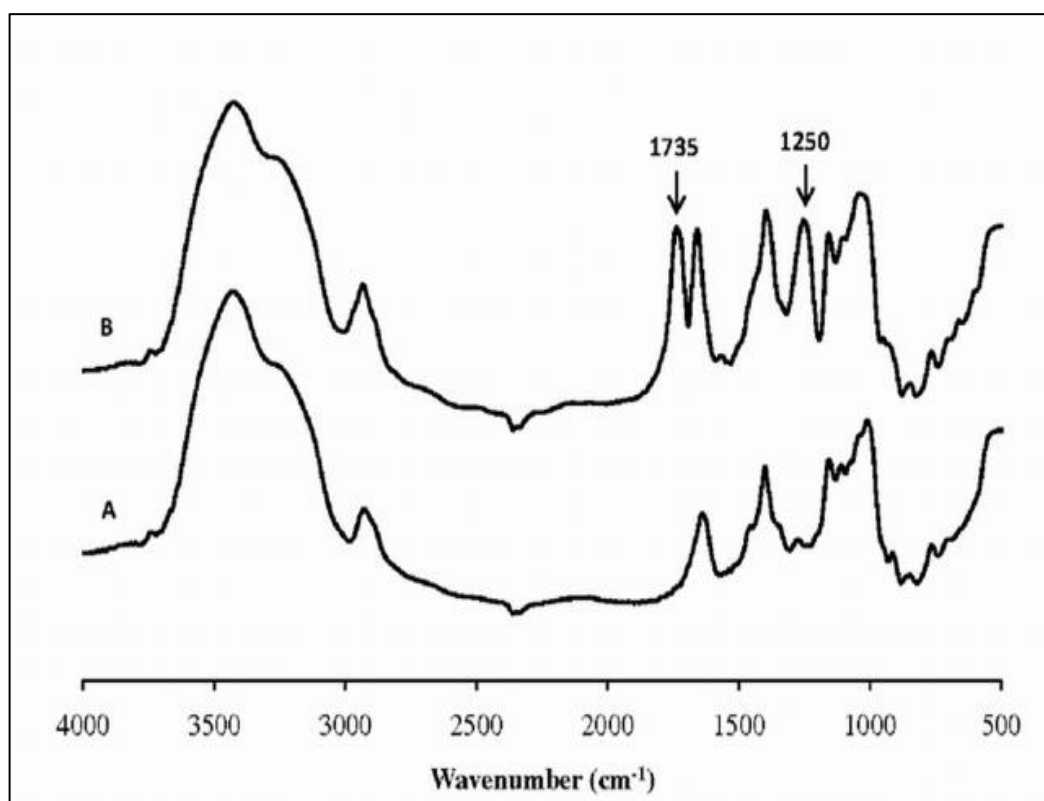
Figure 3.2. FT-IR Spectra of Dextran and DA: (A) Dextran and (B) DA.

3.3.2. Preparation and Characterization of PEG/DAs Microspheres

PEG was used as the major encapsulation vehicle due to its excellent solubility in aqueous and organic solvents, biocompatibility, and ability to inhibit adhesion to protein. The DAs obtained were insoluble in organic solvents but with the help of PEG, PEG/DA could serve as drug carrier. With the double emulsion method, protein and DA were dissolved in distilled water, while PEG was dissolved in chloroform. When the two solutions were mixed with the help of an emulsifier (PVA 2% w/v), the hydrophilic and hydrophobic components partitioned themselves so that the polymers entrapped protein.

The results of SEM demonstrated that the shape of PEG/DAs microspheres was spherical (Figure 3.3) with a particle size less than 1 μm. The particle size by SEM was confirmed with that found by a light scattering analyzer. As shown in Table 3.2, the particle sizes of PEG/DAs microspheres were 0.74 – 0.85 μm in diameter, increasing as the degree of substitution of DA increased. An increase in the degree of substitution results in an increase in the molecular weight of the dextran derivatives (108). Increasing the molecular weight of DAs enhanced the viscosity of the aqueous phase, which reduces the efficiency of mixing and formation of larger emulsion droplets. Thus, the higher DA resulted in larger particles. In Figure 3.3A, the background of the image might be a large particle which was not removed by filter during isolation process.

Table 3.2. Characterization of PEG Microspheres and PEG/DAs Microspheres[a] (mean ± standard error of the mean, $n = 6$)

Microsphere Samples	Degree of Substitution	Particle Size (μm)	EE (%)	$t_{90\%}$ (min)[b]
PEG	_	0.759 ± 0.018	53.2 ± 1.5	21
PEG/DA1	0.60	0.743 ± 0.009	56.3 ± 1.2	31
PEG/DA2	0.78	0.817 ± 0.005*	61.7 ± 2.0*	69
PEG/DA3	0.96	0.851 ± 0.011*†§	70.5 ± 3.4*†§	118

[a] PEG/DA microspheres prepared with 1 g PEG and 0.3 g modified dextran
[b] time to release 90% of the encapsulated BSA
* = $p < 0.05$ vs PEG/DA1; † $p < 0.05$ vs PEG/DA2; § $p < 0.05$ vs PEG
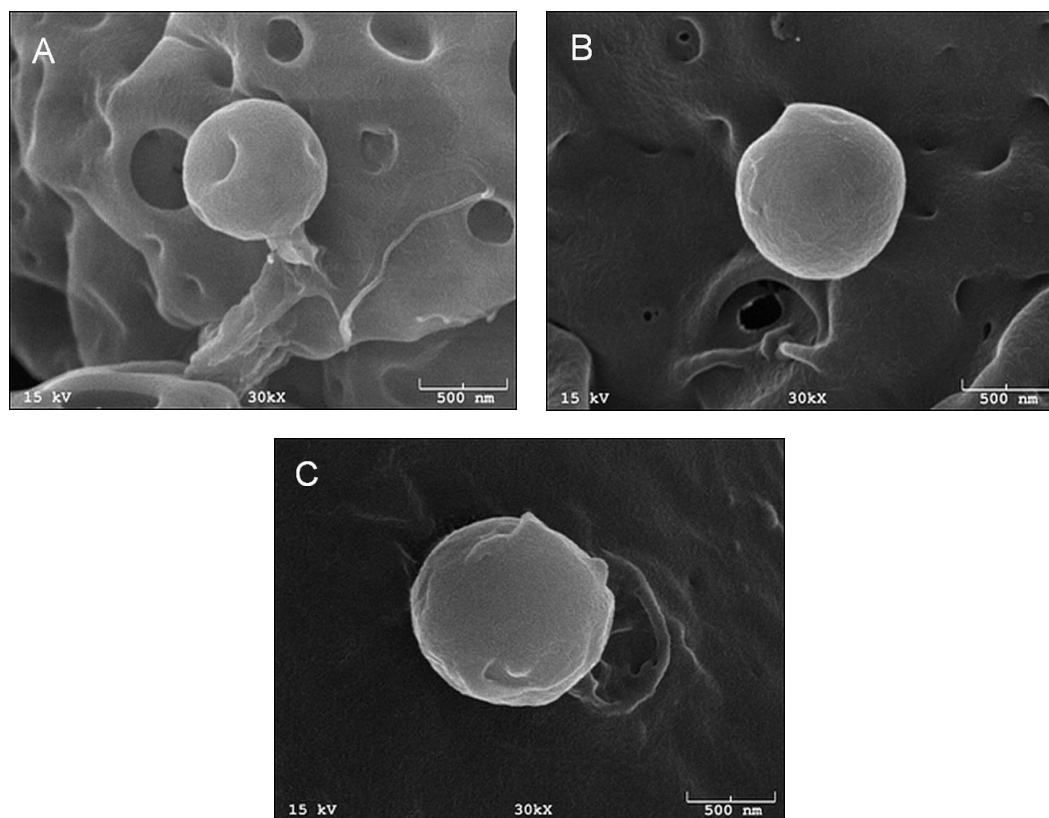
Figure 3.3. SEM Images of PEG/DAs Microspheres: (A) PEG/DA1, (B) PEG/DA2, and (C) PEG/DA3 Microspheres

The EE (%) of PEG/DAs microspheres was found to depend on the degree of substitution (Table 3.2). The encapsulation efficiency increased from $56.3 \pm 1.2\%$ to $70.5 \pm 3.4\%$ with the degree of substitution of DA increasing from 0.60 to 0.96. Higher degree of substitution was associated with improvements in the encapsulation efficiency due to enhanced interactions. These interactions include hydrogen bonding between amine and carboxylic groups in BSA, and hydroxyl groups in DA as well as hydrophobic interactions between hydrophobic amino acids of BSA (109) and the acetyl group in DA during emulsification (104). The encapsulation efficiency of PEG microspheres was lower than that of PEG/DAs microspheres due to the lack of hydrophobic bonding.

3.3.3. In Vitro Release Study

To study the protein release behavior, PEG/DAs microspheres were suspended in PBS pH 7.4 and the free protein level *in vitro* determined as a function of time. The release of BSA from PEG/DAs microspheres was comprised of a reduced initial "burst phase" followed by a slower "sustained release phase" (Figure 3.4). PEG/DA1 microspheres exhibited the fastest release of BSA while PEG/DA3 microspheres showed the slowest release of BSA up to 180 min.
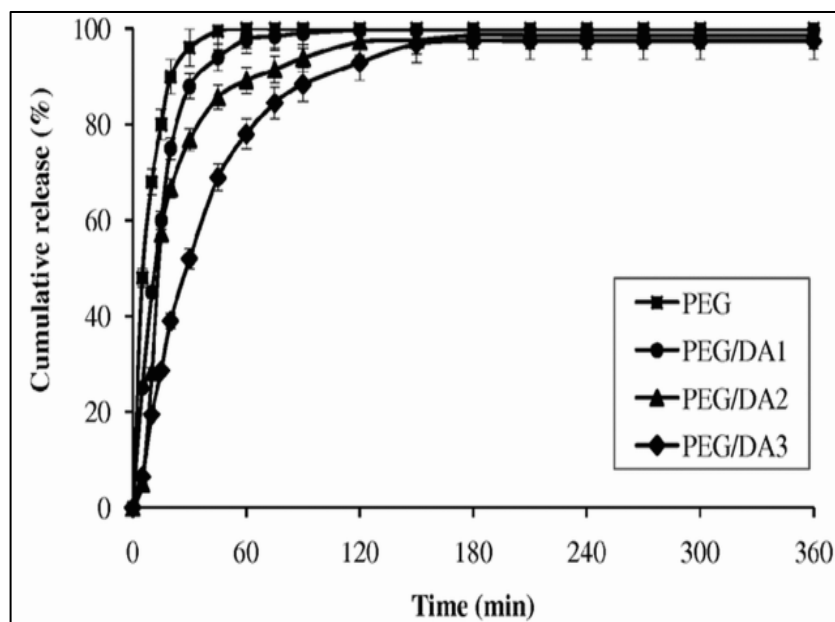
Figure 3.4. *In Vitro* Release Study of BSA from PEG and PEG/DAs Microspheres (mean ± standard error of the mean, $n = 5$).

$t_{90\%}$, defined as the time to release 90% of the encapsulated BSA, was found from release profiles for different PEG/DAs microspheres. The longer $t_{90\%}$, the larger reduction of the burst effect. As shown in Table 3.2, $t_{90\%}$ increased from 31 to 118 min as the degree of substitution of DA rose from 0.60 to 0.96. In contrast, $t_{90\%}$ of plain PEG microspheres was 21 min. Not surprisingly, the release of BSA from PEG microspheres was very fast due to the high solubility of PEG in water. These results indicated that greater hydrophobicity of DA leads to slower release of BSA from microspheres as expected. The release rate of BSA depended on the degree of substitution because the enhanced interactions between BSA and DAs contribute to prevent fragmentation of the microspheres, resulting in a reduction of the initial burst. Moreover, higher degrees of substitution led to fewer favorable interactions with solvent as well as larger particles which dissolve more slowly than smaller particles. With a $t_{90\%}$ of 118 min, PEG/DA3

43

microspheres provided the release of BSA on the scale of hours (180 min). This is a promising observation for the prevention of reocclusion of an artery because complementary action to rapid reperfusion with delayed release of a PA appears viable.

The morphological change of PEG/DA3 microspheres in PBS pH 7.4 solution was investigated via SEM. After 30 min, swelling and loss of spherical shape of microspheres were observed (Figure 3.5). Properties of the constituent polymers help to explain the mechanism of release and the distorted shape. On contact with water, PEG and dextran absorb water and swell due to their hydrophylicity (110-112), leading to release of protein and an increase in size of the microspheres by an order of magnitude. Distortion can be attributed to microphase separation of the polymers and stresses resulting from a difference in swelling ratio of PEG and DA. Swelling ratio is generally important when discussing crosslinked hydrogels which have been made of PEG and dextran. But this does not apply for this system since there are no crosslinks. In the absence of crosslinks to maintain a monolithic structure, no final expansion point exists to determine a specific swelling ratio. With size of 5-10 μm, it can be expected that microparticles may be removed by the reticuloendothelial system (RES) and some may block capillaries until they dissolve.
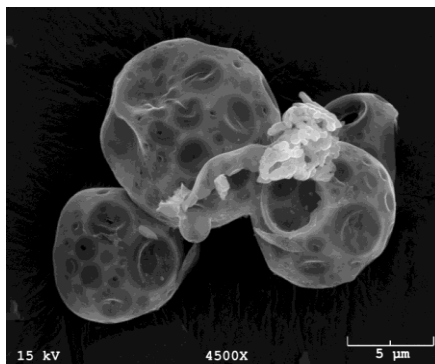
Figure 3.5. SEM Image of PEG/DA3 Microspheres after 30 min in PBS pH 7.4 Solution at 37°C.

3.3.4. Calculation of the Amount of BSA Released In Vitro from Mixtures of PEG and PEG/DA3 Microspheres

If a mixture of PEG and PEG/DA3 microspheres is used to encapsulate a PA for thrombolysis, we hypothesize that the amount of encapsulated PA released from the mixture at 30 min is sufficient for rapid perfusion while the amount released afterward up to 180 min might address reocclusion. The concept of using a mixture of microspheres allows for design to achieve the dual functionality. This can be demonstrated computationally for the release of BSA.

For this purpose, BSA was used as a model protein for predicting the amount of an active agent released *in vitro* from the mixtures of PEG and PEG/DA microspheres. Mathematical fits were obtained for release rates from PEG and PEG/DA3 microspheres (Figure 3.6) to predict amount delivered *in vitro* over a period of hours when constrained to a target level at 30 min. Results for BSA mass released *in vitro* at different times for various mixtures of PEG and PEG/DA3 microspheres are presented in Table 3.3.
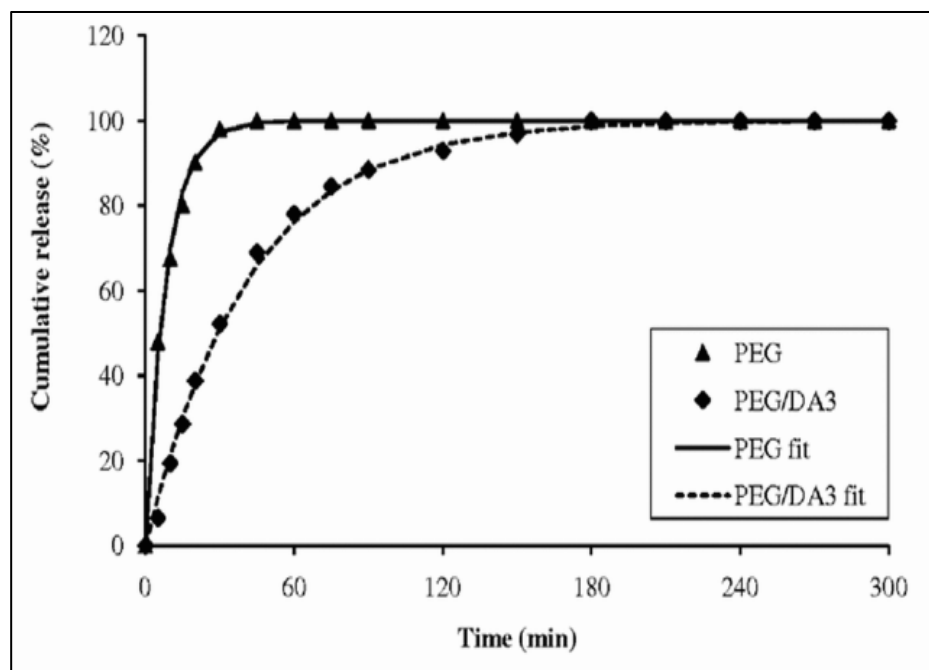
Figure 3.6. Release Data for PEG and PEG/DA3 Microspheres with Linearized Regression Fit [$Y_{PEG} = 100(1 - e^{-0.12t})$; $Y_{PEG/DA3} = 100(1 - e^{-0.024t})$].

Table 3.3. Prediction of BSA Released *In Vitro* from Mixtures of PEG and PEG/DA3 Microspheres Subject to a Target Level for 30 min

Mixture	BSA Encapsulated in PEG Microspheres (mg)	BSA Encapsulated in PEG/DA3 Microspheres (mg)	Released BSA Mass (mg)	
			30 min	**180 min**
1	10	40	30.26	49.47
2	15	30	29.99	44.60
3	20	20	29.72	39.73
4	25	10	29.45	34.87

In clinical practice, it should be appreciated that the dynamics of the fibrinolytic system are very complex with many species involved (113). The initial delivery of a PA rapidly depletes the circulatory concentration of plasminogen. Sustained release allows time for recovery of plasminogen concentration, but also inhibitors, e.g. PAI-1, circulating antibodies and α_2-antiplasmin. Events at the residual thrombus where lysis and clot formation compete are most important. On the basis of half-life data, this approach can be expected to favor the former.

3.4. Conclusions

In this study, DAs with various degrees of substitution were successfully synthesized by the reaction of dextran with acetic anhydride in LiCl/DMF 2% (w/v) system in an effort to prepare the slow-acting microspheres via the modified double emulsion method. Particle size, EE (%), and release rate of PEG/DAs microspheres depended on the degree of substitution of DA. Increasing the degree of substitution of DA resulted in increases of particle size and EE (%), and a slower release rate of protein from PEG/DAs microspheres. PEG/DA3 microspheres exhibited the release of BSA on the scale of hours (180 min), more slowly than that of PEG microspheres. The amount of BSA released from mixtures of PEG and PEG/DA3 microspheres was calculated mathematically to predict delivery *in vitro* over a period of hours when constrained at 30 min. Therefore, the mixtures of PEG and PEG/DA3 microspheres can be considered as a promising means to prevent reocclusion after thrombolysis, in addition to addressing the initial thrombotic crisis.

Chapter 4 - A Mixture of Polyethylene Glycol and Chitosan-Eudragit Microspheres for a Rapid Reperfusion and Prevention of Reocclusion after Thrombolytic Therapy: An *In Vitro* Thrombolysis Study[2]

4.1. Introduction

Cardiovascular disease is considered to be the primary cause of death in the United States. More than 83 million Americans have been diagnosed with one or more types of cardiovascular disease (1), including coronary heart disease, stroke, deep vein thrombosis, and pulmonary embolism (27). Formation of an occlusive blood clot inside a blood vessel is a leading cause of common cardiovascular disease. Thrombolytic therapy is an available means to dissolve the occlusive thrombus and achieve patency besides other methods such as angioplasty and stent placement. This method includes administration of a plasminogen activator (PA) [e.g. tissue-type plasminogen activator (tPA), streptokinase (SK), urokinase] to break up the clot and restore flow (4). The major goal of thrombolytic therapy for myocardial infarction is to minimize the time during which the coronary artery remains occluded by rapidly achieving reperfusion and salvaging tissue. However, after achievement of reperfusion, a putative second thrombus may occur at the site leading to formation of another blockage (114).

---

[2] This work has been submitted to *International Journal of Pharmaceutics.*

Reocclusion of coronary arteries after thrombolytic therapy occurs in 7–32% of patients (7) and increases the level of mortality (8).

Encapsulation shows great promise in improving the performance of PAs. PA-containing liposomes and nano- or microspheres accelerate thrombolysis by providing a rapid release of PAs near or even within blood clot regions (17, 65, 86), so that blood clots dissolve more quickly (9, 18, 115, 116). Drug carriers with PAs have been targeted to thrombi by attaching ligands, e.g. RGD (Arg-Gly-Asp) peptides or gamma-chain peptide sequence of fibrinogen, to the surface of liposomes and nanoparticles (17, 19, 86) or by using magnetic nanoparticles to localize thrombolysis (20, 21). Similarly, ultrasound has been used in combination with encapsulation to facilitate release at the clot site (90, 91, 117). In a novel approach, Korin et al. (70) have proposed shear activation of PA-containing nanoparticles as a targeting strategy which might show promise in addressing the channeling phenomenon that can occur with thrombolysis. Results with drug delivery systems like these indicate their great potential for fibrinolytic therapy including a recent report that liposomal encapsulated tPA attenuates bleeding complications (19)

However, the above strategies only focus on improvement in the delivery of the PAs to the site of thrombus for a rapid reperfusion and a decrease of bleeding complications, not on prevention of reocclusion after thrombolysis. Encapsulation enhances the efficacy of PAs in part by protection of these agents from the premature inactivation by antibodies or PAI-1 in the circulation, yielding increased half-lives and thus showing some promise in addressing reocclusion (9, 16, 66, 118). A link between half-life and reocclusion has long been known (12, 61) and experiment confirms the

expectation with encapsulation. Specifically, Leach et al. (23) observed fewer reocclusion episodes with SK in polyethylene glycol (PEG) microspheres in an animal model of myocardial infarction.

The purpose of this study is to examine formulations that would not only restore blood flow rapidly, but also would act to prevent formation of another blockage and further loss of tissue. We have developed microspheres which exhibit the release of active agent on the scale of hours. These microspheres can be used with PEG microspheres, which dissolve in minutes, to provide complementary action with delayed release to prevent a putative second thrombus. We used polymethacrylate polymer (Eudragit FS30D) for development and testing of delayed release microspheres. Eudragit FS30D (termed Eud hereafter) is the trade name of a copolymer of methyl acrylate, methyl methacrylate and methacrylic acid which is soluble at pH above 7.0, and is commonly used in pharmaceutical industry for drug controlled-release (119). In addition, Eud microspheres were modified with chitosan (CS), as CS has been shown to be a biodegradable, biocompatible and non-toxic natural polymer (120), widely applied in drug delivery systems (121, 122) and for tissue engineering constructs (123). Experiments included the preparation and characterization of Eud/SK and CS-Eud/SK microspheres, and an *in vitro* thrombolytic study for testing the protracted clot-lytic efficacy of mixtures of PEG/SK and Eud/SK microspheres and mixtures of PEG/SK and CS-Eud/SK microspheres.

4.2. Materials and Methods

4.2.1. Materials

CS (medium molecular weight: 190-310 kDa) with 75-85% deacetylation, poly(vinyl alcohol) (PVA, 87-90% hydrolyzed, average molecular weight: 30-70 kDa), BSA, methylene chloride, 1-ethyl-3-(3-dimethylaminopropyl)-carbodiimide (EDC), N-hydroxysuccinimide (NHS), 2-(N-morpholino)ethanesulfonic acid (MES), SK (10,000 IU) were purchased from Sigma-Aldrich (St. Louis, MO). PEG (molecular weight: 20 kDa) was obtained from Polysciences (Warrington, PA). Eud FS30D [poly(methyl acrylate-*co*-methyl methacrylate-*co*-methacrylic acid) = 7:3:1] (average molecular weight: 220 kDa) was a gift from Evonik Röhm GmbH (Darmstadt, Germany). Eud was supplied in a form of an aqueous dispersion with 30 % dry substance. The product was purified by dialysis of the solution against distilled water for 2 days using a regenerated cellulose membrane with a MWCO of 3500 g/mol (Fisherbrand, Fisher Scientific). Then, the sample was lyophilized for 24 h to obtain a white powder.

4.2.2. Preparation of Eud/SK Microspheres

Eud/SK microspheres were prepared by a double emulsion method (124). Briefly, SK (250,000 IU) was dissolved in 0.5 mL distilled water at room temperature. Eud (0.5 g) was dissolved separately in 5 mL methylene chloride and added to SK solution. This mixture was sonicated at 60 W for 45 s using a Sonic Dismembrator 60 (Fisher Scientific). The primary emulsion was mixed with 10 mL of PVA 3% (w/v), vortexed for 30 s, and sonicated at 60 W for 30 s to produce W/O/W emulsion. Then, 100 mL of PVA 0.3% (w/v) was added to the emulsion. The suspension was mechanically stirred at 1200 rpm for 6 h at room temperature to remove the organic

solvent. The microspheres were isolated by centrifugation (1000 × g for 10 min) and washed with distilled water by vortexing for 30 s and then centrifuging several times to remove the residual PVA and solvent. The washed microspheres were suspended in distilled water (2 mL) and lyophilized for 20 h.

4.2.3. Preparation of CS-Eud/SK Microspheres

0.3 g Eud/SK microspheres was dispersed in 10 mL MES (pH 5.5) containing EDC (0.3 g) and NHS (0.2 g) (the molar ration of EDC to NHS = 1:1.1) for 60 min. Then, 20 mL of 1.5% (w/v) CS solution in 1% acetic acid was added to this suspension (mass ratio of Eud to CS =1:1) and the mixture stirred for 24 h at room temperature. Microspheres were collected by centrifugation (1000 × g for 10 min) and washed several times with distilled water by vortexing for 30 s and then centrifuging. Washed microspheres were suspended in distilled water (2 mL) and lyophilized for 20 h (125).

4.2.4. Particle Size

Particle diameter was determined using a laser diffraction particle size analyzer (Beckman Coulter LS230). Particle size measurements are based on diffraction patterns formed by the scattering of light by microparticles. Particle sizes were obtained and analyzed using the accompanying software of the instrument.

4.2.5. Drug Encapsulation Efficiency

Encapsulation efficiency (EE) of Eud/SK and CS-Eud/SK microspheres was determined with commercial assay both by the protein content present in the microspheres as well as the activity of the protein. Activity of SK is normally expressed

by international unit (IU) in which one IU was defined as the amount of enzyme activity that converts 1 μmol of substrate per minute per liter (126).

The content of entrapped SK in the microspheres was determined using the bicinchoninic acid protein assay (Pierce Chemical, Rockford, IL) after dissolving the microspheres (10 mg in 2 mL PBS pH 7.4) completely for 24 h. The concentration of the dissolved SK was determined spectrophotometrically at 562 nm (Shimadzu UV-2450). Samples were compared to that of a standard curve of SK with blank microspheres (9, 65).

The activity of encapsulated SK was determined using a chromogenic assay (Sekisui Diagnostics, Stamford, CT) (65, 126) after dissolving the microspheres (5 mg in 1 mL PBS pH 7.4) completely for 24 h. Samples were collected, incubated with fresh plasma at 37°C in a 96-well plate for 1 min, allowing the formation of the plasminogen-SK complex. The plasmin-lysis chromogenic substrate (S-2251) was added to the complex. The substrate was cleaved by the plasmin, releasing p-nitroaniline which was measured spectrophotometrically at 405 nm (Synergy HT plate reader, Bio-Tek). The photometric signal was linear with respect to activity of SK originally present in the samples compared to that of a standard curve of SK with blank microspheres.

EE (%) was calculated using the following equation:

$$EE(\%) = \frac{Actual\ SK\ loading\ (content\ or\ activity) \times 100}{Total\ SK\ (content\ or\ activity)} \tag{5}$$

4.2.6. Morphology of the Microspheres

The surface morphology of the microspheres was examined using a scanning electron microscope (SEM) (JEOLJSM-880). A small amount of freeze-dried microspheres was loaded on an aluminum stub with double-sided adhesive tape. Samples were sputter coated with gold and examined by SEM at 15 kV.

Particle morphology was also studied using a transmission electron microscope (TEM) (JEOL 2000-FX). A small amount of microspheres was placed on a 300 mesh copper grid coated with carbon film and stained by 2% (w/v) phosphotungstic acid. Then, after the samples were air-dried at room temperature, the morphology of the stained microspheres was imaged by TEM.

To assess the mechanism of SK release from CS-Eud/SK microspheres, the morphological change of CS-Eud/SK microspheres in PBS pH 7.4 was monitored via SEM. Microspheres (20 mg) were dispersed in 10 mL PBS pH 7.4 at 37°C. After 2 h and 6 h, samples were collected by centrifuge at $1000 \times g$ for 10 min and then lyophilized for 15−20 h.

4.2.7. Fourier Transform Infrared (FT-IR) Spectroscopy

Infrared spectra were obtained by Nicolet 6700 FT-IR Spectrometer. Dried samples (CS, blank Eud and CS-Eud microspheres) were ground with KBr powder, and pressed into pellets for FT-IR examination.

4.2.8. Preparation of PEG/SK Microspheres

PEG/SK microspheres were prepared by a modified double emulsion method in which 100,000 IU of SK was encapsulated in 1 g of PEG, as described earlier (9, 65).

The content and activity of encapsulated SK were determined using the above described bicinchoninic acid protein assay and chromogenic assay.

4.2.9. In Vitro Release Study:

Eud/SK or CS-Eud/SK microspheres (50 mg) were dispersed in 25 mL PBS pH 7.4 in test tubes, respectively. The test tubes were placed in an orbital shaker at 37°C and agitated at 80 rpm. At specified time points, a small volume of solution (1 mL) was drawn for testing. Samples were collected using filters of 0.2 μm pore sizes and 25 mm diameter over 12 h. PBS pH 7.4 solution was replenished to maintain a constant sink volume. The amount of SK release was determined using the above described bicinchoninic acid method.

To determine the SK release from mixtures of microspheres, a mixture of PEG/SK microspheres (50 mg) and Eud/SK microspheres (90 mg) or of PEG/SK microspheres (50 mg) and CS-Eud/SK microspheres (100 mg) were dispersed in 25 mL PBS pH 7.4 in test tubes, separately. The test tubes were placed in an orbital shaker at 37°C and agitated at 80 rpm. At specified time points, a small volume of solution (1 mL) was drawn for testing. PBS solution was replenished to maintain a constant sink volume. The amount of SK release was determined using the above described chromogenic assay.

The *in vitro* release profiles of SK were fitted to the zero-order model, first-order model, Higuchi square root model and Hixson–Crowell cube root model (127, 128). The model with the highest correlation coefficient between the experimentally obtained data and the fitted data was selected.

4.2.10. In Vitro Thrombolytic Study

4.2.10.1. Preparation of Plasma Blood Clot

A blood clot was formed in a 0.2 cm (ID) glass capillary tube (Fisher Scientific) as described previously (65, 129). Briefly, the capillary tubes were etched in a dilute solution of hydrofluoric acid and the interior surface coated with a thin layer of fibrin for enhancement of clot adherence. Blood samples were collected from healthy donors and anticoagulated with 0.13 M sodium citrate (1: 9 in volume). Platelet-rich plasma (PRP) and platelet-poor plasma (PPP) were obtained by centrifugation of blood collection tube in a centrifuge (Beckman AccuSpin) at $150 \times g$ for 10 min and $4600 \times g$ for 20 min, respectively. Then, a small volume of the mixture of 50 μL PRP, 50 μL PPP, 100 μL thrombin 2 NIH/mL and 16 μL of 0.25 M $CaCl_2$ was injected into a capillary tube and then left to form a 3-cm plasma clot for 1 h at 37°C.

4.2.10.2. In Vitro Lysis Study

Study formulations included: free SK, PEG/SK, Eud/SK and CS-Eud/SK microspheres. Encapsulated SK in PEG/SK microspheres was 2500 IU (approximately 50 mg of microspheres), in Eud/SK microspheres was 12500 IU (approximately 90 mg of microspheres), and in CS-Eud/SK microspheres was 12500 IU (approximately 100 mg of microspheres). Four fibrinolytic formulation mixtures were studied (Table 4.1):

I) Free SK (2500 IU) + Blank CS-Eud microspheres

II) PEG/SK (2500 IU) microspheres + Free SK (12500 IU)/Blank CS-Eud microspheres

III) PEG/SK (2500 IU) microspheres + Eud/SK (12500 IU) microspheres,

IV) PEG/SK (2500 IU) microspheres + CS-Eud/SK (12500 IU) microspheres.

56

Table 4.1. Fibrinolytic Formulation Mixtures

Formulation	Streptokinase (IU)			
	Free SK	**PEG/SK**	**Eud/SK**	**CS-Eud/SK**
I	2500	–	–	0
II	12500	2500	–	0
III	–	2500	12500	–
IV	–	2500	–	12500

The dose fractionation of SK activity between PEG/SK and Eud/SK microspheres or CS-Eud/SK microspheres was 1: 5. The lysis study consisted of a series of experiments with a lysis test immediately after addition of the microspheres to plasma and additional lysis tests after the microspheres were exposed to plasma for periods of 2 h, 4 h and 6 h.

To carry out a lysis test, an occluded capillary tube oriented vertically was connected by Tygon lab tubing to a horizontally mounted graduated glass pipette. The height of the tubing from the upper surface of the plasma clot to the glass pipette was 61 cm. Firstly, the glass pipette and tubing were filled with a solution of 5 mL PBS pH 7.4, 2 mL PPP (as a source of plasminogen), and the fibrinolytic formulation mixtures. Then, the glass pipette was connected to a PBS buffer reservoir to achieve a hydrostatic pressure of 45 mm Hg/3-cm clot. Pressure was kept constant throughout the experiment. The lysis time required to dissolve the clot was monitored. The mixture in the collection dish was retained for the next stage of the lysis experiment (Figure 4.1).

For a series of "reocclusion" lysis experiments at 2 h, 4 h and 6 h, the mixture in the collection dish was centrifuged at $1000 \times g$ for 10 min, rinsed with distilled water

and centrifuged again to collect the undissolved microspheres. The glass pipette was filled with the mixture of the obtained microspheres in 5 mL PBS at pH 7.4, and 2 mL PPP and connected to another occluded capillary tube representing a secondary thrombus. The clot lysis time was recorded and the mixture in the collection dish was collected for the next stage of the lysis experiment (Figure 4.2).
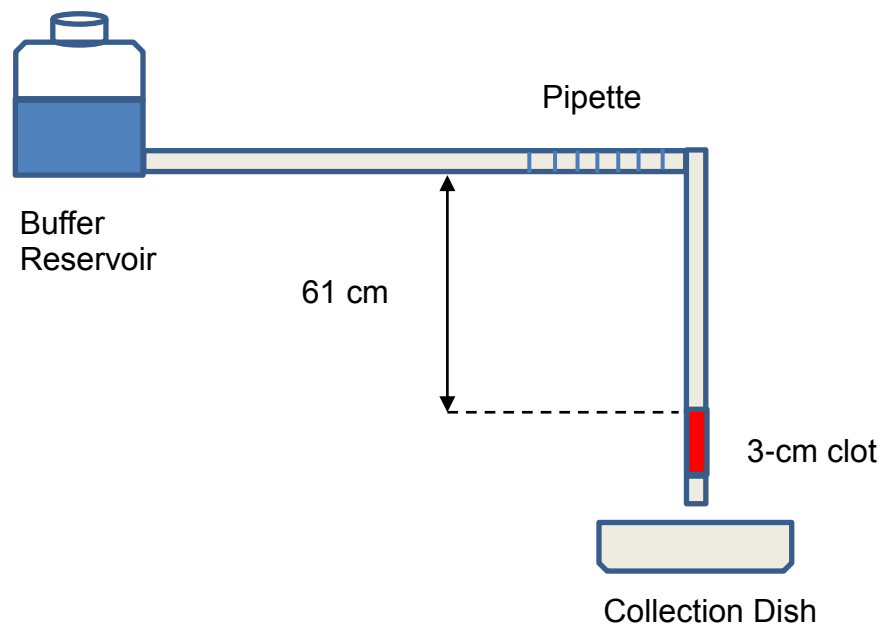
Figure 4.1. *In Vitro* Thrombolytic Experiment (65, 129).
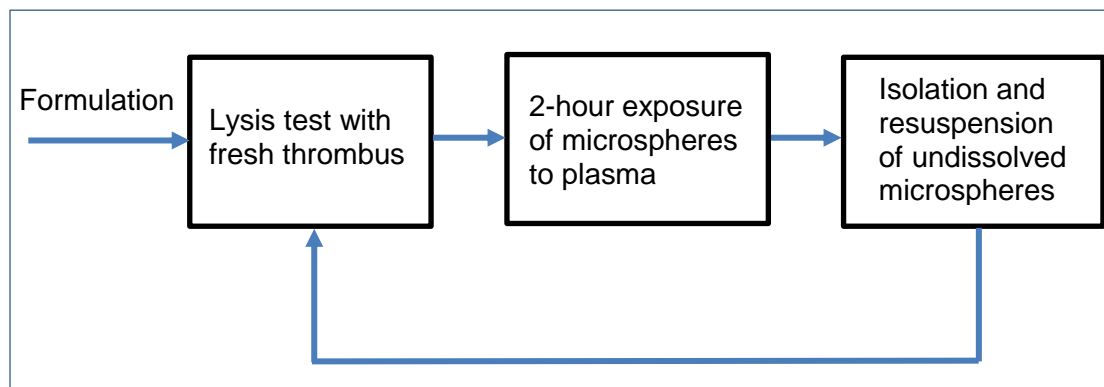
Figure 4.2. Reocclusion Lysis Test Scheme.

4.2.11. Statistical Analysis:

Unless otherwise stated, all data are presented as mean ± standard error of the mean. Student's t-test was used to determine significance between two groups. P-values less than 0.05 were considered significant.

4.3. Results

4.3.1. Characterization of Eud/SK and CS-Eud/SK Microspheres

Eud/SK microspheres were successfully prepared using the double emulsion method. CS-Eud/SK microspheres were formed by surface modification of Eud/SK microspheres with CS using covalent bond synthesis (Figure 4.3). In this method, the carboxyl group of Eud was chemically coupled with the primary amino group of CS by EDC/NHS. Firstly, carboxyl groups on the surface of Eud/SK microspheres were activated by EDC/NHS and then reacted with the amino group of CS (130).
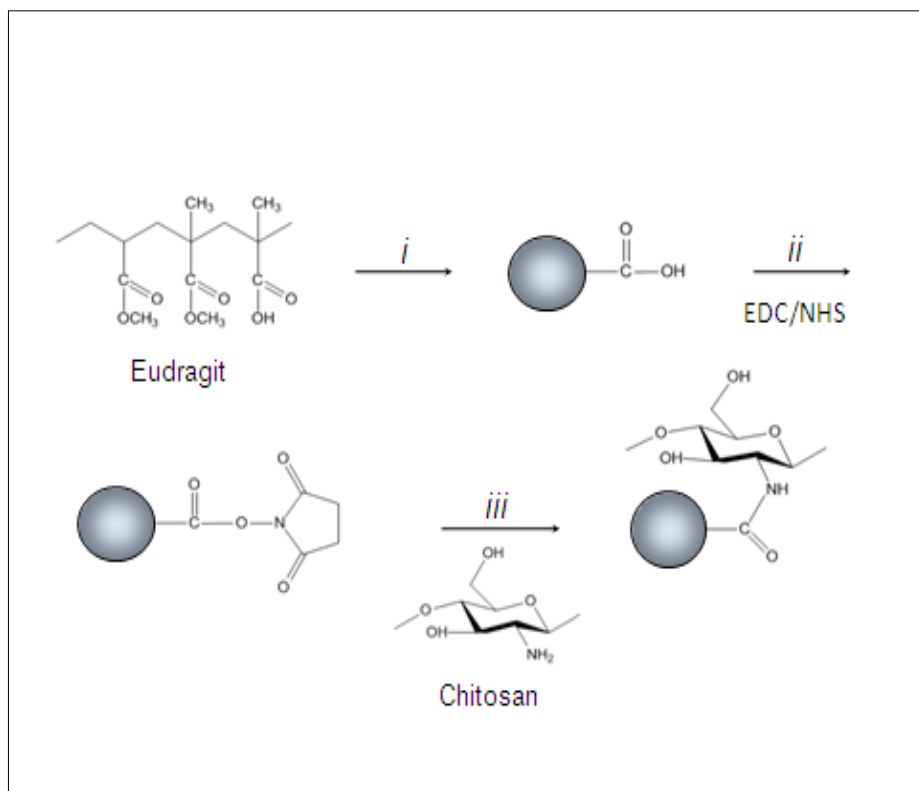
Figure 4.3. Preparation of Eud/SK and CS-Eud/SK Microspheres:
(*i*) Preparation of Eud/SK Microspheres via the Double Emulsion Method.
(*ii*) Activation of Carboxyl Group on the Surface of Microspheres by EDC/NHS.
(*iii*) Reaction of Activated Carboxyl Group with Amine Group of CS.

FT-IR spectra confirmed the successful conjugation of CS to the Eud microspheres (Figure 4.4). In the spectra of blank Eud and CS-Eud microspheres, the peaks at 1735 and 1733 cm^{-1}, respectively, correspond to the C=O stretching vibration from carboxylic acid groups (131). The spectrum of CS exhibits peaks of amide groups: amide I band (C=O stretch of acetyl group) at 1654 cm^{-1} and amide II band (N-H stretch) at 1570 cm^{-1} (125) while the spectrum of blank CS-Eud microspheres displays the amide bond peak at 1651 cm^{-1}.
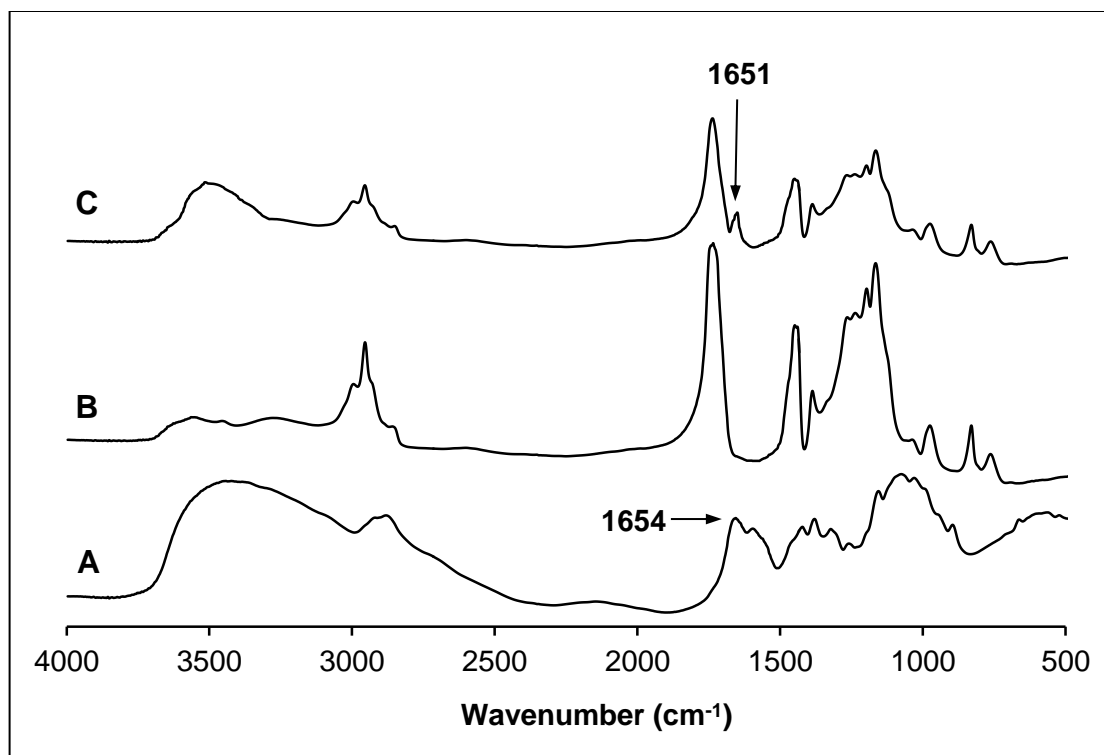
Figure 4.4. FT-IR Spectra of CS, Blank Eud and CS-Eud Microspheres: (A) CS, (B) Blank Eud Microspheres, and (C) Blank CS-Eud microspheres.

The EE (%) based on protein content or protein activity of CS-Eud/SK microspheres was significant lower than that of Eud/SK microspheres (Table 4.2). The EE (%) of CS-Eud/SK microspheres was determined based on the content or activity of SK obtained after the covalent bonding process over the initial total content or activity of SK, while the EE (%) of Eud/SK microspheres was determined based on the content or activity of SK obtained before the covalent bonding process over the same initial total content or activity of SK according to equation (5). The EE (%) based on protein content or protein activity of PEG/SK microspheres has also been presented in Table 4.2 and are consistent with a previous study (65).

Table 4.2. Characterization of PEG/SK, Eud/SK and CS-Eud/SK Microspheres (mean ± standard error of the mean, $n = 5$)

Microspheres	Particle Size (μm)	EE (%)	
		Protein Content	Activity
PEG/SK	0.802 ± 0.023	84.4 ± 3.1	52.6 ± 2.8
Eud/SK	0.726 ± 0.015	90.1 ± 2.7	61.4 ± 3.4
CS-Eud/SK	0.813 ± 0.018*	85.3 ± 2.2*	50.6 ± 2.9*

* = p<0.05 vs. Eud/SK

SEM images confirmed that the shapes of Eud/SK and CS-Eud/SK microspheres were spherical with smooth surface and a particle size less than 1 μm (Figure 4.5). Moreover, the particle size by SEM confirmed that found by light scattering where Eud/SK microspheres had a particle size of 0.726 ± 0.015 μm. A statistically significant difference in size was observed after modification with CS. The mean particle diameter of Eud/SK microspheres was smaller than that of CS-Eud/SK microspheres (0.726 ± 0.015 μm vs 0.813 ± 0.018 μm, p<0.05) (Table 4.2). The increase in size of CS-Eud/SK microspheres in comparison with that of Eud/SK microspheres was attributed to bonding of CS to the surface of Eud/SK microspheres.
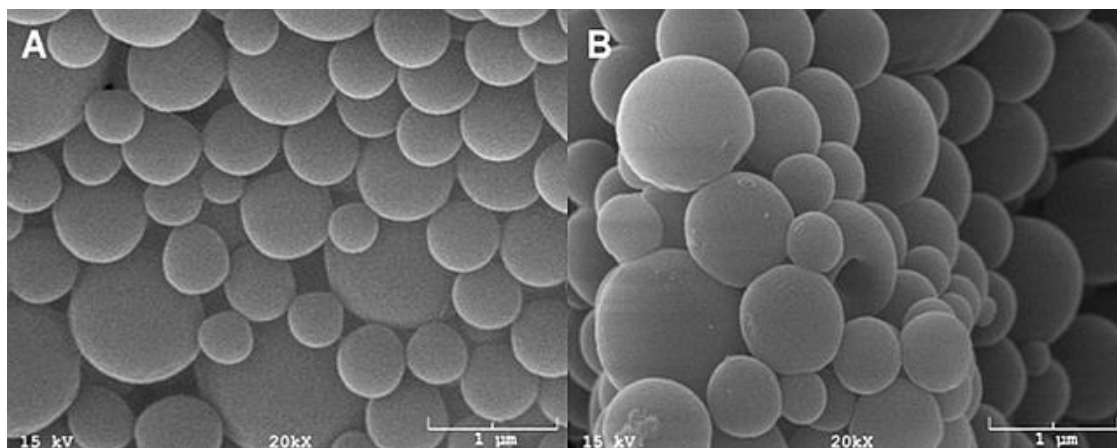
Figure 4.5. SEM Images of (A) Eud/SK Microspheres and (B) CS-Eud/SK Microspheres.

TEM images showed that Eud/SK and CS-Eud/SK microspheres were non-homogenous matrices due to the different ratios of components in Eud copolymer (methylacrylate:methylmethacrylate:methacrylic acid = 7:3:1). Furthermore, under the TEM microscope, CS-Eud/SK microspheres were darker than Eud/SK microspheres (Figure 4.6). The component of the dark clustered layers on the surface of CS-Eud/SK microspheres was CS (132). CS layers did not coat the entire surface of the Eud/SK microspheres because the carboxyl groups were randomly distributed along the copolymer chain and the ratio of the free carboxyl groups to the ester groups is approximately 1:10. When conjugating to the carboxyl groups on the surface of Eud/SK microspheres, CS formed nonuniformly clustered layers over the surface, perhaps due to microphase separation of the underlying polymer.
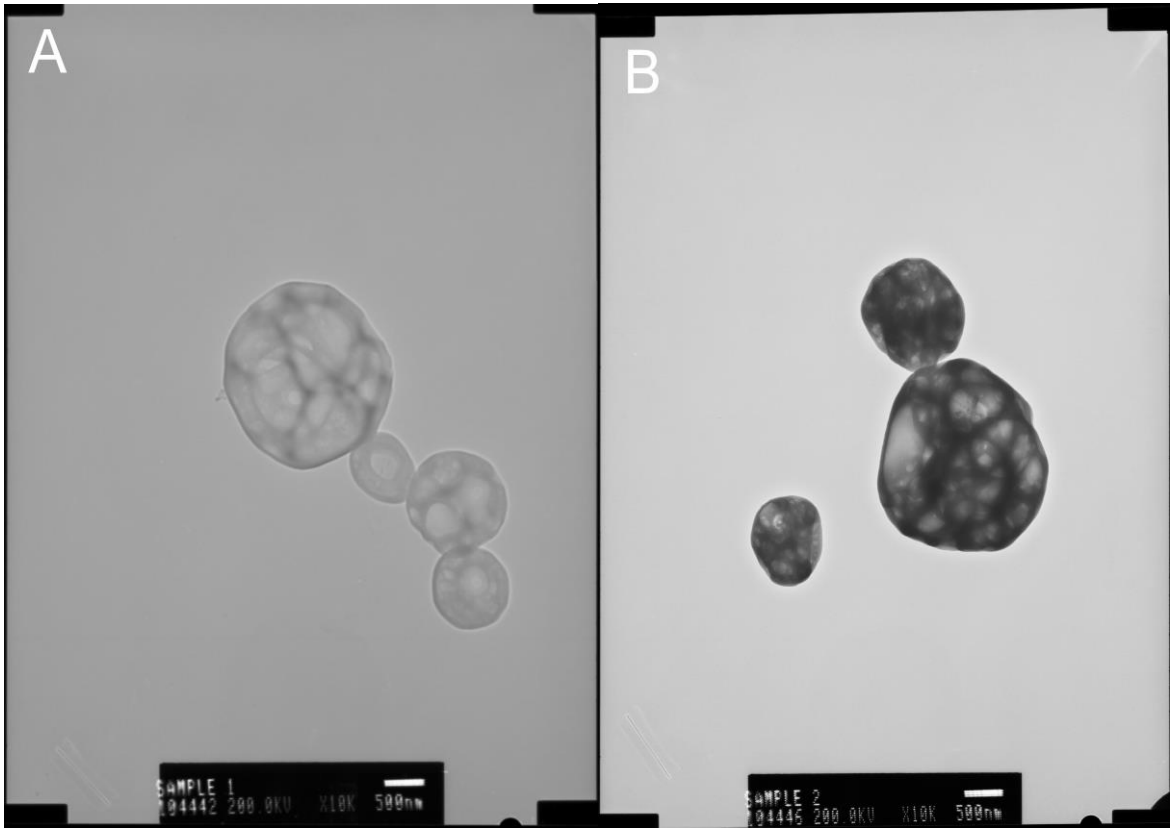
Figure 4.6. TEM Images of (A) Eud/SK Microspheres and (B) CS-Eud/SK Microspheres.

The *in vitro* release profiles of the Eud/SK and CS-Eud/SK microspheres presented similar biphasic configurations, consisting of an initial burst followed by a sustained release (Figure 4.7). CS modification reduced the initial burst so that CS-Eud/SK microspheres had a longer sustained release phase when compared with those of Eud/SK microspheres. For instance, the cumulative releases of SK for Eud/SK and CS-Eud/SK microspheres were 41.4%, and 28.1% at 1 h and 99.3% and 88.6% at 5 h, respectively. Both mixtures of PEG/SK + Eud/SK and PEG/SK + CS-Eud/SK microspheres showed a faster release of the entrapped SK during the first 30 min followed by a continuous release for 5 h and 8 h, respectively. The SK release from

PEG/SK + CS-Eud/SK microspheres within the first 30 min was slightly lower than that

from PEG/SK + Eud/SK microspheres, release of the drug continuing for a total of 8 h

(Figure 4.9).
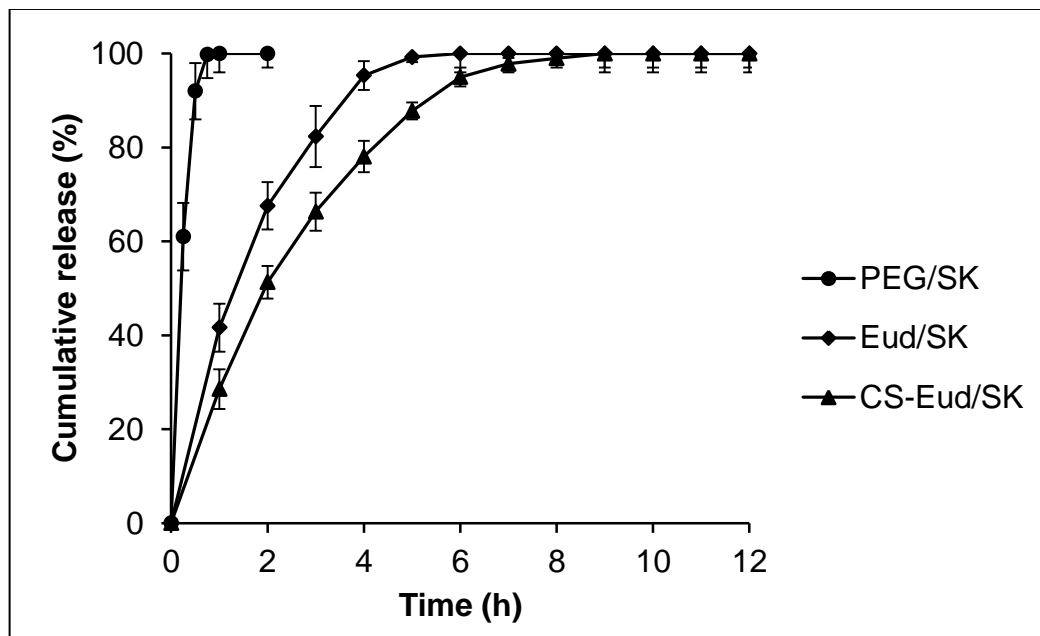
Figure 4.7. *In Vitro* Release Study of SK from PEG/SK, Eud/SK and CS-Eud/SK Microspheres (mean ± standard error of the mean, *n*=5).
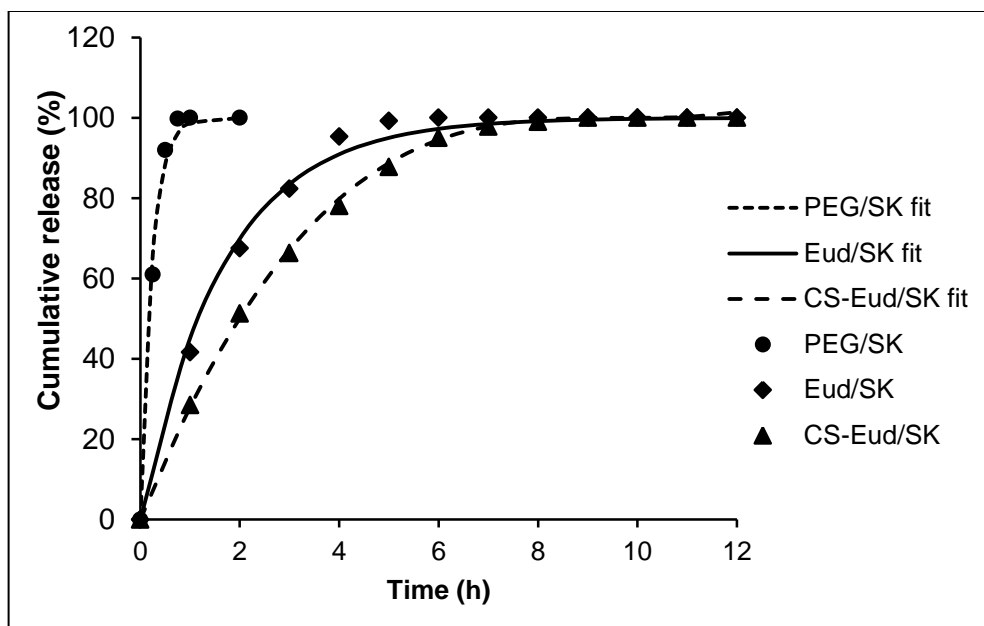
Figure 4.8. Fit of the Mathematical Models to the Experimentally Determined Release of SK from PEG/SK, Eud/SK and CS-Eud/SK Microspheres [$Y_{PEG/SK} = 100(1 - e^{-4.27t})$; $Y_{Eud/SK} = 100(1 - e^{-0.6t})$; $Y_{CS-Eud/SK} = 100(1 - (1 - 0.1t)^3)$].

The release rate constants (k_x) and the correlation coefficients (R^2) between the experimentally obtained and the fitted data calculated by the above-mentioned mathematical models appear in Table 4.3. Release data of PEG/SK and Eud/SK microspheres were found to fit first-order kinetics [$Y_{PEG/SK} = 100(1 - e^{-4.27t})$; $Y_{Eud/SK} = 100(1 - e^{-0.6t})$] while release data for CS-Eud/SK fitted the Hixson-Crowell model [$Y_{CS-Eud/SK} = 100(1 - (1 - 0.1t)^3)$]. Fit of the mathematical models to the experimentally determined release of SK from PEG/SK, Eud/SK and CS-Eud/SK microspheres are presented in Figure 4.8.

Table 4.3. Release Rate Constants (k_x) (mean ± standard error of the mean, $n = 5$) and Correlation Coefficients (R^2) Calculated after Fitting the Release Profiles

Model	Parameters	Microspheres		
		PEG/SK	**Eud/SK**	**CS-Eud/SK**
Zero order	k_o [a]	-38.60 ± 13.34	-15.82 ± 2.79	-15.36 ± 4.37
	R^2	0.7864	0.8531	0.9562
First order	k_1 [b]	4.27 ± 0.90	0.60 ± 0.07	0.40 ± 0.01
	R^2	0.9936	0.9943	0.9927
Higuchi	k_H [c]	79.55 ± 14.65	35.63 ± 0.56	33.77 ± 0.45
	R^2	0.4481	0.7338	0.9138
Hixson-Crowell	k_{HC} [d]	2.23 ± 0.51	0.55 ± 0.04	0.47 ± 0.01
	R^2	0.7934	0.9692	0.9994

[a] the zero-order release rate constant (% h^{-1})
[b] the first-order release rate constant (% h^{-1})
[c] the rate constant obtained according to the Higuchi equation (% $h^{-1/2}$)
[d] the rate constant obtained according to the Hixson–Crowell equation (% h^{-1})
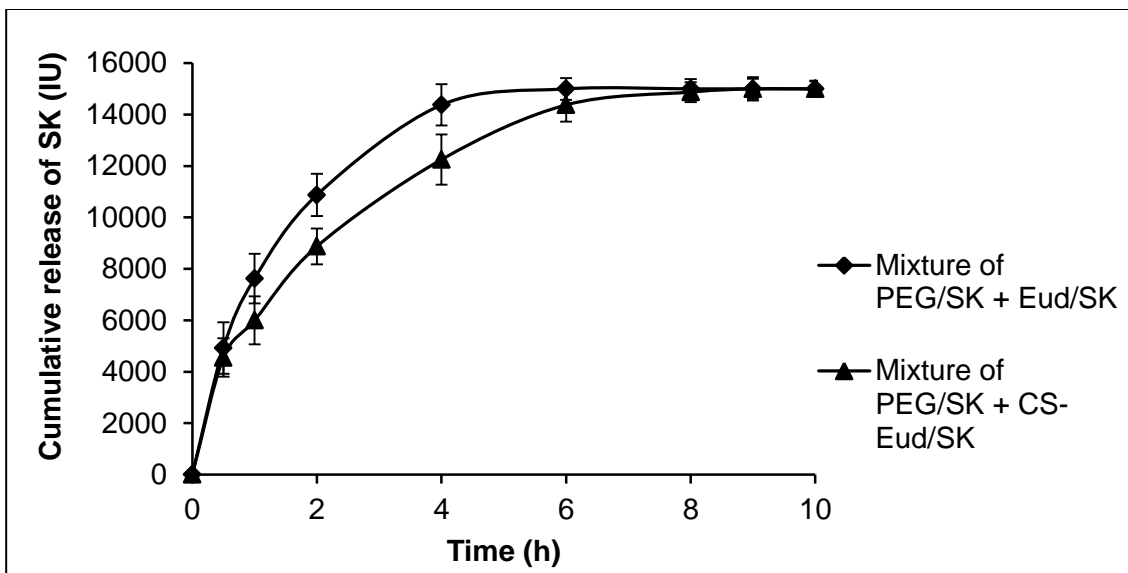
Figure 4.9. *In Vitro* Release Study of SK from Mixtures of PEG/SK + Eud/SK Microspheres and PEG/SK + CS-Eud/SK Microspheres (The Dose Fractionation of SK Activity between PEG/SK and Eud/SK Microspheres or CS-Eud/SK Microspheres was 1:5) (mean ± standard error of the mean, *n*=5).

The morphological change of CS-Eud/SK microspheres in PBS pH 7.4 solution was investigated via SEM. After 2 h, swelling and loss of spherical shape of microspheres were observed (Figure 4.10). After 6 h, additional swelling could be seen. The microspheres had lost their integrity with small fragments resulting from the disintegration evident.
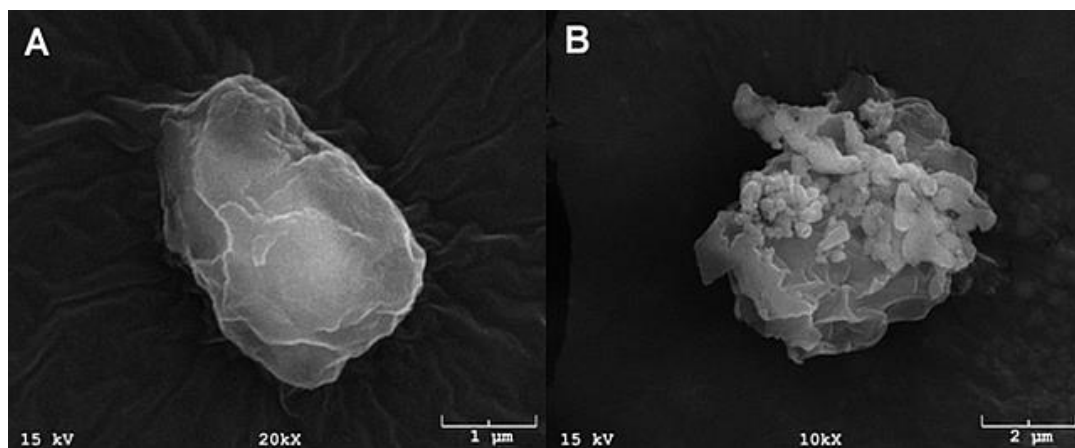
Figure 4.10. SEM Images of CS-Eud/SK Microspheres after 2 h (A) and 6 h (B) in PBS pH 7.4 Solution at 37°C.

4.3.2. In Vitro Thrombolytic Study

At the beginning of the lysis experiments (0 h), the clot lysis times for PEG/SK + Eud/SK and PEG/SK + CS-Eud/SK microspheres were significantly shorter than that of free SK + blank CS-Eud microspheres (Table 4.4). At the stage of the 2 h "reocclusion" lysis experiment, the clot lysis time for PEG/SK+CS-Eud/SK microspheres was reduced 19.7% when compared with that of PEG/SK + Eud/SK microspheres (27.7 ± 0.7 min vs. 34.5 ± 2.3 min, $p<0.05$). After 4 h, the clot lysis time for PEG/SK+ CS-Eud/SK microspheres was 38.4 ± 2.2 min. The PEG/SK + Eud/SK microspheres at 4 h, 6 h and the PEG/SK + CS-Eud/SK microspheres at 6 h showed no evidence of clot lysis after more than 60 min. Similarly, free SK + blank CS-Eud and PEG + free SK/blank CS-Eud microspheres showed no evidence of clot lysis at 2 h, 4 h and 6 h (Table 4.4). Thus, PEG/SK + CS-Eud/SK microspheres retain activity up to 4 h from beginning of the *in vitro* lysis experiment.

Table 4.4. The Clot Lysis Times (min) of Four Fibrinolytic Formulation Mixtures at Different Stages of the Lysis Experiment (The Dose Fractionation of SK Activity Between PEG/SK and Eud/SK Microspheres or CS-Eud/SK Microspheres was 1:5) (mean ± standard error of the mean, $n = 5$)

Microsphere Mixtures	0 h	2 h	4 h	6 h
Free SK (2500 IU) + Blank CS-Eud	19.3 ± 0.9	_	_	_
PEG/SK (2500 IU) + Free SK (12500 IU)/Blank CS-Eud	13.4 ± 1.6	_	_	_
PEG/SK (2500 IU) + Eud/SK (12500 IU)	12.8 ± 1.1*	34.5 ± 2.3	_	_
PEG/SK (2500 IU) + CS-Eud/SK (12500 IU)	14.3 ± 1.3*	27.7 ± 0.7†	38.4 ± 2.2	_

* = p<0.05 vs. Free SK + Blank CS-Eud
† = p<0.05 vs. PEG/SK + Eud/SK

4.4. Discussion

Submicron Eud microspheres with SK were successfully prepared by the double emulsion method and the surface of the microspheres modified with CS while retaining fibrinolytic activity. The EE (%) based on protein content or protein activity of Eud/SK microspheres was higher than that of CS-Eud/SK microspheres because some proteins on the surface of Eud/SK microspheres were dissolved in solution and washed away during coating process. This resulted in the lower EE (%) of CS-Eud/SK microspheres than that of Eud/SK microspheres. It is also possible that some SK activity was lost during the preparation process from exposure to organic solvent, heat with sonication and shear during vortexing.

As a biocompatible polymer, CS has been used elsewhere to coat tPA-magnetic nanoparticles (88) and tPA-PLGA nanoparticles (18, 132) for accelerating thrombolysis or imparting sustained delivery of urokinase and SK (22, 133). Our results indicate CS also contributes to the observed release properties as does Eud. Eud is soluble near neutral pH and commonly used for enteric coating in pharmaceutical industry (119). In medium pH 7.4, the dissolution of Eud starts with the diffusion of water and hydroxyl ion into the polymer matrices to form a gel layer and then the carboxylic acid groups are ionized, facilitating the dissolution of the polymer (134). The presence of CS affects this dissolution process. The pKa of the primary amine groups of CS is between 6.3 and 7.0. Therefore, it is not soluble in PBS pH 7.4 (135) but it absorbs water and swells on contact with PBS pH 7.4. As the Eud interior of the microsphere dissolves, SK is released by desorption from Eud copolymer so that it can diffuse through the swollen CS layer. When CS is conjugated to the surface of Eud microspheres, it acts as a physical barrier to retard water and hydroxyl ion entering the microsphere matrix and to slow the diffusion of SK into the bulk solution. This led to a reduced initial ''burst phase'' and a slower ''sustained release phase'' of CS-Eud/SK microspheres compared with Eud/SK microspheres. The burst effect is undesirable for a controlled release system because it results from dissolution of an uncontrolled portion of protein or drug entrapped on the surface of microspheres when microparticles are immersed in solution. Due to the covalent bonding of CS on the surface, CS-Eud/SK microspheres exhibited a reduction in initial burst effect.

To investigate the mechanism of release SK from CS-Eud/SK microspheres, SEM images of these microspheres were taken after 2 h (A) and 6 h (B) in PBS pH 7.4

71

at 37$^\mathrm{o}$C. On contact with PBS pH 7.4, the swelling of CS and the formation of a gel layer in the matrices led to the loss of spherical shape of CS-Eud/SK microspheres (Figure 4.10A). Dissociation of the carboxylic acid groups in the Eud/SK polymer caused the polymer to expand by charge-charge repulsion, which combined with CS swelling, resulted in the loss of compact structure and disintegration into small fragments (Figure 4.10B).

Prior work had shown that a dosage of 2500 IU of SK was adequate to generate *in vitro* thrombolysis in a capillary tube (65). Therefore, we used an amount of PEG/SK microspheres containing 2500 IU of SK (approximately 50 mg) for rapid fibrinolysis. Based on mathematical fits for release rates from Eud/SK and CS-Eud/SK microspheres (Figure 4.8), the dose of entrapped SK in Eud/SK or CS-Eud/SK microspheres was determined as 12500 IU so that the content of SK released at each stage after 2 h, 4 h and 6 h was approximately 2500 IU for the digestion of the secondary blood clots. The dose fractionation of SK activity between PEG/SK and Eud/SK microspheres or CS-Eud/SK microspheres was 1: 5 and the total dose of entrapped SK in the mixtures of PEG/SK + Eud/SK microspheres or the mixtures of PEG/SK + CS-Eud/SK microspheres was set at 15000 IU.

At the beginning of the lysis experiment (0 h), although Eud/SK microspheres released SK faster than CS-Eud/SK microspheres (Figure 4.7) and the SK released from PEG/SK + Eud/SK microspheres was higher than that from PEG/SK + CS-Eud/SK microspheres (Figure 4.9), there was not a significant difference in the clot lysis times between the two mixtures. The shorter lysis times obtained at 0 h for both PEG/SK + Eud/SK and PEG/SK +CS-Eud/SK microspheres compared with free SK was attributed

to the presence of PEG/SK microparticles (65). With the application of pressure, the SK-encapsulated microspheres were transported into the clot by convection or permeation (129, 136) so that fibrinolysis proceeded within the clot as well as at the leading edge (65).

After 2 h, 4 h and 6 h, only Eud/SK microspheres or CS-Eud/SK microspheres remain for the "reocclusion" experiments, because PEG/SK microspheres dissolved completely after 45 min. Comparison of the release rates (Figure 4.7) and lysis results (Table 4.4) at 2 h and 4 h reveals the unusual nature of thrombolysis with encapsulated PA. One generally expects the activity of an agent to be proportional to the amount released. However, the opposite is true for this system with activity corresponding to the amount of encapsulated agent remaining. CS-Eud/SK exhibits faster lysis even though SK releases more slowly. This results from distributed intraclot thrombolysis which occurs with encapsulated PAs. Microspheres penetrate and release inside the thrombus leading to the fibrinolytic reaction throughout the volume of the clot rather than being limited to its surface. With fluorophore-tagged, encapsulated PA, Leach proved the fibrinolytic reaction proceeded to create SK associated voids throughout the interior of a thrombus (65). In contrast, the reaction only took place at the leading edge of the thrombus with the free agent, consistent with the report by Blinc (137), Diamond (138), and others (139, 140). Encapsulation blocks adsorption of SK at the surface and allows penetration overcoming high affinity, high surface area and low flow strongly favor binding of SK at the leading edge. Beside the pressure-driven hydrodynamic forces facilitating microsphere penetration, we note the electrostatic force between the positive potentials of CS on the surface of CS-Eud/SK microspheres and negative

73

potentials of fibrin of the blood clot at pH of 7.4 as another mechanism driving the CS-Eud/SK microspheres to associate with the matrix of the blood clot and release of SK therein (17, 18). At the 4 h stage, the clot lysis time of CS-Eud/SK microspheres was longest (38.4 ± 2.2 min) because by that time the SK available from CS-Eud/SK microspheres was gradually diminishing.

In the *in vitro* lysis experiment, the presence of CS coating on the surface of Eud/SK microspheres induced a much slower release of SK up to 8 h which would seem to provide clot-lytic efficacy in prevention of second blockage up to 4 h. A 3-cm clot is a stringent test for reocclusion since a reservoir of circulating PA in the body would presumably act before the thrombus reached that length. The test however only provides a comparison of thrombolytic activity with the delayed released formulations and serves as evidence of a potential approach to address reocclusion.

For clinical practice, after administration a mixture of PEG/SK + CS-Eud/SK microspheres for thrombolytic therapy, microspheres are envisioned to rapidly accumulate on thrombus surface and within the thrombus. Evidences from a number of studies in a different species indicate that encapsulated PA when released within minutes will break up the thrombus and restore flow faster than free PA. This study has demonstrated that longer release times leading to extended half-life in plasma can be expected to offer protection from reocclusion episodes.

Finally, we note that while Eud is a pH-sensitive material and has been widely employed in pharmaceutical industry for controlled-release of drugs, it is not biodegradable and its fate in circulation is not known (141). Recently however, Eud nanoparticles have been locally infused to treat in-stent restenosis following

74

percutaneous transluminal coronary angioplasty in a swine model (142). It has also been used in vivo for arteriovenous malformation (143, 144) If Eud is not approved for intravenous administration, other materials that have both pH-sensitive and biodegradable properties could apply the principles reported herein. Knowledge of this study can provide the basis for improvement of therapies for heart attack and stroke.

4.5. Conclusions

In this study, CS was successfully conjugated to the surface of Eud/SK microspheres by covalent bonding. This led to CS-Eud/SK microspheres with a lower EE (%) based on protein content or protein activity, and a much slower release of SK when compared with those of Eud/SK microspheres. *In vitro* thrombolytic study showed that a mixture of PEG/SK and CS-Eud/SK microspheres could break up the blood clot rapidly while also providing clot-lytic efficacy for prevention of a second blockage up to 4 h.

Chapter 5 - Modified Dextran/Heparin-Based Triggered Release Microspheres for Cardiovascular Delivery of Therapeutic Drugs Using Protamine as a Stimulus[3]

5.1. Introduction

Thrombolytic drugs [e.g. tissue-specific plasminogen activator (tPA), streptokinase, and urokinase] actively dissolve clots by inducing fibrinolytic activity. They convert the proenzyme plasminogen to the active enzyme plasmin, which in turn breaks up the fibrin clot. But thrombolytic therapy has a possible serious uncontrolled bleeding side effect due to non-specific and systemic activation of these agents (5). Moreover, thrombolytic agents have short half-lives which need to be used with the higher dosages in clinical therapeutics, leading to increased risk of bleeding complications. In fact, this side effect can occur in as many as 20% patients receiving plasminogen activators (18). Therefore, a drug delivery system that releases these agents in a triggerable manner is desirable to prolong their circulatory half-lives and protect these agents from inactivation by components in the circulatory system and antibodies. Systems offering an on-demand controlled release might enhance therapeutic efficacy and reduce systemic side effects of thrombolysis. While our interest in thrombolysis motivated this work, we note its potential for controlled delivery of other agents.

---

[3] This work has been submitted to *Journal of Microencapsulation*.

Various triggering mechanisms have been described for drug delivery systems including pH (145), temperature (146), light (147), ultrasound (148) and magnetic stimuli (149). Recently, a heparin (HP)/protamine-based prodrug system has been developed for the controlled delivery of tPA at the clot site (24, 25). In this approach, cation-modified tPA was attached to a HP-antifibrin complex via ionic attraction. Protamine, a competitive HP inhibitor, was used as a triggering agent to release the active tPA from the prodrug for clot dissolution. Similarly, a HP/protamine-based system has been applied for delivery of the anticancer agents (150). Based on the electrostatic interactions between HP and ammonium moieties in modified dextrans, we offer a new triggerable drug delivery system in which a drug agent is physically entrapped inside microspheres formed by the double emulsion method (151). This offers promise in extending prior work with HP/protamine to the delivery of a wide range of species without requiring chemical modification of the agent.

Dextran is a biocompatible and biodegradable natural polymer that has been widely used in drug delivery systems. Owing to having many hydroxyl groups, dextran can easily be modified to meet various biomedical applications (94). Of which, cationic dextran polymers have been synthesized (Figure 5.1) by grafting amine-containing species to the backbone of dextran using reductive amination (152-155). To facilitate formation of the microparticles with the double emulsion method, some hydroxyl groups of dextran have been converted to hydrophobic structures yielding an intermediate acetalated dextran (DAC) (99, 108, 156).

In this study, we describe the synthesis of a new amine-modified acetalated dextran polymer which is combined with HP to develop triggered release microspheres.

Amine groups, present as positively charged ammonium ions, will bind with the negatively charged HP. Protamine is then used as a triggering stimulus to release crystal violet (CV), a model drug, from these microspheres. We also investigate the effects of various factors such as the degree of amination and concentration of protamine on the release of CV from microspheres.

5.2. Materials and Methods

5.2.1. Materials

Dextran from *Leuconostoc spp.* (average molecular weight: 70 kDa), poly(vinyl alcohol) (PVA, 87–90% hydrolyzed, average molecular weight: 30–70 kDa), dimethyl sulfoxide (DMSO), chloroform, sodium periodate, 2-methoxypropene, ethylendiamine, protamine sulfate salt from salmon, pyridinium p-toluenesulfonate sodium, 2,4,6-trinitrobenzenesulfonic acid (TNBS), CV (molecular weight: 407.9 g/mol) were purchased from Sigma-Aldrich (St. Louis, MO). HP sodium was purchased from Fisher Scientific (Pittsburgh, PA).

5.2.2. Synthesis of Dextran-Amine (DEXAM) Conjugates

5.2.2.1. Oxidation of Dextran

Dextran (3.0 g) was dissolved in 30 mL water. To this solution was separately added potassium periodate (0.8 g or 1.2 g), and the mixture was vigorously stirred for 6 h in the dark at room temperature. The product was purified by dialysis of the solution against distilled water using a regenerated cellulose membrane with a MWCO of 3500 g/mol (Fisherbrand, Fisher Scientific) for 48 h. Then, the sample was lyophilized for 24

h to obtain a white powder. The obtained products were designated as DO1 or DO2, respectively (154).

5.2.2.2. Acetalation of Oxidized Dextran

DO1 (2 g) was dissolved in 40 mL of DMSO at 90°C under nitrogen gas. After complete dissolution, the mixture was cooled down to room temperature and pyridinium p-toluenesulfonate (0.186 g) was added followed by 2-methoxypropene (14.4 mL) to the reaction vessel. The reaction continued at room temperature for 6 h under nitrogen gas and was quenched with triethylamine (1 mL). Product isolation followed from precipitation in distilled water, centrifugation (1000 × g for 5 min), removal of the supernatant, and washing several times with distilled water before lyophilizing for 24 h. The obtained product was designated as DAC1 (99, 108).

DO2 (2 g) was reacted similarly with 2-methoxypropene (14.4 mL or 7.2 mL) yielding products which were designated as DAC2 or DAC3, respectively.

5.2.2.3. DEXAM Conjugates

Modified dextran of 2 g (DAC1, DAC2 or DAC3) was dissolved in 60 mL of DMSO at 90°C under nitrogen gas. After complete dissolution, the mixture was cooled down to room temperature. Ethylendiamine (8 mL) was added and stirred for 22 h at room temperature. Then, sodium borohydride (2.0 g) was added to the reaction vessel and stirred for 24 h at room temperature. The product was precipitated in distilled water and was isolated by centrifugation at 1000 × g for 5 min, and then was washed with distilled water, followed by centrifugation and removal of the supernatant before lyophilizing for 24 h. The obtained products were designated as DEXAM1, DEXAM2, and DEXAM3, respectively (154, 155).

5.2.3. Characterization of DEXAM Conjugates

5.2.3.1. Determination of Degree of Oxidation

Degree of oxidation was determined according to the literature (154, 157). In brief, aqueous DO1and DO2 solutions (0.1 mg/mL) were prepared and absorbances of samples were measured at 562 nm with a plate reader (Synergy HT plate reader, Bio-Tek) using a microplate reductometric bicinchoninic acid assay (Micro BCA, Protein Assay Kit, Pierce). An aqueous dextran solution (0.1 mg/mL) was used as a blank in the absorbance measurements. The degree of oxidation (the aldehyde content) was calculated according to the calibration curve formed from the absorbances of a series of glucose solutions (0.01, 0.025, 0.05, 0.075, 0.1 mg/mL).

5.2.3.2. Determination of Degree of Acetalation by the NMR Method

The acetal content was determined by NMR analysis as described in the literature (99). In brief, DAC was suspended in deuterium oxide and hydrolyzed with deuterium chloride. Then, the NMR spectra of DAC were recorded (Varian VNMRS 400 MHz NMR Spectrometer). Based on the integration of reference NMR signals for acetone and methanol at 2.1 and 3.3 ppm, respectively, the content of acetal groups was calculated.

5.2.3.3. Determination of Primary Amines by the TNBS Method

The primary amine content was determined as described previously (153). In brief, DEXAM (10 mg) was dissolved in 10 mL pH 4.0 acetate. 20 µL of freshly prepared aqueous TNBS solution (15 mg/mL) was added to 600 µL of this solution, followed by adding 200 µL of pH8.5 sodium bicarbonate buffer, vortexed for 1 min,

and incubated for 2 h at 37°C. Then, 600 µL of 1 N HCl solution was added, vortexed for 1 min, and gently sonicated for 2 min to remove bubbles. Absorbances of samples were measured spectrophotometrically at 410 nm (Shimadzu UV-2450). A sample of dextran was used as a blank in the absorbance measurements. The primary amine content was calculated according to the calibration curve of ethylenediamine.

5.2.3.4. Fourier Transform Infrared (FT-IR) Spectroscopy

Infrared spectra were obtained by Nicolet 6700 FT-IR Spectrometer. Dried samples were ground with KBr powder, and pressed into pellets for FT-IR examination.

5.2.4. Development and Characterization of Microspheres

5.2.4.1. Preparation of Microspheres by W/O/W Double Emulsion Method

Microspheres were prepared by a double emulsion method (124). Briefly, HP sodium and CV (5 mg) was dissolved in 0.6 mL distilled water. DEXAM conjugates (0.3 g) were dissolved separately in 3 mL of chloroform. The two solutions were mixed for 30 s and sonicated at 45 W for 1 min using a sonicator (Sonic Dismembrator 60, Fisher Scientific). The primary emulsion was mixed with 6 mL of PVA 3% (w/v), sonicated for 30 s to produce W/O/W emulsion. Then, 50 mL of PVA 0.3% (w/v) was added to the emulsion. The suspension was mechanically stirred at 1200 rpm for 3 h at room temperature to remove the organic solvent. The microspheres were isolated by centrifugation (1000 × *g* for 10 min) and washed with distilled water by vortexing for 30 s and then centrifuging several times to remove the residual PVA and solvent. The washed microspheres were suspended in distilled water (1 mL) and lyophilized for 20 h.

In separate runs, the amount of HP sodium was a 1/3 or 1/2 mass ratio of the amount of dextran-amine conjugates. These microspheres were designated as DEXAM/HP1/3 and DEXAM/HP1/2, respectively.

5.2.4.2. Drug Encapsulation Efficiency

CV microspheres of 10 mg were allowed to dissolve completely in 10 mL pH 4.0 acetate buffer for 12 h. The content of entrapped CV in the microspheres was determined spectrophotometrically (Shimadzu UV-2450) at 590 nm (158). Encapsulation efficiency (EE) (%) was calculated using the following equation:

$$EE(\%) = \frac{Actual\ CV\ loading \times 100}{Total\ CV} \tag{6}$$

5.2.4.3. Particle Size

Particle diameter was determined using a laser diffraction particle size analyzer (Beckman Coulter LS230). Particle size measurements are based on diffraction patterns formed by the scattering of light by microparticles. Particle sizes were obtained and analyzed using the accompanying software of the instrument.

5.2.4.4. In Vitro CV Release Study

Microspheres (25 mg) were dispersed in 10 mL of phosphate-buffered saline solution (PBS 10 mM, pH 7.4) in test tubes. Protamine sulfate was added to test tubes to make 0.1%, 0.25% or 0.5% solution. The test tubes were placed in an orbital shaker at $37^{o}C$ and agitated at 80 rpm**.** At specific time points, 2 mL of solution was drawn and filtered for testing. 2 mL of 0.1%, 0.25% or 0.5% protamine in PBS 10 mM, pH 7.4 was

replenished to maintain a constant sink volume. The CV release rate was continuously measured with spectrophotometer (Shimadzu UV-2450) at 590 nm.

5.2.4.5. SEM Images

To assess the mechanism of CV release from DEXAM/HP microspheres, the morphological change of microspheres in 0.5% protamine /PBS pH 7.4 was monitored with SEM (Zeiss NEON 40 EsB). DEXAM2/HP1/2 microspheres (20 mg) were dispersed in 10 mL 0.5% protamine /PBS pH 7.4 at 37°C. After 15 min, 1 h, 2 h, 4 h, 6 h and 12 h, samples were collected by centrifuge at $1000 \times g$ for 10 min and then lyophilized for 15–20 h. A small amount of freeze-dried microspheres was loaded on an aluminum stub with double-sided adhesive tape. Samples were sputter coated with gold and examined by SEM at 15 kV.

5.2.5. Statistical Analysis

Unless otherwise stated, all data are presented as mean ± standard error of the mean. Student's t-test was used to determine significance between two groups. P-values less than 0.05 were considered significant.

5.3. Results

5.3.1. Characterization of DEXAM Conjugates

DEXAM conjugates were synthesized by using the reductive amination reaction method to graft ethylenediamine to the backbone of the modified dextran that had been previously acetalated (Figure 5.1). First, dextran was oxidized using sodium periodate to obtain the dialdehyde derivative. Second, this derivative was acetalated to transform water-soluble dextran into a hydrophobic polymer which was suitable for preparation of

microspheres by the double emulsion method. Finally, the acetalated dialdehyde polymer was reacted with ethylendiamine and reduced by borohydride to form DEXAM conjugates.

The product was characterized by FT-IR (Figure 5.2) with the spectrum of DAC showing peaks of acetal groups at 2989, 1386, and 1239 cm^{-1}, consistent with a previous study (108) . The FT-IR spectrum of DEXAM displayed an amine peak at 1062 cm^{-1} (159).
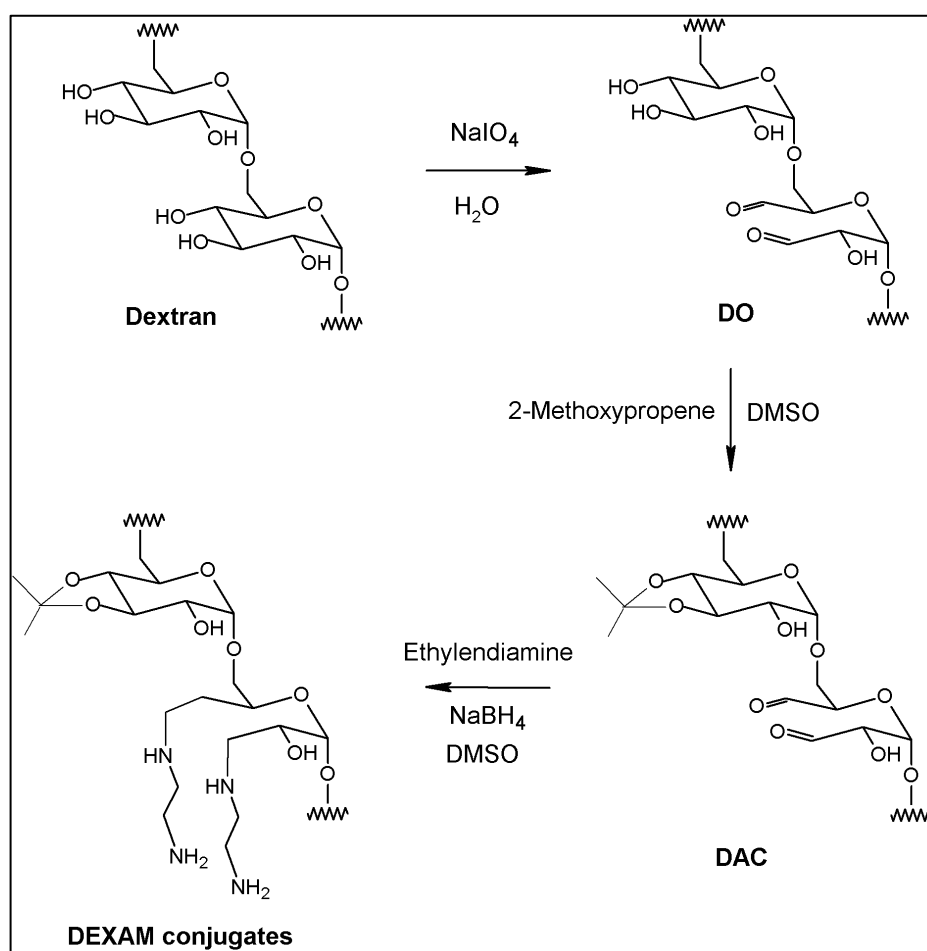
Figure 5.1. Synthesis of DEXAM Conjugates.
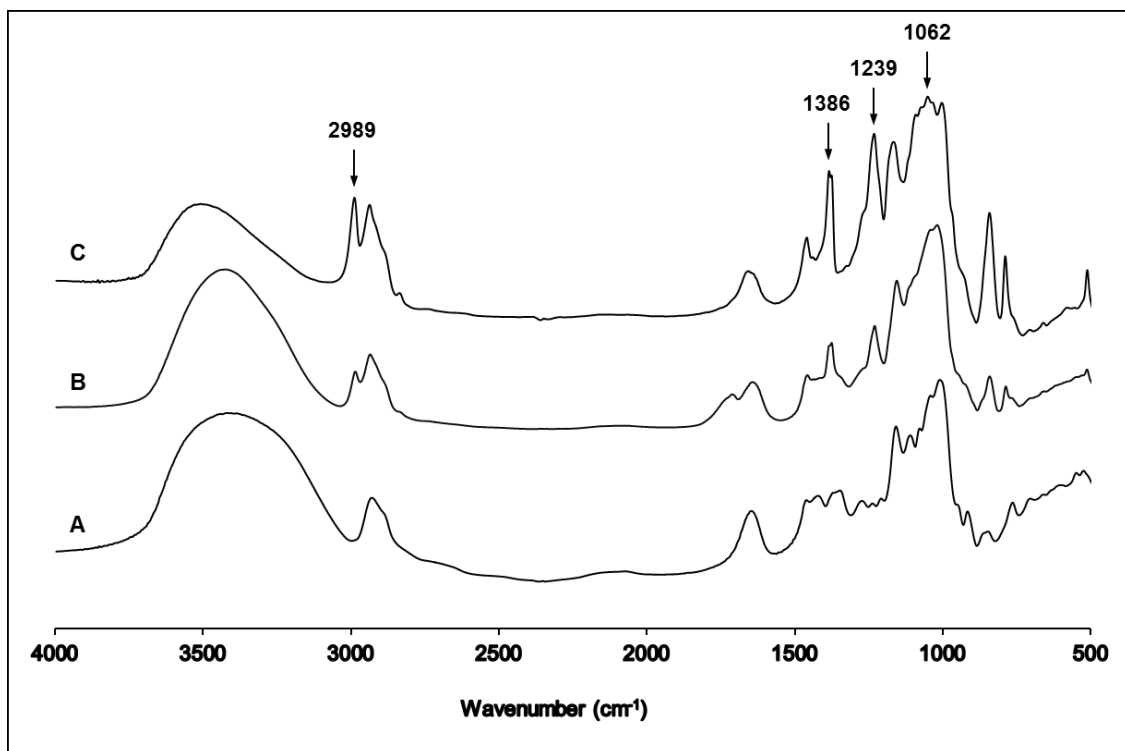
Figure 5.2. FT-IR spectra of (A) Dextran, (B) DAC and (C) DEXAM Conjugates.

The degree of oxidation, degree of acetalation and the primary amine content are presented in Table 5.1. Increasing the amount of sodium periodate in the oxidation reaction of dextran (0.8 to 1.2 g) resulted in a greater degree of oxidation from 9.8 ± 0.15 mol aldehyde /100 mol anhydroglucose unit (AGU) of DO1 to 12.7 ± 0.44 mol aldehyde /100 mol AGU of DO2 ($p < 0.05$). This led to increasing the primary amine content from 7.4 ± 0.3 mol primary amine/100 mol AGU of DEXAM1 to 9.9 ± 0.2 and 10.1 ± 0.2 mol primary amine/100 mol AGU of DEXAM2 and DEXAM3, respectively, ($p < 0.05$) which indicated the amount of ethylenediamine grafted on the dextran backbone. These results are consistent with previous studies (152, 153).

Table 5.1. Characterization of the Modified Dextran (mean ± standard error of the mean, $n = 6$)

Sample	Degree of Oxidation (mol aldehyde/100 mol AGU)[a]	Degree of Acetalation (mol acetalated hydroxyls /100 mol AGU)[b]	The Primary Amine Content (mol primary amine/100 mol AGU)
DEXAM1	9.8 ± 0.15	188.9 ± 3.3	7.4 ± 0.3
DEXAM2	12.7 ± 0.44*	178.8 ± 3.4	9.9 ± 0.2[‡]
DEXAM3	12.7 ± 0.44*	159.6 ± 2.8[†]	10.1 ± 0.2[‡]

[a] Degree of oxidation in DO derivatives; * = $p<0.05$ vs. DO1
[b] Degree of acetalation in DAC derivatives; [†] = $p<0.05$ vs. DAC2
[‡] = $p<0.05$ vs. DEXAM1

In contrast, increasing the degree of oxidation led to slight drop in the degree of acetalation from 188.9 ± 3.3 mol acetalated hydroxyls/100 mol AGU of DAC1 (63.0% of the available hydroxyl groups was modified) to 178.8 ± 3.4 mol acetalated hydroxyls/100 mol AGU of DAC2 indicating that 59.6% of the available hydroxyl groups were modified. Decreasing the amount of 2-methoxypropene from 14.4 mL to 7.2 mL in the acetalation reaction of DO2 resulted in decreasing the acetal content of DAC [178.8 ± 3.4 vs.159.6 ± 2.8 mol acetalated hydroxyls/100 mol AGU (53.2% of the available hydroxyl groups was modified), $p<0.05$)]. Due to the presence of acetal groups, the obtained DEXAM1, DEXAM2 and DEXAM3 are insoluble in aqueous media.

5.3.2. Development and Characterization of DEXAM/HP Microspheres

As shown in Table 5.2, the particle size of DEXAM/HP microspheres was 1.2 - 1.6 μm in diameter, varying with the primary amine content of DEXAM. Moreover, when the amount of HP for preparation of DEXAM2/HP microspheres was reduced, the size of the obtained microspheres was found to decrease. The mean particle diameter of DEXAM2/HP1/3 microspheres was smaller than that of DEXAM2/HP1/2 microspheres (1.247 ± 0.027 μm vs.1.563 ± 0.026 μm, p<0.05).

Table 5.2. Characterization of DEXAM/HP Microspheres (mean ± standard error of the mean, $n = 6$)

Microspheres	Mass Ratio[a]	Particle Size (μm)	EE (%)
DEXAM1/HP1/2	1: 1/2	1.367 ± 0.018	78.4 ± 2.6
DEXAM2/HP1/2	1: 1/2	1.563 ± 0.026*[†]	89.6 ± 2.0*[†]
DEXAM3/HP1/2	1: 1/2	1.607 ± 0.044*	91.0 ± 2.5*
DEXAM2/HP1/3	1: 1/3	1.247 ± 0.027	79.1 ± 1.8

[a] DEXAM: HP
* = p<0.05 vs. DEXAM1/HP1/2
[†] = p<0.05 vs. DEXAM2/HP1/3

EE (%) of DEXAM/HP microspheres was found to depend on the primary amine content and the amount of HP for preparation of DEXAM/HP microspheres (Table 5.2). The EE (%) increased from 78.4 ± 2.6% to 91.0 ± 2.5% as the primary amine content of DEXAM rose from 7.4 ± 0.3 to 10.1 ± 0.2 mol primary amine/100 mol AGU. The EE (%) of DEXAM2/HP microspheres was decreased when the amount of

HP for preparation of DEXAM2/HP microspheres was reduced (89.6 ± 2.0% of DEXAM2/HP1/2 microspheres vs. 79.1 ± 1.8% of DEXAM2/HP1/3 microspheres, p<0.05).

5.3.2.1. In Vitro CV Release Study

We investigated the effect of variables such as chemical properties of DEXAM polymer, mass ratios between DEXAM and HP, and concentrations of protamine on the release profile of CV. It was observed that protamine accelerated the release of CV (Figure 5.3) which was negligible in its absence. The release of CV from DEXAM2/HP1/2 microspheres was increased from 27.6% to 59.1% at 4 h when the concentration of protamine was changed from 0.1% to 0.5%. The percentage released was based on the amount of CV released with time over the actual amount of CV encapsulated in microspheres.

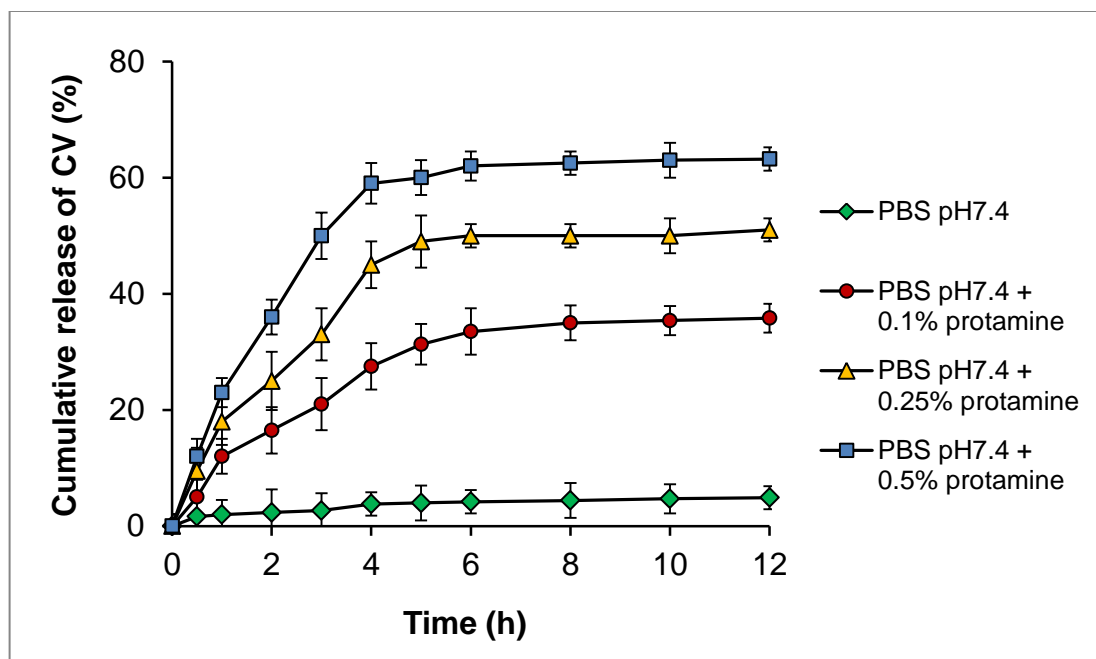**Figure 5.3.** *In Vitro* Release of CV from DEXAM2/HP1/2 Microspheres with Time as a Function of Concentration of Protamine (mean ± standard error of the mean, $n = 5$).
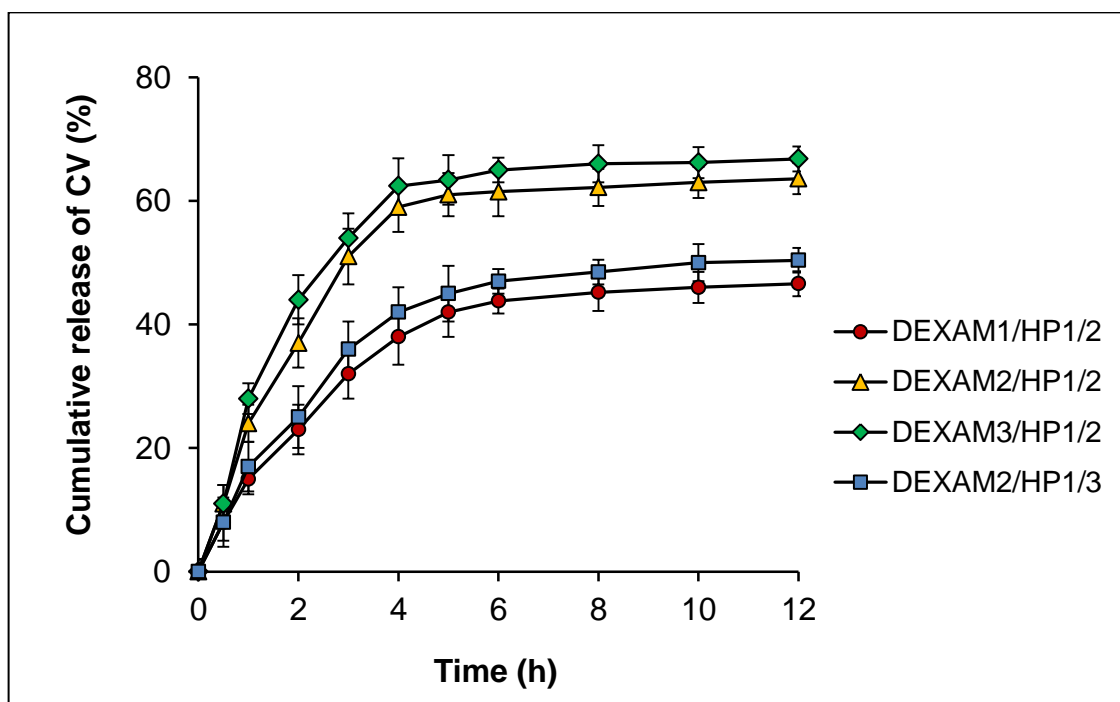
Figure 5.4. *In Vitro* Release of CV from DEXAM/HP Microspheres with Time as Functions of the Primary Amine Content or the Amount of HP with a Fixed Concentration of Protamine (0.5%) (mean ± standard error of the mean, $n = 5$).

The release profile of CV from DEXAM/HP microspheres was also dependent on the primary amine content and the amount of HP when suspended in a fixed concentration of protamine (0.5%) (Figure 5.4). Increasing the primary amine content of DEXAM (DEXAM1/HP1/2, DEXAM2/HP1/2, DEXAM3/HP1/2 microspheres) or the amount of HP when preparation of microspheres (DEXAM2/HP1/2, DEXAM2/HP1/3 microspheres) resulted in accelerating of CV release. DEXAM3/HP1/2 microspheres released 62.4% of entrapped CV after 4 h. In contrast, DEXAM1/HP1/2 microspheres released only 43% of entrapped CV after 5 h.

5.3.2.2. SEM Images

SEM images demonstrated that the shapes of DEXAM/HP microspheres were spherical with a fairly smooth particle surface (Figure 5.5). Particle size of approximately 1.5 µm by SEM confirms findings by light scattering.
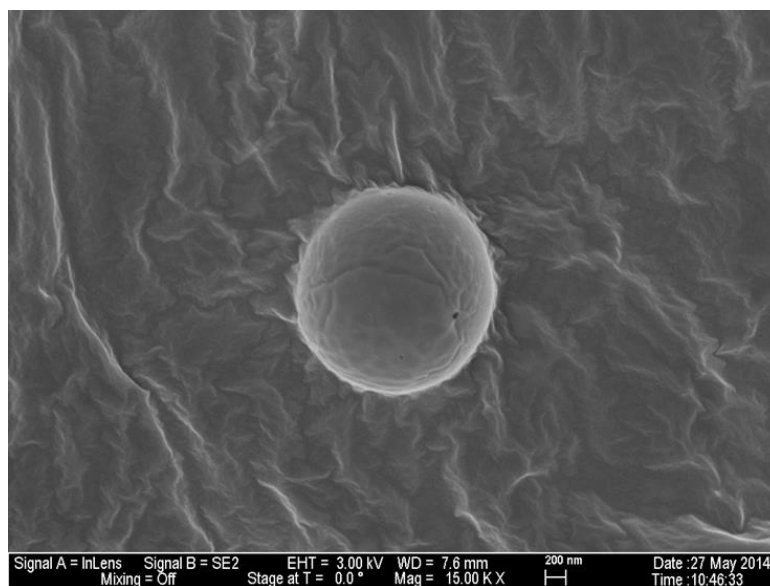
Figure 5.5. SEM Image of DEXAM/HP Microspheres.

To understand the mechanism of CV release from microspheres, the morphological change of DEXAM2/HP1/2 microspheres in 0.5% protamine /PBS pH 7.4 was monitored by SEM (Figure 5.6). The SEM images showed that protamine bound to the surface of microspheres after 15 min (Figure 5.6A). Then, the surface of microspheres becomes rough with pores gradually appearing on the surface of microspheres after 1 h (Figure 5.6B). Next, more cracks and pores can be seen on the surface at 2 h while only remnants of an outer coating is visible at 4 h (Figure 5.6C and 5.6D). Only a porous interior structure can be seen after 6 h and 12 h (Figure 5.6E and 5.6F).
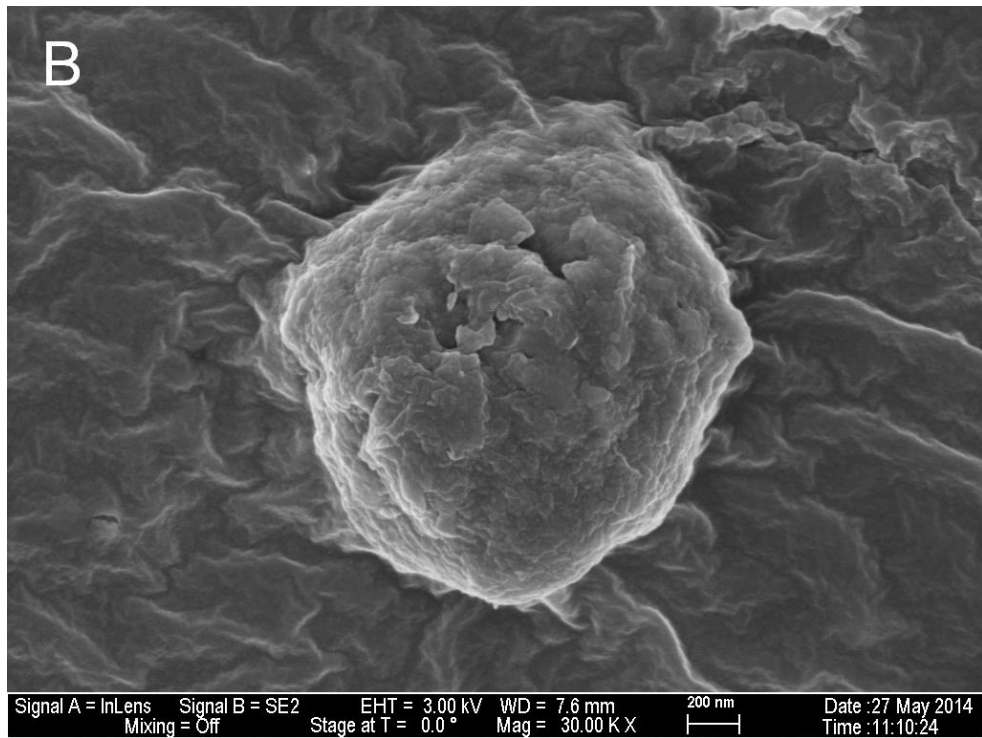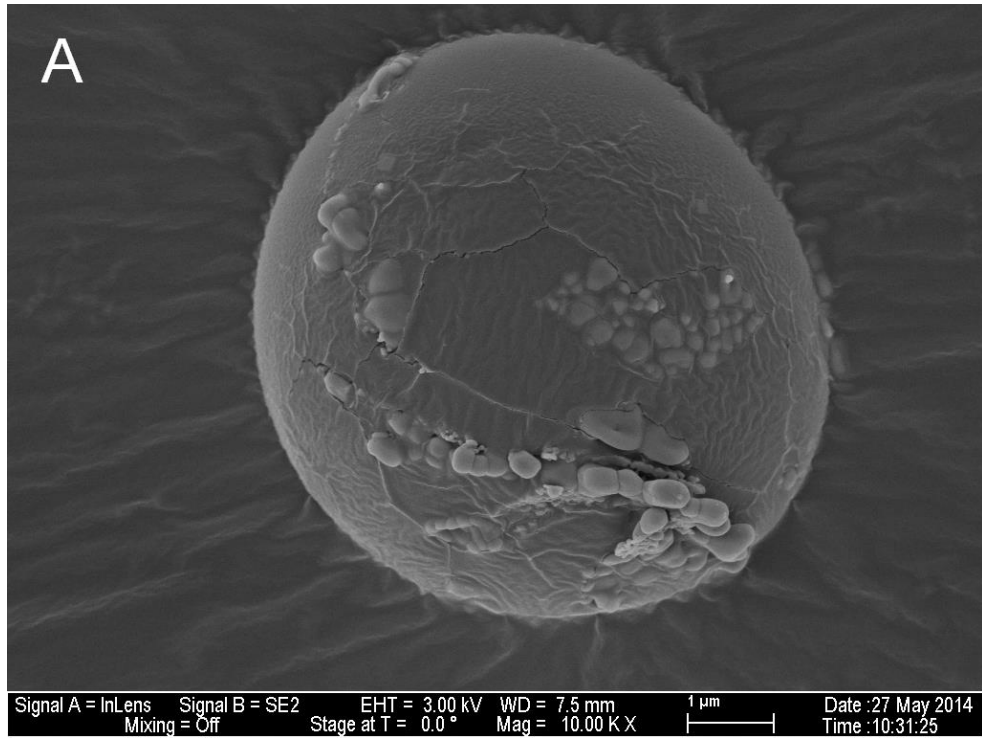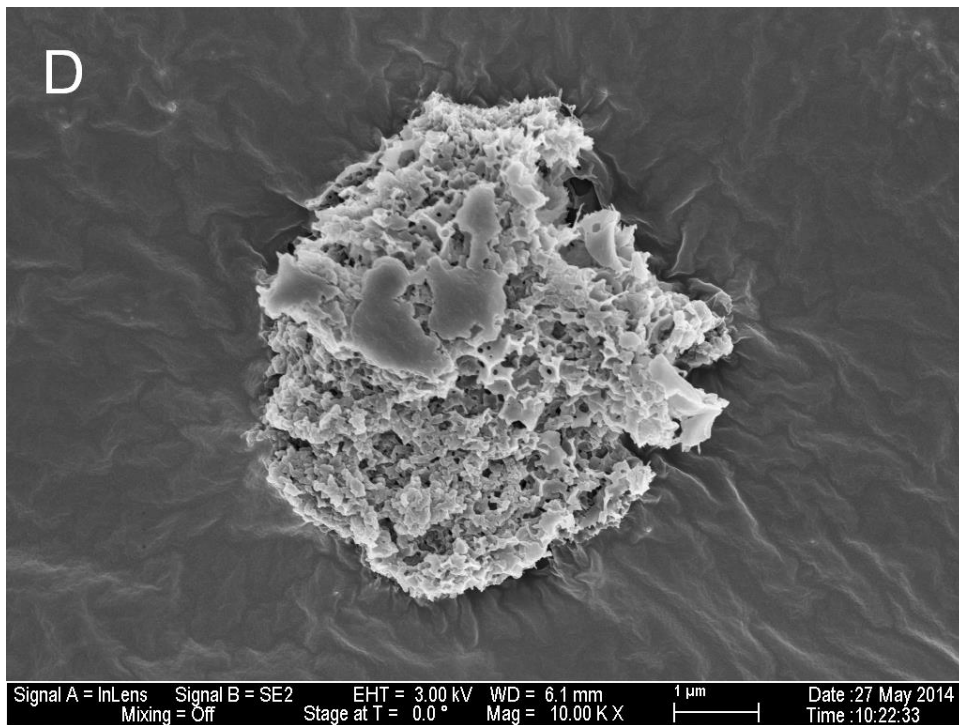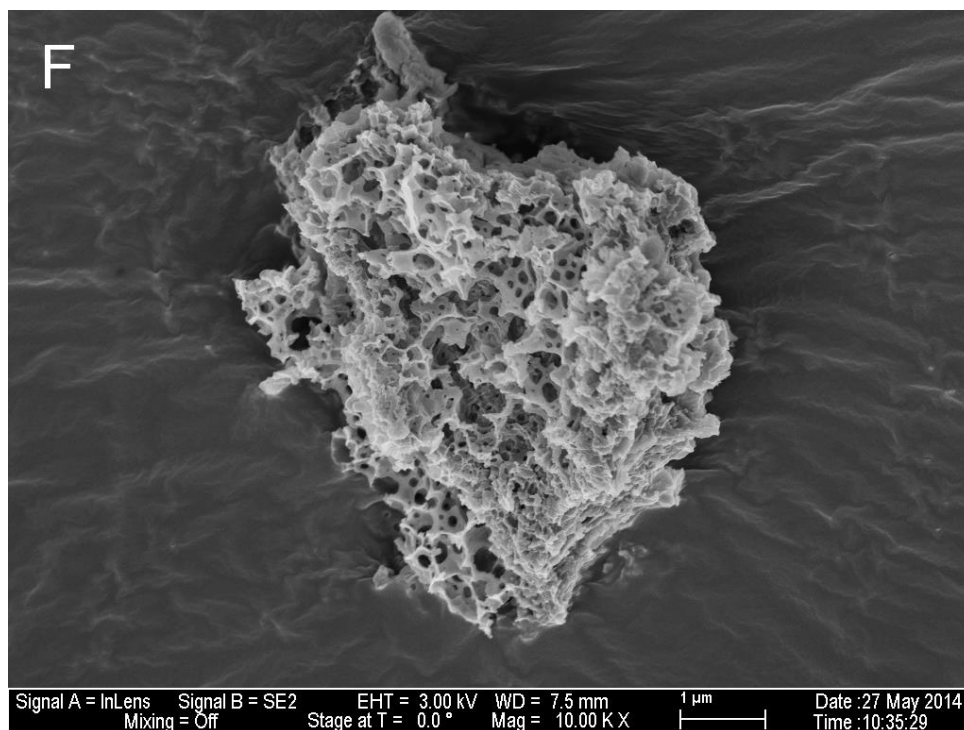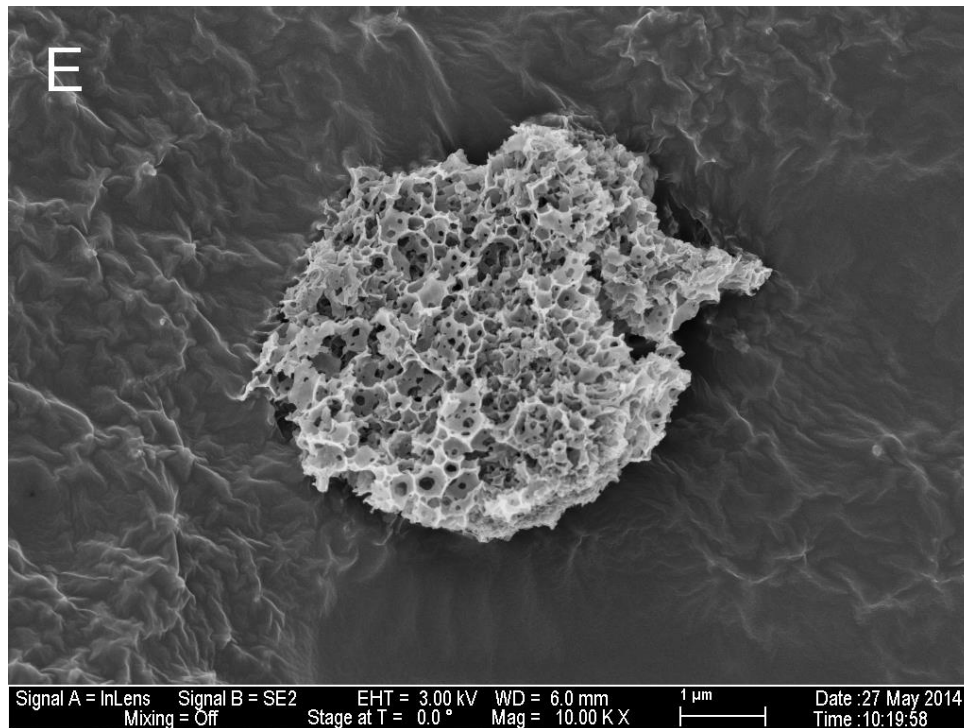
Figure 5.6. SEM Images of DEXAM2/HP1/2 Microspheres in 0.5 % Protamine /PBS pH 7.4 after (A) 15 min, (B) 1 h, (C) 2 h, (D) 4 h, (E) 6 h and (F) 12 h.

5.4. Discussion

HP is a highly sulfated glycosaminoglycan and has negative charges under physiologic conditions (160). Its use as an anticoagulant is well known (161). Protamine, a positively charged protein, forms a complex with HP by electrostatic interactions. Protamine binds strongly to HP, displaces typical gegenions, and inhibits its mode of action (162). Protamine sulfate has been widely utilized clinically to reverse heparin-induced anticoagulation (163, 164). In clinical practice, the dose of protamine is determined by the HP exposure: 1 mg of protamine sulfate neutralises 80-100 IU of HP (165). The lethal dose (LD_{50}) of protamine sulfate is 100 mg/kg in mice (166). In this study, we used protamine sulfate with concentrations ranged from 0.1% to 0.5% (w/v) to determine whether or not protamine would trigger the release of CV from DEXAM/HP microspheres.

Based on the electrostatic interactions of HP with cationic polymers, other drug delivery systems have been developed for biomedical applications (167-169). In this study, we investigated a triggerable drug delivery system incorporating the biodegradable and biocompatible polymer dextran. CV was encapsulated inside DEXAM/HP microspheres via packing by the emulsion process and the electrostatic bindings between DEXAM conjugates and HP.

In this study, we did not use bovine serum albumin (BSA) as a model protein because when determining the amount of BSA encapsulated in DEXAM/HP microspheres by bicinchoninic acid (BCA) method, the aldehyde groups of DEXAM conjugates also reacted with BCA reagents, leading to inaccurate results. This reaction

is used to determine the degree of oxidation (the aldehyde content) of DEXAM conjugate (see *5.2.3.1*). Instead, we use CV as a model drug.

DEXAM conjugates were synthesized using the reductive amination reaction method (Figure 5.1). Acetal groups of DEXAM conjugates help to transform water-soluble dextran into a hydrophobic polymer. We found the primary amine content affects the characteristics of DEXAM/HP microspheres because the positive charges of DEXAM interacted with the negative charges of HP, contributing to the structural integrity of the microspheres. The higher primary amine content, the more HP and DEXAM aggregated in the microspheres, leading to increase the particle size.

CV is a triaminotriphenylmethane dye with a cationic tertiary amine group (170) which allows CV to interact and form complexes with negatively charged HP in the internal water phase as they were encapsulated in the modified dextran microparticles. Thus, the larger amount of HP was entrapped, the higher EE (%) of DEXAM/HP microspheres.

The same trend was observed when increasing the amount of HP resulted in an increase the particle size and EE (%) of DEXAM/HP microspheres with a fixed content of the primary amine (DEXAM2/HP1/2 and DEXAM2/HP1/3 microspheres). In fact, in the fabrication process of microspheres, a high HP concentration in the internal water phase enhanced the viscosity of primary emulsion, which reduced the efficiency of mixing and formation of larger emulsion droplets (171, 172). The interaction between DEXAM conjugates and HP at the O-W interface during the double emulsion process seemed to form an outer shell of microspheres which can be observed in Figure 6C and 6D. The size of microspheres increases with the amount of DEXAM or HP because

more complexes form at the interface. Therefore, the higher amount of HP led to the larger microparticles.

Electrostatic interactions of DEXAM conjugates, HP, and protamine help to explain the mechanism of CV release from microspheres that was monitored via SEM images. In the absence of protamine, the microspheres are fairly stable with approximately 5% of CV released after 12 h in PBS pH 7.4. This CV release is attributed to the diffusion of CV or HP on the surface of microspheres into medium. When protamine was present, HP on the surface of the microspheres gradually binds to protamine and dissociates from DEXAM with degradation of the microspheres. HP/ protamine might be dissolved into the surround medium. During this process, there is a competition between protamine and DEXAM conjugates to bind with HP. As HP disaggregates, the outer shell of microspheres is eroding, leading to the appearance of pores on the surface of microspheres (Figure 5.6C and 5.6D). Water and protamine continue to penetrate microspheres, resulting in the disaggregation and dissolution of HP lodged inside microspheres and accelerating CV release. When HP is completely disaggregated, the remnant of microspheres appears (Figure 5.6E and 5.6F). This remnant is DEXAM conjugates which is not degradable in pH 7.4 medium due to the acetal groups (108) . The DEXAM/HP microspheres do not completely release their CV payloads because more than 30% of CV is still entrapped inside these remaining cores

The release rate of CV depended on the disaggregation rate of HP from microspheres due to interact with protamine. So that when we changed the concentration of protamine, the disaggregation rate of HP changed accordingly, leading to changing of the release rate of CV. The release rate of CV also depended on the

primary amine content of DEXAM conjugates. The higher primary amine content, the larger amount of HP aggregated in microspheres, leads to the more HP disaggregate from microspheres when suspended in a fix concentration of PS.

To improve the cumulative amount of CV released from microspheres, we can enhance the primary amine content of DEXAM conjugates by using dextran with low molecular weight because oxidized dextran with lower molecular weight (9.3-40 kDa) may resulted in higher aldehyde content and therefore in a higher the primary amine content (152, 153).

5.5. Conclusions

In this study, DEXAM conjugates with various primary amine contents were successfully synthesized by the reductive amination reaction method in an effort to be combined with HP to develop the triggered release microspheres using protamine as a triggering agent. The primary amine contents and amount of HP affected the characteristics of the DEXAM/HP microspheres. In addition, protamine triggered the release of CV from DEXAM/HP microspheres. Future studies using dextran with lower molecular weight to maximize the encapsulated drug release.

Chapter 6 - Conclusions and Future Work

6.1. Conclusions

The overall goal of this research was the design, synthesis, characterization and testing of microspheres which *i*) are suitable for extension the half-life of SK for prevention of reocclusion *in vitro*, and *ii*) provide a general controlled release by triggered release mechanism for cardiovascular delivery of therapeutic drugs. This chapter summarizes the concluding remarks of this work and the knowledge gained from the previous chapters.

6.1.1. Summaries from Chapter 3

- DA with various degrees of substitution was successfully synthesized by the reaction of dextran with acetic anhydride.

- A series of PEG/DAs microspheres were prepared by a modified double emulsion method and tested with BSA functioning as a model protein.

- Increasing the degree of substitution of DA resulted in slower release of BSA from PEG/DAs microspheres

- PEG/DA3 microspheres provided the release of BSA on the scale of hours (180 min)

- The percentage of BSA released from PEG and PEG/DA3 microspheres with time (min) was modeled mathematically [$Y_{PEG} = 100(1 - e^{-0.12t})$; $Y_{PEG/DA3} = 100(1 -$

e$^{-0.024t}$)] in order to predict cumulative delivery from mixtures *in vitro* over a period of hours when constrained to a target level at 30 min.

6.1.2. Summaries from Chapter 4

- CS was successfully conjugated to the surface of Eud/SK microspheres by covalent bonding.

- With CS coating on the surface, CS-Eud/SK microspheres exhibited a lower EE (%) based on protein content or SK activity and a much slower release of SK up to 8 h when compared with those of Eud/SK microspheres.

- *In vitro* lysis experiment: mixture of PEG + CS-Eud/SK microspheres could break up the blood clot rapidly while also provide clot-lytic efficacy for prevention of second blockage up to 4 h.

- Counter-intuitively, slower release of SK from CS-Eud/SK microspheres led to faster thrombolysis as a result of greater penetration of agent into the thrombus and the mechanism of distributed intraclot thrombolysis.

6.1.3. Summaries from Chapter 5

- DEXAM conjugates were successfully synthesized using reductive amination reaction.

- HP bound to positively charged ammonium ions of the DEXAM conjugates, contributing to the structural integrity of the microspheres.

- Binding of protamine to HP creates conformational changes leading to mechanical stresses and release of the encapsulated CV.

- Release of CV from microspheres varied with primary amine content of DEXAM conjugates, amount of HP, and concentration of protamine added.

6.2. Future Work

Based on this work and the design of thrombolytic formulations for rapid reperfusion and prevention of another blockage, several important research steps can be pursued in the near future.

Following our current work on testing the thrombolytic formulations on dissolving plasma blood clot *in vitro* (Chapter 4), the future work needs to test the pharmacokinetic profile and thrombolytic efficacy of the formulation mixture of PEG/SK + CS-Eud/SK microspheres in animal models.

We have designed a general controlled release drug delivery system based on protamine induced degradation DEXAM/HP microspheres (Chapter 5). Binding constants for the interaction between DEXAM conjugates and HP, and between protamine and HP need to be determined to characterize the competitive binding between DEXAM conjugates and protamine to HP. In addition, we have shown that increasing the primary amine content of DEXAM conjugate results in increasing the CV release from DEXAM/HP microspheres. Therefore, as further steps of the project, we hypothesize that using dextran with lower molecular weight (9.3-40 kDa) in the reductive amination reactions for synthesis of DEXAM conjugates can improve the CV release from microspheres because the lower molecular weight of dextran used results in the higher primary content of DEXAM conjugates. With the higher amine content of DEXAM conjugates, we can attach ligands, such as anti-fibrin antibody, to the surface of microspheres to target drug carriers to thrombi for improvement of thrombolysis.

References

1. Go AS, Mozaffarian D, Roger VL, Benjamin EJ, Berry JD, Blaha MJ, et al. Heart disease and stroke statistics-2014 Update: A report from the American heart association. Circulation. 2014;129(3):E28-E292.

2. Baker WF. Thrombolytic therapy. Clin Appl Thromb Hemost. 2002;8(4):291-314.

3. Banerjee A, Chisti Y, Banerjee UC. Streptokinase - A clinically useful thrombolytic agent. Biotechnol Adv. 2004;22(4):287-307.

4. Kunamneni A, Abdelghani TTA, Ellaiah P. Streptokinase - The drug of choice for thrombolytic therapy. J Thromb Thrombolysis. 2007;23(1):9-23.

5. Lippi G, Mattiuzzi C, Favaloro EJ. Novel and emerging therapies: thrombus-targeted fibrinolysis. Semin Thromb Hemost. 2013;39(1):48-58.

6. Armstrong PW, Collen D. Fibrinolysis for acute myocardial infarction: current status and new horizons for pharmacological reperfusion, part 1. Circulation. 2001;103(23):2862-66.

7. Gyongyosi M, Wexberg P, Kiss K, Yang P, Sperker W, Sochor H, et al. Adaptive remodeling of the infarct-related artery is associated with recurrent ischemic events after thrombolysis in acute myocardial infarction. Coronary Artery Dis. 2001;12(3):167-72.

8. Ohman EM, Califf RM, Topol EJ, Candela R, Abbottsmith C, Ellis S, et al. Consequences of reocclusion after successful reperfusion therapy in acute myocardial-infarction. Circulation. 1990;82(3):781-91.

9. Leach JK, O'Rear EA, Patterson E, Miao P, Johnson AE. Accelerated thrombolysis in a rabbit model of carotid artery thrombosis with liposome-encapsulated and microencapsulated streptokinase. Thromb Haemost. 2003;90(1):64-70.

10. Badimon L, Chesebro JH, Badimon JJ. Thrombus formation on ruptured atherosclerotic plaques and rethrombosis on evolving thrombi. Circulation. 1992;86(6):74-85.

11. Eisenberg PR. Mechanisms of reocclusion after coronary thrombolysis. Z Kardiol. 1993;82:175-78.

12. Marder VJ, Sherry S. Thrombolytic therapy: current status. N Engl J Med. 1988;318(23):1512-20.

13. Gold HK, Leinbach RC, Garabedian HD, Yasuda T, Johns JA, Grossbard EB, et al. Acute coronary reocclusion after thrombolysis with recombinant human tissue-type plasminogen activator: prevention by a maintenance infusion. Circulation. 1986;73(2):347-52.

14. Johns JA, Gold HK, Leinbach RC, Yasuda T, Gimple LW, Werner W, et al. Prevention of coronary artery reocclusion and reduction in late coronary artery stenosis after thrombolytic therapy in patients with acute myocardial infarction. A randomized study of maintenance infusion of recombinant human tissue-type plasminogen activator. Circulation. 1988;78(3):546-56.

15. Kalbfleisch J, Thadani U, Littlejohn JK, Brown G, Magorien R, Kutcher M, et al. Evaluation of a prolonged infusion of recombinant tissue-type plasminogen activator (Duteplase) in preventing reocclusion following successful thrombolysis in acute myocardial infarction. Am J Cardiol. 1992;69(14):1120-27.

16. Nguyen PD, Orear EA, Johnson AE, Patterson E, Whitsett TL, Bhakta R. Accelerated thrombolysis and reperfusion in a canine model of myocardial-infarction by liposomal encapsulation of streptokinase. Circ Res. 1990;66(3):875-78.

17. Wang SS, Chou NK, Chung TW. The t-PA-encapsulated PLGA nanoparticles shelled with CS or CS-GRGD alter both permeation through and dissolving patterns of blood clots compared with t-PA solution: An in vitro thrombolysis study. J Biomed Mater Res A. 2009;91A(3):753-61.

18. Chung TW, Wang SS, Tsai WJ. Accelerating thrombolysis with chitosan-coated plasminogen activators encapsulated in poly-(lactide-co-glycolide) (PLGA) nanoparticles. Biomaterials. 2008;29(2):228-37.

19. Absar S, Nahar K, Kwon YM, Ahsan F. Thrombus-targeted nanocarrier attenuates bleeding complications associated with conventional thrombolytic therapy. Pharm Res. 2013;30(6):1663-76.

20. Bi F, Zhang J, Su YJ, Tang YC, Liu JN. Chemical conjugation of urokinase to magnetic nanoparticles for targeted thrombolysis. Biomaterials. 2009;30(28):5125-30.

21. Yang HW, Hua MY, Lin KJ, Wey SP, Tsai RY, Wu SY, et al. Bioconjugation of recombinant tissue plasminogen activator to magnetic nanocarriers for targeted thrombolysis. Int J Nanomed. 2012;7:5159-73.

22. Jin HJ, Zhang H, Sun ML, Zhang BG, Zhang JW. Urokinase-coated chitosan nanoparticles for thrombolytic therapy: preparation and pharmacodynamics in vivo. J Thromb Thrombolysis. 2013;36(4):458-68.

23. Leach JK, Patterson E, O'Rear EA. Encapsulation of a plasminogen activator speeds reperfusion, lessens infarct and reduces blood loss in a canine model of coronary artery thrombosis. Thromb Haemost. 2004;91(6):1213-18.

24. Liang JF, Park YJ, Song H, Li YT, Yang VCM. ATTEMPTS: A heparin/protamine-based prodrug approach for delivery of thrombolytic drugs. J Control Release. 2001;72(1-3):145-56.

25. Park YJ, Liang JF, Song H, Li YT, Naik S, Yang VC. ATTEMPTS: A heparin/protamine-based triggered release system for the delivery of enzyme drugs without associated side-effects. Adv Drug Deliv Rev. 2003;55(2):251-65.

26. Naik SS, Liang JF, Park YJ, Lee WK, Yang VC. Application of "ATTEMPTS" for drug delivery. J Control Release. 2005;101(1-3):35-45.

27. Vaidya B, Agrawal GP, Vyas SP. Functionalized carriers for the improved delivery of plasminogen activators. Int J Pharm. 2012;424(1-2):1-11.

28. Mackman N. Triggers, targets and treatments for thrombosis. Nature. 2008;451(7181):914-18.

29. Furie B, Furie BC. Mechanisms of disease: Mechanisms of thrombus formation. N Engl J Med. 2008;359(9):938-49.

30. Bennett PC, Silverman SH, Gill PS, Lip GYH. Peripheral arterial disease and Virchow's triad. Thromb Haemost. 2009;101(6):1032-40.

31. Wolberg AS, Aleman MM, Leiderman K, Machlus KR. Procoagulant activity in hemostasis and thrombosis: Virchow's triad revisited. Anesth Analg. 2012;114(2):275-85.

32. Loscalzo J. Nitric oxide insufficiency, platelet activation, and arterial thrombosis. Circ Res. 2001;88(8):756-62.

33. Cines DB, Pollak ES, Buck CA, Loscalzo J, Zimmerman GA, McEver RP, et al. Endothelial cells in physiology and in the pathophysiology of vascular disorders. Blood. 1998;91(10):3527-61.

34. Vane JR, Botting RM. Pharmacodynamic profile of prostacyclin. Am J Cardiol. 1995;75(3):A3-A10.

35. Holme PA, Orvim U, Hamers M, Solum NO, Brosstad FR, Barstad RM, et al. Shear-induced platelet activation and platelet microparticle formation at blood flow conditions as in arteries with a severe stenosis. Arterioscler Thromb Vasc Biol. 1997;17(4):646-53.

36. Bentzon JF, Otsuka F, Virmani R, Falk E. Mechanisms of plaque formation and rupture. Circ Res. 2014;114(12):1852-66.

37. Sen Gupta A. Nanomedicine approaches in vascular disease: a review. Nanomed-Nanotechnol Biol Med. 2011;7(6):763-79.

38. Bark DL, Jr., Ku DN. Wall shear over high degree stenoses pertinent to atherothrombosis. J Biomech. 2010;43(15):2970-77.

39. Lijfering WM, Flinterman LE, Vandenbroucke JP, Rosendaal FR, Cannegieter SC. Relationship between venous and arterial thrombosis: A review of the literature from a causal perspective. Semin Thromb Hemost. 2011;37(8):884-95.

40. Rajan L, Moliterno DJ. New anticoagulants in ischemic heart disease. Curr Cardiol Rep. 2012;14(4):450-56.

41. Singer OC, Humpich MC, Fiehler J, Albers GW, Lansberg MG, Kastrup A, et al. Risk for symptomatic intracerebral hemorrhage after thrombolysis assessed by diffusion-weighted magnetic resonance imaging. Ann Neurol. 2008;63(1):52-60.

42. Karnabatidis D, Spiliopoulos S, Tsetis D, Siablis D. Quality improvement guidelines for percutaneous catheter-directed intra-arterial thrombolysis and mechanical thrombectomy for acute lower-limb ischemia. Cardiovasc Interv Radiol. 2011;34(6):1123-36.

43. Kim IS, Choi HG, Choi HS, Kim BK, Kim CK. Prolonged systemic delivery of streptokinase using liposome. Arch Pharm Res. 1998;21(3):248-52.

44. Sikri N, Bardia A. A history of streptokinase use in acute myocardial infarction. Tex Heart Inst J. 2007;34(3):318-27.

45. Mundada LV, Prorok M, DeFord ME, Figuera M, Castellino FJ, Fay WP. Structure-function analysis of the streptokinase amino terminus (residues 1-59). J Biol Chem. 2003;278(27):24421-27.

46. Wang XQ, Lin XL, Loy JA, Tang J, Zhang XJC. Crystal structure of the catalytic domain of human plasmin complexed with streptokinase. Science. 1998;281(5383):1662-65.

47. Boxrud PD, Fay WP, Bock PE. Streptokinase binds to human plasmin with high affinity, perturbs the plasmin active site, and induces expression of a substrate recognition exosite for plasminogen. J Biol Chem. 2000;275(19):14579-89.

48. Lijnen HR, Collen D. Molecular basis of thrombolytic therapy. J Nucl Cardiol. 2000;7(4):373-81.

49. Nolan M, Bouldin SD, Bock PE. Full time course kinetics of the streptokinase-plasminogen activation pathway. J Biol Chem. 2013;288(41):29482-93.

50. Boxrud PD, Bock PE. Coupling of conformational and proteolytic activation in the kinetic mechanism of plasminogen activation by streptokinase. J Biol Chem. 2004;279(35):36642-49.

51. Aisina RB, Mukhametova LI, Tyupa DV, Gershkovich KB, Gulin DA, Varfolomeev SD. Streptokinase-polyethylene glycol conjugates with increased stability and reduced side effects. Russ J Bioorg Chem. 2014;40(5):516-25.

52. Greineder CF, Howard MD, Carnemolla R, Cines DB, Muzykantov VR. Advanced drug delivery systems for antithrombotic agents. Blood. 2013;122(9):1565-75.

53. Berger H, Pizzo SV. Preparation of polyethylene glycol-tissue plasminogen activator adducts that retain functional activity: characteristics and behavior in three animal species. Blood. 1988;71(6):1641-47.

54. Runge MS, Bode C, Matsueda GR, Haber E. Antibody-enhanced thrombolysis: targeting of tissue plasminogen activator *in vivo*. Proc Natl Acad Sci U S A. 1987;84(21):7659-62.

55. Veronese FM. Peptide and protein PEGylation: A review of problems and solutions. Biomaterials. 2001;22(5):405-17.

56. Rajagopalan S, Gonias SL, Pizzo SV. A nonantigenic covalent streptokinase polyethylene glycol complex with plasminogen activator function. J Clin Invest. 1985;75(2):413-19.

57. Brucato FH, Pizzo SV. Catabolism of streptokinase and polyethylene glycol-streptokinase: Evidence for transport of intact forms through the biliary system in the mouse. Blood. 1990;76(1):73-79.

58. Sakuragawa N, Shimizu K, Kondo K, Kondo S, Niwa M. Studies on the effect of PEG-modified urokinase on coagulation fibrinolysis using beagles. Thromb Res. 1986;41(5):627-35.

59. Moreadith RW, Collen D. Clinical development of PEGylated recombinant staphylokinase (PEG-Sak) for bolus thrombolytic treatment of patients with acute myocardial infarction. Adv Drug Deliv Rev. 2003;55(10):1337-45.

60. Torchilin VP. Targeting of drugs and drug carriers within the cardiovascular system. Adv Drug Deliv Rev. 1995;17(1):75-101.

61. Kim JY, Kim JK, Park JS, Byun Y, Kim CK. The use of PEGylated liposomes to prolong circulation lifetimes of tissue plasminogen activator. Biomaterials. 2009;30(29):5751-56.

62. Heeremans JLM, Prevost R, Bekkers MEA, Los P, Emeis JJ, Kluft C, et al. Thrombolytic treatment with tissue-type plasminogen activator (t-PA) containing liposomes in rabbit: A comparison with free t-PA. Thromb Haemost. 1995;73(3):488-94.

63. Perkins WR, Vaughan DE, Plavin SR, Daley WL, Rauch J, Lee L, et al. Streptokinase entrapment in interdigitation-fusion liposomes improves thrombolysis in an experimental rabbit model. Thromb Haemost. 1997;77(6):1174-78.

64. Heeremans JLM, Prevost R, Feitsma H, Kluft C, Crommelin DJA. Clot accumulation characteristics of plasminogen-bearing liposomes in a flow system. Thromb Haemost. 1998;79(1):144-49.

65. Leach JK, Patterson E, O'Rear EA. Distributed intraclot thrombolysis: mechanism of accelerated thrombolysis with encapsulated plasminogen activators. J Thromb Haemost. 2004;2(9):1548-55.

66. Piras AM, Chiellini F, Fiumi C, Bartoli C, Chiellini E, Fiorentino B, et al. A new biocompatible nanoparticle delivery system for the release of fibrinolytic drugs. Int J Pharm. 2008;357(1-2):260-71.

67. Chiellini F, Piras AM, Gazzarri M, Bartoli C, Ferri M, Paolini L, et al. Bioactive polymeric materials for targeted administration of active agents: Synthesis and evaluation. Macromol Biosci. 2008;8(6):516-25.

68.   Tang ZC, Li D, Wang XJ, Gong H, Luan YF, Liu Z, et al. A t-PA/nanoparticle conjugate with fully retained enzymatic activity and prolonged circulation time. J Mater Chem B. 2015;3(6):977-82.

69.   Yurko Y, Maximov V, Andreozzi E, Thompson GL, Vertegel AA. Design of biomedical nanodevices for dissolution of blood clots. Mater Sci Eng C. 2009;29(3):737-41.

70.   Korin N, Kanapathipillai M, Matthews BD, Crescente M, Brill A, Mammoto T, et al. Shear-activated nanotherapeutics for drug targeting to obstructed blood vessels. Science. 2012;337(6095):738-42.

71.   Kwon YM, Li YT, Naik S, Liang JF, Huang YZ, Park YJ, et al. The ATTEMPTS delivery systems for macromolecular drugs. Expert Opin Drug Deliv. 2008;5(11):1255-66.

72.   Huang Y, Park YS, Wang J, Moon C, Kwon YM, Chung HS, et al. ATTEMPTS system: A macromolecular prodrug strategy for cancer drug delivery. Curr Pharm Des. 2010;16(21):2369-76.

73.   Qureshi AI, Siddiqui AM, Kim SH, Hanel RA, Xavier AR, Kirmani JF, et al. Reocclusion of recanalized arteries during intra-arterial thrombolysis for acute ischemic stroke. Am J Neuroradiol. 2004;25(2):322-28.

74.   Yamada Y, Furui H, Furumichi T, Yamauchi K, Yokota M, Saito H. Possible mechanism of vascular reocclusion after initially successful thrombolysis with recombinant tissue-type plasminogen activator. Am Heart J. 1991;121(6):1618-27.

75.   Wada K, Umemura K, Nishiyama H, Saniabadi AR, Takiguchi Y, Nakano M, et al. A chemiluminescent detection of superoxide radical produced by adherent leucocytes to the subendothelium following thrombolysis: Studies with a photochemically induced thrombosis model in the guinea pig femoral artery. Atherosclerosis. 1996;122(2):217-24.

76. Rapaport E. Thrombolysis, anticoagulation, and reocclusion. Am J Cardiol. 1991;68(16):E17-E22.

77. Coller BS. Augmentation of thrombolysis with antiplatelet drugs. Coronary Artery Dis. 1995;6(12):911-14.

78. Brouwer MA, van den Bergh P, Aengevaeren WRM, Veen G, Luijten HE, Hertzberger DP, et al. Aspirin plus coumarin versus aspirin alone in the prevention of reocclusion after fibrinoilysis for acute myocardial infarction - Results of the Antithrombotics in the Prevention of Reocclusion In Coronary Thrombolysis (APRICOT)-2 trial. Circulation. 2002;106(6):659-65.

79. Antman EM, Giugliano RP, Gibson CM, McCabe CH, Coussement P, Kleiman NS, et al. Abciximab facilitates the rate and extent of thrombolysis - Results of the thrombolysis in myocardial infarction (TIMI) 14 trial. Circulation. 1999;99(21):2720-32.

80. Barlinn K, Becker U, Puetz V, Dzialowski I, Kunz A, Kepplinger J, et al. Combined treatment with intravenous abciximab and intraarterial tPA yields high recanalization rate in patients with acute basilar artery occlusion. J Neuroimaging. 2012;22(2):167-71.

81. Pulicherla KK, Kumar A, Gadupudi GS, Kotra SR, Rao K. In vitro characterization of a multifunctional staphylokinase variant with reduced reocclusion, produced from salt inducible E. coli GJ1158. Biomed Res Int. 2013:12.

82. Marder VJ. Thrombolytic therapy: 2001. Blood Rev. 2001;15(3):143-57.

83. Uyttenboogaart M, De Keyser J, Luijckx GJ. Thrombolysis for acute ischemic stroke. Curr Top Med Chem. 2009;9(14):1285-90.

84. Verheugt FWA. New anticoagulants in ischemic heart disease. Presse Med. 2005;34(18):1325-29.

85. Elbayoumi TA, Torchilin VP. Liposomes for targeted delivery of antithrombotic drugs. Expert Opin Drug Deliv. 2008;5(11):1185-98.

86. Vaidya B, Nayak MK, Dash D, Agrawal GP, Vyas SP. Development and characterization of site specific target sensitive liposomes for the delivery of thrombolytic agents. Int J Pharm. 2011;403(1-2):254-61.

87. Kaminski MD, Xie Y, Mertz CJ, Finck MR, Chen H, Rosengart AJ. Encapsulation and release of plasminogen activator from biodegradable magnetic microcarriers. Eur J Pharm Sci. 2008;35(1-2):96-103.

88. Chen J-P, Yang P-C, Ma Y-H, Wu T. Characterization of chitosan magnetic nanoparticles for in situ delivery of tissue plasminogen activator. Carbohydr Polym. 2011;84(1):364-72.

89. Shaw GJ, Meunier JM, Huang S-L, Lindsell CJ, McPherson DD, Holland CK. Ultrasound-enhanced thrombolysis with tPA-loaded echogenic liposomes. Thromb Res. 2009;124(3):306-10.

90. Smith DAB, Vaidya SS, Kopechek JA, Huang S-L, Klegerman ME, McPherson DD, et al. Ultrasound-triggered release of recombinant tissue-type plasminogen activator from echogenic liposomes. Ultrasound Med Biol. 2010;36(1):145-57.

91. Uesugi Y, Kawata H, Jo J-i, Saito Y, Tabata Y. An ultrasound-responsive nano delivery system of tissue-type plasminogen activator for thrombolytic therapy. J Control Release. 2010;147(2):269-77.

92. Ye M, Kim S, Park K. Issues in long-term protein delivery using biodegradable microparticles. J Control Release. 2010;146(2):241-60.

93. Sinha VR, Bansal K, Kaushik R, Kumria R, Trehan A. Poly-epsilon-caprolactone microspheres and nanospheres: an overview. Int J Pharm. 2004;278(1):1-23.

94. Heinze T, Liebert T, Heublein B, Hornig S. Functional polymers based on dextran. In: Klemm D, editor. Polysaccharides II. Advances in Polymer Science. 2052006. p. 199-291.

95. Mehvar R. Dextrans for targeted and sustained delivery of therapeutic and imaging agents. J Control Release. 2000;69(1):1-25.

96. Dhaneshwar SS, Kandpal M, Gairola N, Kadam SS. Dextran: A promising macromolecular drug carrier. Indian J Pharm Sci. 2006;68(6):705-14.

97. Wich PR, Frechet JMJ. Degradable dextran particles for gene delivery applications. Aust J Chem. 2012;65(1):15-19.

98. Ouchi T, Saito T, Kontani T, Ohya Y. Encapsulation and/or release behavior of bovine serum albumin within and from polylactide-grafted dextran microspheres. Macromol Biosci. 2004;4(4):458-63.

99. Broaders KE, Cohen JA, Beaudette TT, Bachelder EM, Frechet JMJ. Acetalated dextran is a chemically and biologically tunable material for particulate immunotherapy. Proc Natl Acad Sci U S A. 2009;106(14):5497-502.

100. Chiewpattanakul P, Covis R, Vanderesse R, Thanomsub B, Marie E, Durand A. Design of polymeric nanoparticles for the encapsulation of monoacylglycerol. Colloid Polym Sci. 2010;288(9):959-67.

101. Aumelas A, Serrero A, Durand A, Dellacherie E, Leonard M. Nanoparticles of hydrophobically modified dextrans as potential drug carrier systems. Colloids Surf B Biointerfaces. 2007;59(1):74-80.

102. Vandijkwolthuis WNE, Franssen O, Talsma H, Vansteenbergen MJ, Vandenbosch JJK, Hennink WE. Synthesis, characterization, and polymerization of glycidyl methacrylate derivatized dextran. Macromolecules. 1995;28(18):6317-22.

103. Hussain MA, Shahwar D, Tahir MN, Sher M, Hassan MN, Afzal Z. An efficient acetylation of dextran using in situ activated acetic anhydride with iodine. J Serb Chem Soc. 2010;75(2):165-73.

104. Yang HJ, Park IS, Na K. Biocompatible microspheres based on acetylated polysaccharide prepared from water-in-oil-in-water (W1/O/W2) double emulsion

method for delivery of type II diabetic drug (exenatide). Colloids Surf A Physicochem Eng Asp. 2009;340(1-3):115-20.

105. Kim SH, Chu CC. Synthesis and characterization of dextran-methacrylate hydrogels and structural study by SEM. J Biomed Mater Res. 2000;49(4):517-27.

106. Ogawa K, Hirai I, Shimasaki C, Yoshimura T, Ono S, Rengakuji S, et al. Simple determination method of degree of substitution for starch acetate. Bull Chem Soc Jpn. 1999;72(12):2785-90.

107. Thummala AS, Leach JK, O'Rear EA. Factors affecting the particle size and in vitro release of bovine serum albumin from polyethylene glycol microparticles. Biomed Sci Instrum 2003;39:318–23.

108. Bachelder EM, Beaudette TT, Broaders KE, Dashe J, Frechet JMJ. Acetal-derivatized dextran: An acid-responsive biodegradable material for therapeutic applications. J Am Chem Soc. 2008;130(32):10494-5.

109. Carter DC, Ho JX. Structure of serum albumin. Adv Protein Chem. 1994;45:153-203.

110. Jiang WL, Schwendeman SP. Stabilization and controlled release of bovine serum albumin encapsulated in poly(D, L-lactide) and poly(ethylene glycol) microsphere blends. Pharm Res. 2001;18(6):878-85.

111. Park SJ, Kim SH. Preparation and characterization of biodegradable poly (1-lactide)/poly(ethylene glycol) microcapsules containing erythromycin by emulsion solvent evaporation technique. J Colloid Interface Sci. 2004;271(2):336-41.

112. Liu G, Hong X, Jiang M, Yuan W. Sustained-release G-CSF microspheres using a novel solid-in-oil-in-oil-in-water emulsion method. Int J Nanomed. 2012;7:4559-69.

113. Tuliani VV, Orear EA. Circulatory concentrations of fibrinolytic species during thrombolytic therapy estimated by stirred-tank reactor analysis. Pharm Res. 1997;14(8):1051-57.

114. Anand S, Kudallur V, Pitman EB, Diamond SL. Mechanisms by which thrombolytic therapy results in nonuniform lysis and residual thrombus after reperfusion. Ann Biomed Eng. 1997;25(6):964-74.

115. Khoobehi B, Peyman GA. Accelerated thrombolysis and reperfusion in a primate model of branch vein occlusion by liposomal encapsulation of streptokinase. Invest Ophthalmol Vis Sci. 1997;38(4):4879-79.

116. Mukhametova LI, Aisina RB, Tyupa DV, Medvedeva AS, Gershkovich KB. Properties of streptokinase incorporated into polyethylene glycol microcapsules. Russ J Bioorg Chem. 2013;39(4):390-96.

117. Torno MD, Kaminski MD, Xie YM, Meyers RE, Mertz CJ, Liu X, et al. Improvement of in vitro thrombolysis employing magnetically-guided microspheres. Thromb Res. 2008;121(6):799-811.

118. Holt B, Sen Gupta A. Streptokinase loading in liposomes for vascular targeted nanomedicine applications: Encapsulation efficiency and effects of processing. J Biomater Appl. 2012;26(5):509-27.

119. Dvorackova K, Rabiskova M, Muselik J, Gajdziok J, Bajerova M. Coated hard capsules as the pH-dependent drug transport systems to ileo-colonic compartment. Drug Dev Ind Pharm. 2011;37(10):1131-40.

120. Sinha VR, Singla AK, Wadhawan S, Kaushik R, Kumria R, Bansal K, et al. Chitosan microspheres as a potential carrier for drugs. Int J Pharm. 2004;274(1-2):1-33.

121. Zhang D, Sun P, Li P, Xue AB, Zhang XK, Zhang HY, et al. A magnetic chitosan hydrogel for sustained and prolonged delivery of Bacillus Calmette-Guerin in the treatment of bladder cancer. Biomaterials. 2013;34(38):10258-66.

122. Guo HJ, Zhang DR, Li CY, Jia LJ, Liu GP, Hao LL, et al. Self-assembled nanoparticles based on galactosylated O-carboxymethyl chitosan-graft-stearic acid conjugates for delivery of doxorubicin. Int J Pharm. 2013;458(1):31-38.

123. Chicatun F, Pedraza CE, Muja N, Ghezzi CE, McKee MD, Nazhat SN. Effect of chitosan incorporation and scaffold geometry on chondrocyte function in dense collagen type I hydrogels. Tissue Eng Part A. 2013;19(23-24):2553-64.

124. Panyam J, Dali MA, Sahoo SK, Ma WX, Chakravarthi SS, Amidon GL, et al. Polymer degradation and in vitro release of a model protein from poly(D,L-lactide-co-glycolide) nano- and microparticles. J Control Release. 2003;92(1-2):173-87.

125. Ma FK, Li J, Kong M, Liu Y, An Y, Chen XG. Preparation and hydrolytic erosion of differently structured PLGA nanoparticles with chitosan modification. Int J Biol Macromol. 2013;54:174-79.

126. Couto LT, Donato JL, De Nucci G. Analysis of five streptokinase formulations using the euglobulin lysis test and the plasminogen activation assay. Brazilian J Med Biol Res. 2004;37(12):1889-94.

127. Hughes GA. Nanostructure-mediated drug delivery. Dis Mon. 2005;51(6):342-61.

128. Kathleen D, Vandervoort J, Van den Mooter G, Ludwig A. Evaluation of ciprofloxacin-loaded Eudragit((R)) RS100 or RL100/PLGA nanoparticles. Int J Pharm. 2006;314(1):72-82.

129. Wu JH, Siddiqui K, Diamond SL. Transport phenomena and clot dissolving therapy: an experimental investigation of diffusion-controlled and permeation-enhanced fibrinolysis. Thromb Haemost. 1994;72(1):105-12.

130. Staros JV, Wright RW, Swingle DM. Enhancement by N-hydroxysulfosuccinimide of water-soluble carbodiimide-mediated coupling reactions. Anal Biochem. 1986;156(1):220-22.

131. Mustafin RI, Bodrov AV, Kemenova VA, Rombaut P, Van den Mooter G. Interpolymer interaction between countercharged types of Eudragit(A (R)) RL30D and FS30D in binary films as a method of drug release modification in oral delivery systems. Pharm Chem J. 2012;46(1):45-49.

132. Mahmoodi M, Khosroshahi ME, Atyabi F. Early experimental results of thrombolysis using controlled release of tissue plasminogen activator encapsulated by PLGA/CS nanoparticles delivered by pulse 532 nm laser. Dig J Nanomater Biostruct. 2011;6(3):889-905.

133. Modaresi SMS, Mehr SE, Faramarzi MA, Gharehdaghi EE, Azarnia M, Modarressi MH, et al. Preparation and characterization of self-assembled chitosan nanoparticles for the sustained delivery of streptokinase: an in vivo study. Pharm Dev Technol. 2014;19(5):593-97.

134. Nguyen DA, Fogler HS. Facilitated diffusion in the dissolution of carboxylic polymers. Aiche J. 2005;51(2):415-25.

135. Chakravarthi SS, Robinson DH. Enhanced cellular association of paclitaxel delivered in chitosan-PLGA particles. Int J Pharm. 2011;409(1-2):111-20.

136. Blinc A, Francis CW. Transport processes in fibrinolysis and fibrinolytic therapy. Thromb Haemost. 1996;76(4):481-91.

137. Blinc A, Planinsic G, Keber D, Jarh O, Lahajnar G, Zidansek A, et al. Dependence of blood clot lysis on the mode of transport of urokinase into the clot - A magnetic resonance imaging study in vitro. Thromb Haemost. 1991;65(5):549-52.

138. Diamond SL, Anand S. Inner clot diffusion and permeation during fibrinolysis. Biophys J. 1993;65(6):2622-43.

139. Collet JP, Montalescot G, Lesty C, Weisel JW. A structural and dynamic investigation of the facilitating effect of glycoprotein IIb/IIIa inhibitors in dissolving platelet-rich clots. Circ Res. 2002;90(4):428-34.

140. Sakharov DV, Nagelkerke JF, Rijken DC. Rearrangements of the fibrin network and spatial distribution of fibrinolytic components during plasma clot lysis - Study with confocal microscopy. J Biol Chem. 1996;271(4):2133-38.

141. Kohane DS, Anderson DG, Yu C, Langer R. pH-triggered release of macromolecules from spray-dried polymethacrylate microparticles. Pharm Res. 2003;20(10):1533-38.

142. Zago AC, Raudales JC, Attizzani G, Matte BS, Yamamoto GI, Balvedi JA, et al. Local delivery of sirolimus nanoparticles for the treatment of in-stent restenosis. Catheter Cardiovasc Interv. 2013;81(2):E124-E29.

143. Arakawa H, Murayama Y, Davis CR, Howard DL, Baumgardner WL, Marks MP, et al. Endovascular embolization of the swine rete mirabile with Eudragit-E 100 polymer. Am J Neuroradiol. 2007;28(6):1191-96.

144. Tamura G, Kato N, Yamazaki T, Akutsu Y, Hosoo H, Kasuya H, et al. Endovascular embolization of brain arteriovenous malformations with Eudragit-E. Neurol Med Chir. 2015;55(3):253-60.

145. Suarez S, Grover GN, Braden RL, Christman KL, Amutairi A. Tunable protein release from acetalated dextran microparticles: A platform for delivery of protein therapeutics to the heart post-MI. Biomacromolecules. 2013;14(11):3927-35.

146. Cheng YX, Hao J, Lee LA, Biewer MC, Wang Q, Stefan MC. Thermally controlled release of anticancer drug from self-assembled gamma-substituted amphiphilic poly(epsilon-caprolactone) micellar nanoparticles. Biomacromolecules. 2012;13(7):2163-73.

147. Park TH, Eyster TW, Lumley JM, Hwang S, Lee KJ, Misra A, et al. Photoswitchable particles for on-demand degradation and triggered release. Small. 2013;9(18):3051-57.

148. Jin HQ, Tan H, Zhao LL, Sun WP, Zhu LJ, Sun YG, et al. Ultrasound-triggered thrombolysis using urokinase-loaded nanogels. Int J Pharm. 2012;434(1-2):384-90.

149. Hu SH, Tsai CH, Liao CF, Liu DM, Chen SY. Controlled rupture of magnetic polyelectrolyte microcapsules for drug delivery. Langmuir. 2008;24(20):11811-18.

150. Huang YZ, Park YS, Wang JX, Moon C, Kwon YM, Chung HS, et al. ATTEMPTS system: a macromolecular prodrug strategy for cancer drug delivery. Curr Pharm Des. 2010;16(21):2369-76.

151. Yang TZ, Nyiawung D, Silber A, Hao JK, Lai L, Bai SH. Comparative studies on chitosan and polylactic-co-glycolic acid incorporated nanoparticles of low molecular weight heparin. AAPS PharmSciTech. 2012;13(4):1309-18.

152. Azzam T, Eliyahu H, Shapira L, Linial M, Barenholz Y, Domb AJ. Polysaccharide-oligoamine based conjugates for gene delivery. J Med Chem. 2002;45(9):1817-24.

153. Azzam T, Raskin A, Makovitzki A, Brem H, Vierling P, Lineal M, et al. Cationic polysaccharides for gene delivery. Macromolecules. 2002;35(27):9947-53.

154. Cohen JL, Schubert S, Wich PR, Cui L, Cohen JA, Mynar JL, et al. Acid-degradable cationic dextran particles for the delivery of siRNA therapeutics. Bioconjug Chem. 2011;22(6):1056-65.

155. Deng WW, Cao X, Wang M, Yang Y, Su WY, Wei YW, et al. Efficient gene delivery to mesenchymal stem cells by an ethylenediamine-modified polysaccharide from mulberry leaves. Small. 2012;8(3):441-51.

156. Kauffman KJ, Do C, Sharma S, Gallovic MD, Bachelder EM, Ainslie KM. Synthesis and characterization of acetalated dextran polymer and microparticles with ethanol as a degradation product. ACS Appl Mater Interfaces. 2012;4(8):4149-55.

157. Doner LW, Irwin PL. Assay of reducing end-groups in oligosaccharide homologs with 2,2'-bicinchoninate. Anal Biochem. 1992;202(1):50-53.

158. Rastogi A, Luo ZQ, Wu ZJ, Ho PS, Bowman PD, Stavchansky S. Development and characterization of a scalable microperforated device capable of long-term zero order drug release. Biomed Microdevices. 2010;12(5):915-21.

159. Giorgini MG, Pelletti MR, Paliani G, Cataliotti RS. Vibrational-spectra and assignments of ethylene-diamine and its deuterated derivatives. J R Spectrosc. 1983;14(1):16-21.

160. Liang YK, Kiick KL. Heparin-functionalized polymeric biomaterials in tissue engineering and drug delivery applications. Acta Biomater. 2014;10(4):1588-600.

161. Lever R, Page CR. Novel drug development opportunities for heparin. Nat Rev Drug Discov. 2002;1(2):140-48.

162. Carr JA, Silverman N. The heparin-protamine interaction: A review. J Cardiovasc Surg. 1999;40(5):659-66.

163. Ainle FN, Preston RJS, Jenkins PV, Nel HJ, Johnson JA, Smith OP, et al. Protamine sulfate down-regulates thrombin generation by inhibiting factor V activation. Blood. 2009;114(8):1658-65.

164. Byun Y, Singh VK, Yang VC. Low molecular weight protamine: A potential nontoxic heparin antagonist. Thromb Res. 1999;94(1):53-61.

165. Baglin T, Barrowcliffe TW, Cohen A, Greaves M, British Comm Stand H. Guidelines on the use and monitoring of heparin. Br J Haematol. 2006;133(1):19-34.

166. http://fresenius-kabi.ca/wp-content/uploads/2015/01/EN_WebInsert_Protamin Sulf.pdf.

167. Tang DW, Yu SH, Ho YC, Mi FL, Kuo PL, Sung HW. Heparinized chitosan/poly(gamma-glutamic acid) nanoparticles for multi-functional delivery of fibroblast growth factor and heparin. Biomaterials. 2010;31(35):9320-32.

168. Reyes-Ortega F, Rodriguez G, Aguilar MR, Lord M, Whitelock J, Stenzel MH, et al. Encapsulation of low molecular weight heparin (bemiparin) into polymeric nanoparticles obtained from cationic block copolymers: properties and cell activity. J Mater Chem B. 2013;1(6):850-60.

169. Saito T, Tabata Y. Preparation of gelatin hydrogels incorporating low-molecular-weight heparin for anti-fibrotic therapy. Acta Biomater. 2012;8(2):646-52.

170. Safarik I, Safarikova M. Detection of low concentrations of malachite green and crystal violet in water. Water Res. 2002;36(1):196-200.

171. Yang YY, Chung TS, Ng NP. Morphology, drug distribution, and in vitro release profiles of biodegradable polymeric microspheres containing protein fabricated by double-emulsion solvent extraction/evaporation method. Biomaterials. 2001;22(3):231-41.

172. Nguyen HX, O'Rear EA. Biphasic release of protein from polyethylene glycol and polyethylene glycol/modified dextran microspheres. J Biomed Mater Res A. 2013;101(9):2699-705.